

Technical Memo

871

Trends in the GloFAS-ERA5 river discharge reanalysis

E. Zsoter^{1,2}, H. Cloke^{2,3,4}, C. Prudhomme¹,
S. Harrigan¹, P. de Rosnay¹, J. Muñoz-Sabater¹,
E. Stephens²

¹ ECMWF Forecast Department

² University of Reading

³ Uppsala University

⁴ Centre of Natural Hazards and Disaster Science (CNDS)

September 2020

Series: ECMWF Technical Memoranda

A full list of ECMWF Publications can be found on our website under:

<http://www.ecmwf.int/en/publications>

Contact: library@ecmwf.int

© Copyright 2020

European Centre for Medium-Range Weather Forecasts, Shinfield Park, Reading, RG2 9AX, UK

Literary and scientific copyrights belong to ECMWF and are reserved in all countries. This publication is not to be reprinted or translated in whole or in part without the written permission of the Director-General. Appropriate non-commercial use will normally be granted under the condition that reference is made to ECMWF.

The information within this publication is given in good faith and considered to be true, but ECMWF accepts no liability for error or omission or for loss or damage arising from its use.

Abstract

The main objective of this study is to analyse the GloFAS-ERA5 river discharge reanalysis for any noticeable change (including gradual trends or discontinuities) in the annual mean time series across the 1979-2018 (40-year) period, and to evaluate how realistic these are compared with available observed river discharge time series.

These variabilities are quantified by linear regression in order to highlight any concerning features in the GloFAS-ERA5 time series.

This work is particularly important for GloFAS, as large trends, discontinuities or other similar features could have a major consequence on the GloFAS flood thresholds in around 50% of catchments, which are based on GloFAS-ERA5, and thus subsequently on the issuing of flood warnings.

In addition, this study also contributes to the understanding of the water cycle variable behaviour in ERA5 (driver of GloFAS-ERA5) and ERA5-Land (higher resolution land reanalysis forced by ERA5, produced offline) by exploring the linear trends in river discharge and related hydrological variables. In exploring the stability of the time series in ERA5, we seek to trigger potential further discussions and research studies, which subsequently should help with the planning and development for the next generation ECMWF reanalysis, ERA6.

1 Introduction

In November 2019, the GloFAS (Global Flood Awareness System) was upgraded to version 2.1 (<https://confluence.ecmwf.int/display/COPSRV/GloFAS+v2.1>). This included two important changes: the release of the official GloFAS-ERA5 river discharge reanalysis, and the revision of the flood threshold computation. The flood thresholds are predefined and specified as a magnitude of river flow for specific return periods; these are used operationally to highlight where upcoming flows may be severe and trigger alerts accordingly. They are computed from river discharge reanalysis by fitting an extreme value distribution onto the annual maxima time series. In the v2.1 upgrade, flood thresholds were recomputed using the 40-year (1979-2018) GloFAS-ERA5 river discharge reanalysis, which is an ERA5-forced hydrological simulation (Harrigan et al. 2020). In addition, the analysis of the v2.1 vs. v2.0 thresholds revealed that over large parts of the world the GloFAS-ERA5 river discharge time series has very noticeable linear trends across the 40-year period.

Linear trends can highlight noticeable change across the 40-year period, be that a gradual shift (i.e. a trend) or a discontinuity (i.e. a step change at one point in the time series). Any noticeable shift in the time series is particularly important as it can hinder the representativity of the GloFAS thresholds, through the characteristically different extreme flood event behaviour in different parts of the 40-year period.

In this study, the changes/shifts in the GloFAS-ERA5 annual mean time series are analysed and quantified by linear regression. The linear trend magnitudes, along the regression lines, are computed for river discharge, as well as for all ERA5 and ERA5-Land variables that directly affect the water budget: precipitation, snowfall, evaporation, 2m temperature, soil water content, runoff and snowmelt. The linear trends in the available river discharge observations are used as verifying truth and compared with the GloFAS-ERA5 river discharge (and also ERA5 runoff) trends.

2 Data and methods

2.1 Global Flood Awareness System

The Global Flood Awareness System (GloFAS; www.globalfloods.eu) is part of the Copernicus Emergency Management Service (CEMS) and has been developed in collaboration between ECMWF, the Joint Research Centre (JRC) of the European Commission with help from research institutions such as the University of Reading (UoR). It monitors and forecasts floods across the world. GloFAS has two complementary systems:

- GloFAS 30-day, that includes daily ensemble flood forecast predictions, out to 30 days ahead, updated daily, based on the ECMWF medium- and extended-range ensemble runoff as input forcing
- GloFAS Seasonal, that provides ensemble hydrological forecasts of unusually low or high flow for calendar weeks up to 16 weeks ahead, updated monthly, based on the ECMWF SEAS5 ensemble runoff as input forcing

GloFAS forecasts possible flood episodes and unusually high/low river flow for all major rivers of the world. It has been an operational service since April 2018 (following a pre-operational phase which started in 2011) with information shown on a dedicated web platform (www.globalfloods.eu; Figure 1).

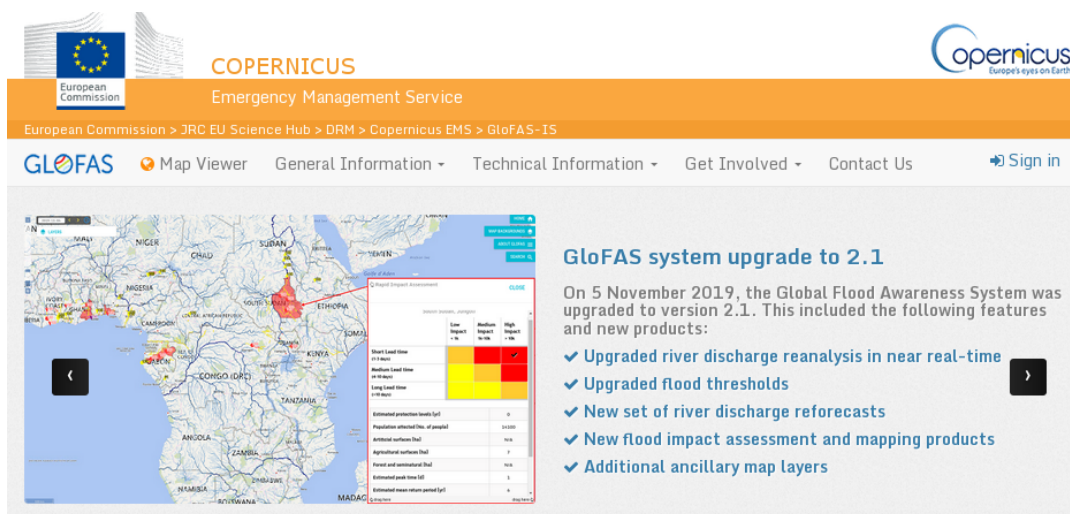


Figure 1. Snapshot of the GloFAS website's landing page.

GloFAS is designed to complement existing national and regional services, and to support national civil protection and international organisations in decision making before major flood events, particularly in large transnational river basins. Forecast information is used by a variety of decision makers, including national and regional water authorities, water resources managers, hydropower companies, civil protection and first line responders, and international humanitarian aid organisations. GloFAS only focuses on larger rivers (mainly over 10.000 km² catchment area) and does not provide real-time forecast information on flash flood risk, pluvial or coastal flooding.

GloFAS river discharge data is produced by coupling the LISFLOOD hydrological and channel routing model (van der Knijff et al., 2010) to the runoff output of the land-surface model of ECMWF NWP

system. The river routing runs with surface and sub-surface runoff inputs on a $0.1^{\circ} \times 0.1^{\circ}$ (~ 10 km resolution) global river network. The surface runoff component directly enters the river channel, while the sub-surface runoff first enters a groundwater module that outputs the water into the river channel after a time delay (Harrigan et al. 2020).

The river state of the real time ensemble GloFAS forecasts is initialised from a hydrological simulation, forced by the fast release version of ERA5 (ERA5T) up until when it is available (a few days behind real time) and then subsequently by the ECMWF ensemble control forecast.

A long term river discharge dataset is required in order to compute the return period flood thresholds in GloFAS 30-day: currently this is the GloFAS-ERA5 reanalysis.

Further description on the GloFAS system is available on the GloFAS internal website at (<https://confluence.ecmwf.int/display/COPSRV/Global+Flood+Awareness+System>) and in Harrigan et al 2020.

2.2 ERA5 and ERA5-Land

ERA5 is ECMWF's 5th generation global climate reanalysis (Hersbach et al., 2020). ERA5 covers the period January 1979 to near real time with a plan to extend to 1950. ERA5 includes one_high-resolution component (~ 31 km horizontal resolution) and a lower resolution ensemble component with 10 members (~ 62 km horizontal resolution).

There are two flavours of ERA5 reanalysis available: the raw ERA5, based on consolidated, quality-checked data, lagging ~ 2 -3 months behind real-time; and ERA5T, which is available 5 days behind real time, but is not fully quality-checked (Hersbach et al., 2020).

ERA5-Land (<https://cds.climate.copernicus.eu/cdsapp#!/dataset/reanalysis-era5-land>) is also analysed for comparative purposes in this study. ERA5-Land is the offline land surface only improved version of ERA5.

ERA5 and ERA5-Land runoff are both produced by the HTESSEL (Hydrology Tiled ECMWF Scheme for Surface Exchanges over Land; Balsamo et al., 2009) land-surface model of the ECMWF Integrated Forecasting System (IFS).

The HTESSEL scheme follows a mosaic (or tiling) approach where the grid boxes are divided into patches (or tiles), with up to six fractions over land (bare ground, low and high vegetation, intercepted water, shaded and exposed snow) and two extra tiles over water (open and frozen water) exchanging energy and water with the atmosphere. HTESSEL is used within the ECMWF IFS in coupled atmosphere-surface mode on time ranges from medium-range to seasonal forecasts.

ERA5 is a coupled application which includes the operational land data assimilation system of ECMWF to assimilate conventional in-situ and satellite observations for land surface variables for the analysis of soil moisture, soil temperature and snow fields (de Rosnay et al., 2014).

ERA5-Land, on the other hand, is a product of an offline HTESSEL simulation without atmosphere-land coupling and land data assimilation, forced by the atmospheric variables (e.g. air temperature and radiation). ERA5-Land is produced at 9 km spatial resolution using downscaled ERA5 atmospheric forcing and a vertical lapse rate correction on temperature. There is no direct coupling or land data assimilation in ERA5-Land (there is only an indirect impact through the ERA5 forcing) and this can

have a large impact on the hydrological cycle (Zsoter et al. 2019), and potentially also on the trends. Other major differences between ERA5 and ERA5-Land are the much higher resolution and the lapse-rate correction in ERA5-Land, which also can have a large impact on the water budget, especially in mountainous areas, changing the snow pack and snowmelt through the temperature differences.

ERA5-Land is analysed in a similar way to ERA5 for hydrological variables, apart from river discharge which is not yet produced for ERA5-Land. In addition, precipitation and snowfall are identical in ERA5 and ERA5-Land (apart from the downscaling) and therefore are not considered further within the ERA5-Land analysis.

2.3 GloFAS-ERA5 reanalysis

The GloFAS-ERA5 river discharge reanalysis is a product of the European Commission’s Copernicus Emergency Management Service (CEMS) and is officially available in the Copernicus Climate Data Store free of charge after registration (<https://cds.climate.copernicus.eu/>).

GloFAS-ERA5 uses surface and sub-surface runoff input from the high-resolution component of the ERA5 reanalysis. It has a fast release version, GloFAS-ERA5T, forced by ERA5T, available 2-5-days behind real time, used in the initialisation of the GloFAS real time forecasts.

A schematic of the key components of the GloFAS-ERA5 and its potential extension GloFAS-ERA5-Land is given in Figure 2.

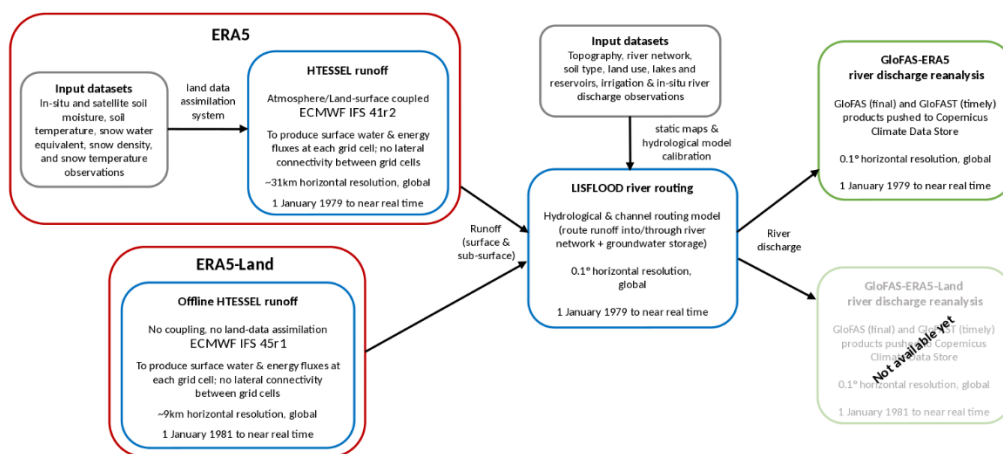


Figure 2. Schematic of the key components of the GloFAS-ERA5 river discharge reanalysis dataset production, including the ERA5 and ERA5-Land climate reanalyses. Adapted from Harrigan et al. 2020.

GloFAS verification studies often use GloFAS-ERA5, serving as a proxy for river discharge observations. More detailed information on GloFAS-ERA5 is available in Harrigan et al. (2020).

2.4 Trend analysis methodology

Although GloFAS-ERA5 starts in 1979, ERA5-Land data are only available from 1981, and thus the trend analysis is based on the common 1981-2018 period of 38 years. At the time of writing, no ERA5-Land river discharge is available, and instead annual averages of runoff are used as a proxy, which is a very good estimate of the river discharge in annual means.

Choice of catchments

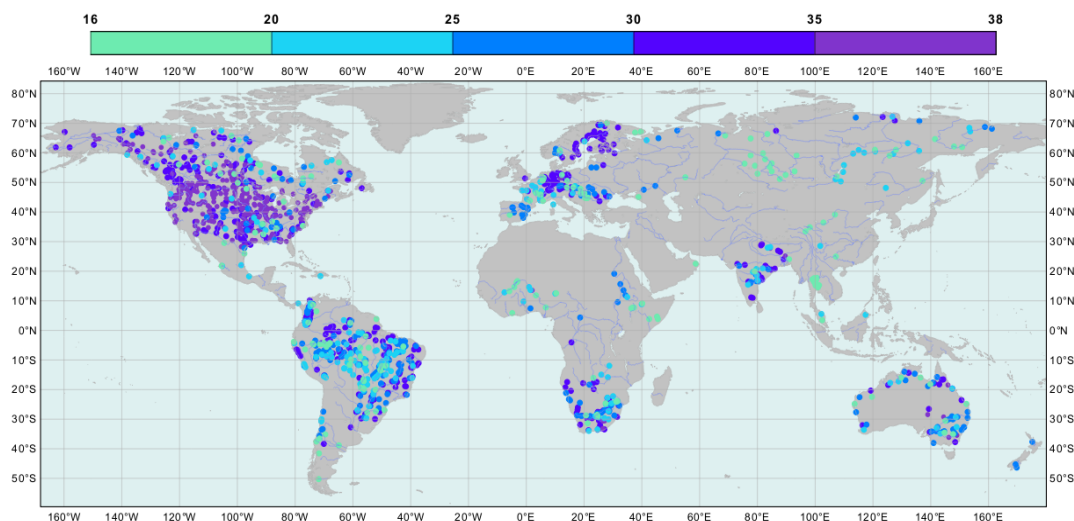


Figure 3. Length of observed river discharge records available for the trend analysis, represented at the catchment outlets. A total of 1324 stations with a minimum of 16 years was processed.

The GloFAS diagnostic catchments are used in this study to analyse the linear trends: a list of 6122 stations with catchment areas varying from about 1.000 km² to 5.4 million km².

On a subset of these catchments, where river discharge observations were available (collected and managed by the JRC), the GloFAS-ERA5 river discharge trends are compared to the equivalent trends, determined from observed river discharge, available in the 1981-2018 period (Figure 3). A total of 1324 stations were selected with a minimum of 16 years of observed daily data. Unfortunately, large parts of the world are poorly observed with large gaps in space and also in time in the 38-year period (Lavers et al., 2019; Rodda et al., 1993; Pavelsky et al., 2014)

Additionally, 33 major world river catchments with good observations are selected for providing detailed analysis of the annual mean time series and linear trend magnitudes (Figure 4). The catchments were selected to cover different parts of the world with the longest possible observation time series.

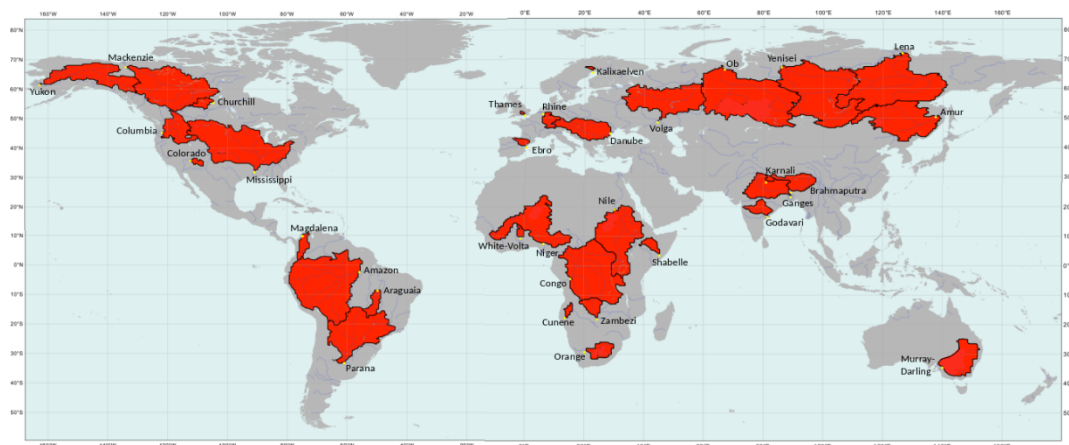


Figure 4. Global river catchments where the trends are provided in Table 2, 3 and A1, and where the hydrographs are shown in the Appendix C with the annual mean time series.

Choice of variables

In addition to the simulated and observed river discharge (Table 1), the surface variables that directly affect the water budget are analysed from ERA5 and ERA5-Land for linear trends. In the HTESSEL terrestrial water budget, precipitation (P) is the incoming water source. The water can stay in one of the water storage reservoirs or leave the land surface. Water reservoirs are the soil, the canopy interception and in solid form the snowpack (the water stored in the snowpack is the snow water equivalent, SWE). The interception accounts for only a very small fraction of the storage and thus it was left out of the analysis. From the soil, which has four layers in HTESSEL, two water reservoir versions are chosen to be analysed. The top layer (SWV7, 0-7cm), which provides an immediate impact to the atmosphere, and the combination of the top three layers (SWV100, 0-100cm) which represents the slower evolving part of the soil that is still more strongly connected to the atmosphere through the vegetation roots.

The snowfall, the solid part of the incoming precipitation (SF), contributes to building the snowpack. Some part of the rain (liquid part of precipitation) and the water from the melting snowpack (SMLT) leave the land surface system as surface runoff (SRO, the surface fraction of RO). Another fraction of the precipitation leaves as intercepted water evaporation. The remaining water (from the incoming rain and the snowmelt) enters the soil and contributes to the soil water reservoir. Some of this water evaporates, either directly from the soil or through the vegetation as transpiration. In total, evaporation in HTESSEL (E, where negative E means the land-surface losing water) is the sum of evaporation of the soil and the interception and also plant transpiration. Finally, some of the water drains from the soil at the bottom at layer 4 and leave the system as subsurface runoff (SSRO, the subsurface fraction of RO).

In order to compare directly with river discharge, the trend analysis is carried out on whole catchment values for each ERA5 and ERA5-Land water budget variable introduced above, after the values on the GloFAS grid are summed together in each of the catchments. This way, essentially the catchment average value is multiplied by the area for the water related variables. The only exception is 2m temperature which was analysed as area average.

Table 1. List of variables analysed for linear trends in this study with their short names, MARS archive codes (see <https://apps.ecmwf.int/codes/grib/param-db/>), the number of processed catchments and a short description.

Short name	Unit	MARS parameter	Number of catchments	Periods	Parameter description
DIS	m^3/s	240.024	5695	1981-2018, 1981-2003 and 2004-2018	GloFAS-ERA5 river discharge
OBS	m^3/s	-	1324	Only 1981-2018 (with variable length)	River discharge observations
DIS-match-OBS	m^3/s	240.024			River discharge observation dates matched GloFAS-ERA5 river discharge

RO-match-OBS	m^3/s	205.128			River discharge observation dates matched runoff outputs of HTESSEL
P	m^3/s	228.128	5698	1981-2018, 1981-2003 and 2004-2018	Precipitation
SF	m^3/s	144.128	3774	1981-2018, 1981-2003 and 2004-2018	Snowfall part of precipitation (same in ERA5 and ERA5-Land apart from downscaling)
RO	m^3/s	205.128	5694	1981-2018, 1981-2003 and 2004-2018	ERA5 sum of surface and sub-surface runoff outputs of HTESSEL
RO-Land	m^3/s	205.128		1981-2018, 1981-2003 and 2004-2018	ERA5-Land sum of surface and sub-surface runoff outputs of HTESSEL
SMLT	m^3/s	145.128	3789	1981-2018, 1981-2003 and 2004-2018	ERA5 snowmelt output of HTESSEL
SMLT-Land	m^3/s	145.128		1981-2018, 1981-2003 and 2004-2018	ERA5-Land snowmelt output of HTESSEL
E	m^3/s	182.128	5698	1981-2018, 1981-2003 and 2004-2018	ERA5 evaporation output of HTESSEL
E-Land	m^3/s	182.128		1981-2018, 1981-2003 and 2004-2018	ERA5-Land evaporation output of HTESSEL
P-E	m^3/s	-	5686	1981-2018, 1981-2003 and 2004-2018	ERA5 precipitation minus evaporation as net water flux to the land-surface in HTESSEL
P-E-Land	m^3/s	-		1981-2018, 1981-2003 and 2004-2018	ERA5-Land precipitation minus evaporation as net water flux to the land-surface in HTESSEL
SWV7	m^3/s	39.128	5698	1981-2018, 1981-2003 and 2004-2018	ERA5 water content in the top 7cm of the soil (layer 1) in HTESSEL
SWV7-Land	m^3/s	39.128		1981-2018, 1981-2003 and 2004-2018	ERA5-Land water content in the top 7cm of the soil (layer 1) in HTESSEL
SWV100	m^3/s	39-41.128	5698	1981-2018, 1981-2003 and 2004-2018	ERA5 water content in the top 1 meter of the soil (layers 1, 2 and 3 together) in HTESSEL
SWV100-Land	m^3/s	39-41.128		1981-2018, 1981-2003 and 2004-2018	ERA5-Land water content in the top 1 meter of the soil (layers 1, 2 and 3 together) in HTESSEL
T2	C°	167.128	5698	1981-2018, 1981-2003 and 2004-2018	ERA5 temperature output at 2 metres in HTESSEL
T2-Land	C°	167.128		1981-2018, 1981-2003 and 2004-2018	ERA5-Land temperature output at 2 metres in HTESSEL

Trend analysis presentation design

This analysis documents the linear trends in the GloFAS-ERA5 river discharge and in the main ERA5 and ERA5-Land water budget variables (Table 1). The trends are shown as maps for all these variables, where the catchment outlets are represented by circles, colour coded by the trend magnitudes, with the size representing the catchment area. In addition, the annual mean time series of all variables are also shown for some major world rivers in the Appendix C, supplemented by some trend related statistics.

As a preliminary check, before the linear trends are computed on the actual river catchments, the global land average annual mean time series of the water cycle variables are analysed for ERA5 (1979-2018) and ERA5-Land (1981-2018). All simulated variables are included in Table 1, extended by snow water equivalent (SWE), surface runoff (SRO) and subsurface runoff (SSRO). This step is carried out to identify if there is any major shift or discontinuity in the global time series. All land grid points are used in the averaging, with exception of the snow water equivalent (SWE), where a mask is applied to remove the glaciers, which are represented by a fixed value of 10 metre (of water equivalent) and thus would severely distort the average values.

The linear trends in the GloFAS-ERA5 river discharge simulations are also compared to the linear trends in the observed river discharge. The river discharge trend errors are assumed to be the difference between the trends in the simulation and the observation annual mean time series. To allow fair comparison, this error computation is done on a special subset of the GloFAS-ERA5 time series that matches the dates when the observations are available (DIS-match-OBS).

As trends in runoff and river discharge are expected to be very similar, the linear trend error, i.e. the difference between the runoff and observed river discharge trends, is calculated to assess how ERA5 and ERA5-Land estimate the changes in river discharge. For runoff trend errors, the observation matching time series are used for both ERA5 (RO-match-OBS) and ERA5-Land (RO-Land-match-OBS), similar to DIS-match-OBS. The impact by ERA5-Land is expressed as the difference between the absolute value of the ERA5-Land runoff linear trend error minus the ERA5 runoff linear trend error.

Even though reanalysis systems are designed with the intention of being independent of the changes in the observing system, it is inevitable that the 38-year reanalysis period has some inhomogeneities in the use of the different meteorological observations, including a known major change in the IMS snow observation use which was analysed further. The operational snow analysis was changed in the ECMWF IFS in 2004, when the 24-km Interactive Multi-Sensor Snow and Ice Mapping System (IMS) snow cover information was introduced, in addition to the SYNOP snow depth measurements. This led to a more realistic representation of the extent of snow cover in the operational analysis (Drusch et al., 2004). Details on ECMWF's snow assimilation can be found in an ECMWF Newsletter article (de Rosnay et al., 2015). In ERA5, the higher resolution (4 km) IMS snow products could be used from 2004, as the high-resolution data was reprocessed and made available to this date.

Moreover, the snow scheme in ECMWF's HTESSEL land-surface model is documented to melt the snow too slowly (Dutra et al. 2012). This, in combination with the use of the IMS snow cover data, could lead to a negative shift in ERA5 snowmelt from 2004, as the excess snow that is not melted by the model could then be removed by the assimilation in areas where in situ observations are not available.

This change is expected to produce a clear discontinuity in the snow related time series, and also contribute indirectly to creating potential shifts in other variables. This would make it possible that the 38-year-based linear trend would reflect mostly the discontinuity. Therefore, in order to see the trends not dependent on this discontinuity, the 38-year period is split in two parts, 1981-2003 (period1, with 23 years) and 2004-2018 (period2, with 15 years). The linear trends are then computed for both periods in the same way as for the whole 38-year period for all variables other than the observation related ones (see Table 1).

Criteria for catchment inclusion

The availability of the river discharge observations varies from catchment to catchment and can be as low as 4-5 years (which is the minimum criteria to include them in the GloFAS observation database). For the trend computation a longer minimum length is needed. The criteria of 16 minimum available years, with at least 330 days available in each year, is set as a compromise considering both the observation availability and the minimum record length for reliable regression analysis (Dai et al., 2009).

For all analysed variables (Table 1), only catchments which have at least 1 m³/s whole catchment value (or river discharge) as sample mean over the 38-year period (or shorter for the observations) and also the 2-year return period flood thresholds are above 20 m³/s are considered for trend analysis. This filters out the very dry catchments for which trends would not be necessarily meaningful or representative, and similarly filters out snowfall and snowmelt for catchments in the warm climate, where the whole catchment values for these variables will be very small. However, for some of the catchments in the tropical belt the trend could still be computed, for those which have some areas over higher orography and thus some snow contribution. These snow related trends should only be interpreted with caution, as especially in the large catchments, such as the Amazon, the snow has extremely small contribution to the total river discharge.

With these criteria, about 1300 catchments could be used for observed river discharge, roughly 3800 catchments for snowfall and snowmelt and about 5700 catchments for all other water cycle variables (see Table 1 for the exact numbers).

Regarding the gaps in the available river discharge observation time series, these were simply left out of the analysis, but the catchments that had at least 16 years of data in total (even if gaps in between) were used regardless of the gaps.

Definition of trend magnitudes

The trend magnitudes are defined after applying a linear regression to the annual mean time series sample. With this the trends are assumed to be linear. This assumption will not be true for all catchments, however, for the sake of this study, this is considered to be sufficient. Linear trends are expected to show if the time series is impacted by larger changes, discontinuities, etc., which could make the flood threshold computation problematic in GloFAS. To help the relative comparison between catchments and variables, the trend T is defined by (following Stahl et al. 2012):

$$T = (10 \cdot S) / M, \quad (1)$$

as the change over a fixed 10-year period, relative to the mean (M) of the n -year period. Here T stands for the trend magnitude at a catchment, S is the slope (annual change as a result of the linear regression), and $M = \text{Mean}(\text{Var}_1, \dots, \text{Var}_n)$, with Var_1 to Var_n denoting the annual mean values from year 1 to year n . The T value gives a measure of the change in a decade. For example, a value of ± 0.1 effectively means the variable increased (decreased) by 10% of the sample mean value over the course of the 10 years. The 10-year fixed period is chosen as a common ground to allow trend comparability for catchments with different observation length.

For 2m temperature, as the only non-water-related variable, the intercomparability with other variables is less important, and also the division by the mean (M) would cause problems (being near 0 in some areas of the world), therefore the trend magnitude is defined as the temperature change in 10 years along the linear regression line ($T=10*S$, where M is replaced by 1).

An alternative trend magnitude was also calculated for all variables, including 2m temperature, by calculating the linear regression on the standardised variable (each annual mean value divided by the standard deviation of the annual mean time series) and T defined by the $10*S$. The standardised trend improves the comparability across variables with very different value ranges (e.g. river discharge and evaporation) and suffer less from the potential issue of division by near 0 values (as it can happen in some isolated cases for P-E). However, the M -based trend (Eq. 1) is more intuitive when interpreting the size of the trends and therefore was selected as the focus of our analysis. In the rest of the paper the ‘raw’ trend, i.e. the original definition of the linear trend with the raw variable (in Eq. 1), is analysed and displayed, with only few exceptions where the standardised trend is mentioned.

In Eq. 1, n is either 38 (1981-2018), 23 (1981-2003) or 15 (2004-2018) for all variables other than the river discharge observation related variables (OBS, DIS-match-OBS, RO-match-OBS and RO-Land-match-OBS; see in Table 1) where it varies between 16 and 38 for the catchments, depending on observation availability.

3 Results

3.1 Global land average annual mean time series for ERA5 and ERA5-Land

The discontinuity in the use of the IMS product from 2004 is a known issue in ERA5. This is clearly present in the global land average annual mean time series of the snow, both for SWE and SMLT (Figure 5). For snowmelt, the change happens from 2004, while for SWE from mainly 2005. This discontinuity, however, seems to be mostly embedded in a general decreasing trend for both variables. ERA5-Land, which does not have land data assimilation as in ERA5, does not show any sign of this change in 2004.

Another very clear shift is seen for precipitation and all the runoff variables in the 1999-2004 period, when these variables suffer a very large drop (Figure 5). There is no such tendency in snowfall, which suggests that the source of this drop must come mainly from warm climate areas where snow is not dominant.

Finally, as expected, the strong upward tendency is present for 2m temperature, with over 1 degree difference between the start and end years of the 40-year period (Figure 5).

ERA5-Land is slightly warmer and generally has more water in the water cycle. It produces more runoff, even though as a balance of much less surface runoff and lot more subsurface runoff. There is more snow in the snowpack with consequently more snowmelt. The soil also has more water but finally less evaporation than in ERA5 (Figure 5).

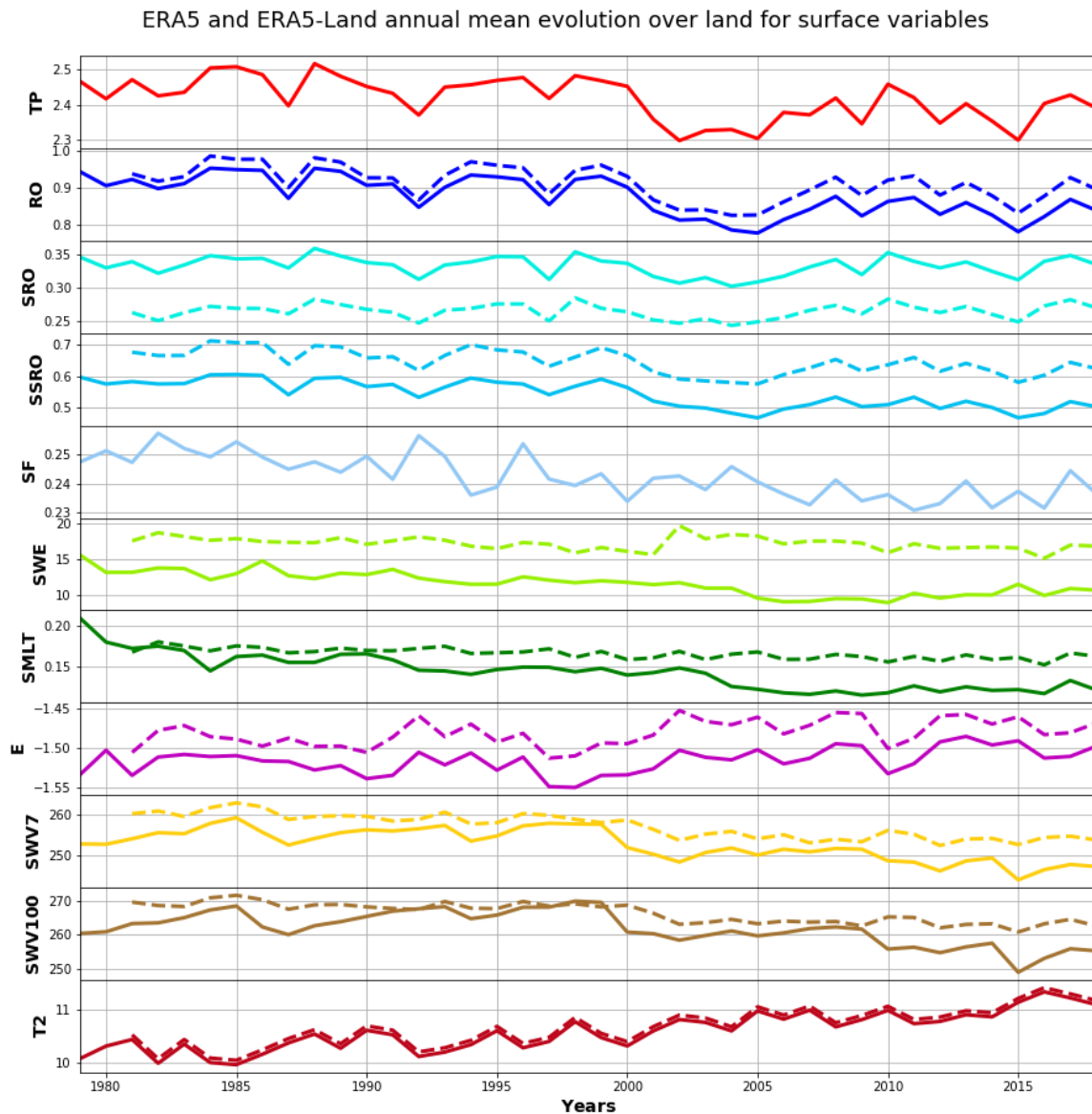


Figure 5. Annual mean time series of global land averages for precipitation (TP), runoff (RO), surface runoff (SRO), subsurface runoff (SSRO), snowfall (SF), snow water equivalent (SWE), snowmelt (SMLT), evaporation (E), soil water content in the top 7 cm (SWV7) and 100 cm (SWV100) and finally 2m temperature (T2) from ERA5 (solid lines) and ERA5-Land (dashed lines) for the 1979-2018 period (ERA5-Land is only available from 1981). TP and SF are the same in ERA5 and ERA5-Land (apart from downscaling to higher resolution in ERA5-Land), so only displayed for ERA5. All variables' unit is mm/day other than 2m temperature which has C.

3.2 Trends in GloFAS-ERA5 river discharge

Over the 1981-2018 period, GloFAS-ERA5 river discharge shows a dominantly negative raw linear trend with almost 80% of catchments exhibiting negative trend magnitudes and about 40% showing a negative value stronger than -0.1 (fraction/decade), i.e. decreasing at least by 10% of the 1981-2018 mean value across the 10-year reference period (Figure 6).

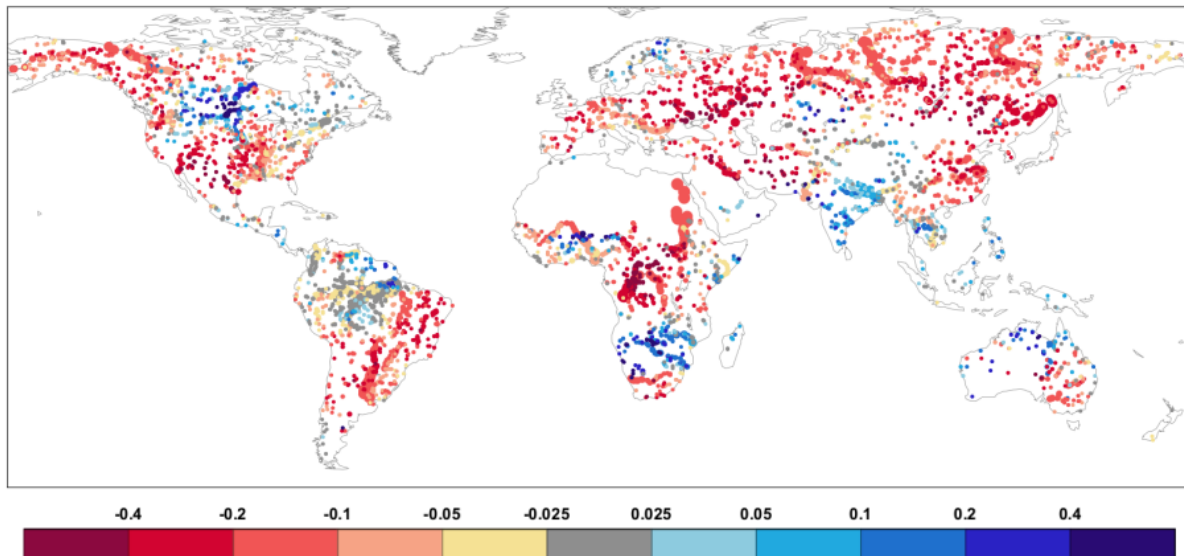


Figure 6. Raw linear trends (fraction/decade) at global river catchments for GloFAS-ERA5 river discharge, based on the 1981-2018 period. The circles represent the catchment outlets, while their size the catchment area.

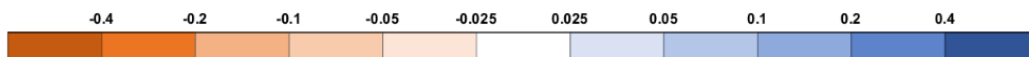
The most negative river discharge trends are found in many of the larger world rivers such as: the Congo and the Nile in Africa; the Ob, Lena, Yenisei and Amur in Russia; the Dnieper and Volga in Europe; the Colorado, Mackenzie and the Yukon in North America; the Yellow and the Yangtze in China; the Tiger and Euphrates in the Middle East and the Sao Francisco, Tocantins and Paraguay in eastern South America.

Positive linear discharge trends can be seen in a few smaller areas, most notably around larger rivers like the Zambezi in South Africa, the Ganges in India and the Nelson in central Canada.

According to the DIS column in Table 2 (and also A1 with the standardised trends), only 8 out of 33 catchments show a positive trend (~25%), while 18 catchments (~55%) reveal larger trends at least with 10% decrease in the 10 years (or more than 1/3 of the standard deviation of the annual mean time series for the standardised trend in A1), making it a very substantial drop in GloFAS-ERA5 river discharge for the whole 1981-2018 period.

Table 2. Raw linear trends (fraction/decade) for selected catchments (see Figure 4) for 1981-2018, for GloFAS-ERA5 river discharge (DIS), ERA5 precipitation (P) and snowfall (SF) and both ERA5 and ERA5-Land snowmelt (SMLT), runoff (RO), evaporation (E), precipitation minus evaporation (P-E), soil moisture in the top 7 cm (SWV7) and 100 cm (SWV100) and 2m temperature (T2). Raw linear trends are also provided for observed river discharge (OBS) and the observation matched GloFAS-ERA5 river discharge (DISm) and ERA5 and ERA5-Land runoff (ROm). Differences in the absolute raw linear trend errors between ERA5-Land and ERA5 are also indicated (Imp). Empty cells correspond to cases for which trend computation was not possible. Coloured cells indicate negative (orange) and positive (blue) trends and also decreasing (green) and increasing (purple) trend errors in ERA5-Land (Imp column). Where there is no raw trend, defined for absolute values less than 0.025, cells are not coloured. Darkening shades show increasing trend magnitudes.

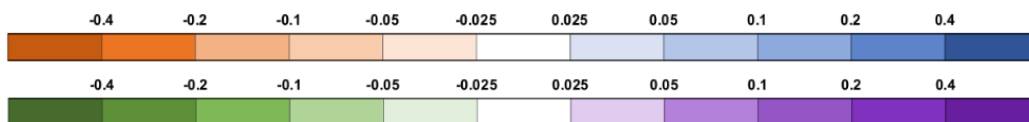
Rivers		DIS	P	SF	SMLT		RO		E		P-E	
		ERA5	ERA5	ERA5	ERA5	ERA5-Land	ERA5	ERA5-Land	ERA5	ERA5-Land	ERA5	ERA5-Land
North Asia	Ob	-0.15	-0.01	-0.03	-0.13	-0.04	-0.11	-0.06	-0.023	-0.018	-0.07	-0.06
	Yenisei	-0.16	-0.02	-0.03	-0.18	-0.03	-0.15	-0.07	-0.016	-0.017	-0.07	-0.08
	Lena	-0.14	0.00	-0.03	-0.24	-0.04	-0.11	-0.04	-0.019	-0.023	-0.04	-0.05
	Amur	-0.26	-0.04	-0.04	-0.39	-0.07	-0.20	-0.16	-0.007	-0.004	-0.16	-0.17
North America	Yukon	-0.14	-0.01	-0.03	-0.13	-0.03	-0.13	-0.03	-0.001	-0.014	-0.01	-0.03
	Mackenzie	-0.12	0.00	-0.01	-0.05	0.00	-0.11	-0.02	-0.008	-0.009	-0.02	-0.03
	Churchill	0.12	0.03	0.03	0.07	0.02	0.07	0.07	-0.009	-0.009	0.15	0.19
	Colorado	-0.11	-0.02	0.01	-0.06	0.01	-0.10	-0.01	0.038	0.021	0.01	-0.01
	Mississippi	-0.09	-0.02	-0.06	-0.08	-0.06	-0.08	-0.07	-0.005	0.006	-0.12	-0.07
Europe	Kalixaelven	0.02	0.03	0.02	-0.06	0.02	0.01	0.05	-0.022	-0.024	0.04	0.04
	Thames	-0.11	0.01	-0.12	0.10	-0.10	-0.11	0.00	0.003	-0.013	0.05	-0.01
	Rhine	-0.12	-0.03	-0.08	-0.15	-0.07	-0.10	-0.08	-0.019	-0.023	-0.08	-0.09
	Danube	-0.09	0.01	-0.04	-0.13	-0.05	-0.08	-0.03	-0.019	-0.026	0.00	-0.02
	Volga	-0.27	-0.03	-0.03	-0.12	-0.03	-0.22	-0.13	-0.024	-0.013	-0.16	-0.14
Ebro	-0.20	0.00	0.04	-0.17	0.04	-0.15	-0.02	0.059	-0.002	0.21	0.00	
South America	Magdalena	-0.03	-0.02				-0.04	-0.03	0.001	-0.008	-0.03	-0.04
	Amazon	-0.02	0.00	-0.12	-0.12	-0.12	-0.02	-0.01	-0.001	-0.004	-0.01	-0.01
	Araguaia	-0.15	-0.06				-0.13	-0.13	0.004	0.015	-0.18	-0.13
Parana	-0.17	-0.05	-0.15	-0.16	-0.16	-0.14	-0.16	0.005	0.019	-0.21	-0.17	
Africa	Nile	-0.11	-0.07				-0.10	-0.12	0.029	0.051	-0.22	-0.15
	Niger	-0.06	-0.02				-0.05	-0.07	-0.028	0.007	-0.35	-0.06
	Shabelle	-0.04	-0.03				-0.04	-0.03	0.021	0.027	-0.08	-0.03
	White-Volta	0.14	-0.03				0.12	0.07	-0.044	0.038	-0.67	0.25
	Congo	-0.30	-0.08				-0.25	-0.28	0.005	0.008	-0.33	-0.30
	Zambesi	0.08	0.01				0.06	0.08	0.022	0.010	0.12	0.06
	Cunene	0.12	0.05				0.09	0.15	0.045	-0.048	1.25	0.09
Orange	-0.20	-0.07	-0.02	-0.04	-0.03	-0.16	-0.17	0.090	0.048	7.83	-0.47	
South Asia	Brahmaputra	-0.02	-0.02	-0.05	-0.01	-0.05	-0.02	-0.03	-0.012	-0.007	-0.03	-0.03
	Ganges	0.07	0.03	-0.05	0.02	-0.04	0.06	0.05	-0.011	-0.006	0.06	0.05
	Godavari	0.10	0.05				0.10	0.11	-0.018	-0.015	0.13	0.12
	Karnali	0.03	0.01	-0.08	-0.05	-0.07	0.03	0.01	-0.012	-0.008	0.01	0.01
Australia	Murray	-0.11	-0.07	-0.13	-0.19	-0.13	-0.10	-0.14	0.035	0.056	-0.11	-0.32



(continues on next page)

Table 2. Raw linear trends (fraction/decade) for selected catchments (see Figure 4) for 1981-2018 (continued)

Rivers		SWV 0-7		SWV 0-100		T2		OBS	DISm	ROm		
		ERA5	ERA5-Land	ERA5	ERA5-Land	ERA5	ERA5-Land	-	ERA5	ERA5	ERA5-Land	Imp
North Asia	Ob	-0.006	-0.006	-0.007	-0.009	0.22	0.22	0.02	-0.16	-0.12	-0.04	-0.081
	Yenisei	-0.010	-0.010	-0.006	-0.014	0.36	0.35	0.04	-0.15	-0.14	-0.05	-0.097
	Lena	-0.004	-0.001	-0.002	-0.001	0.37	0.36	0.04	-0.17	-0.12	-0.06	-0.065
	Amur	-0.024	-0.019	-0.012	-0.024	0.32	0.31	-0.33	-0.65	-0.52	-0.40	-0.128
North Amrica	Yukon	-0.009	-0.002	-0.014	-0.001	0.40	0.39	0.02	-0.20	-0.18	-0.04	-0.140
	Mackenzie	-0.006	-0.003	-0.007	-0.003	0.34	0.33	0.04	-0.12	-0.10	-0.01	-0.095
	Churchill	0.003	0.006	0.007	0.008	0.13	0.12	0.20	0.22	0.11	0.07	0.045
	Columbia	-0.027	-0.015	-0.027	-0.011	0.34	0.32	-0.02	-0.13	-0.11	-0.03	-0.078
	Colorado	-0.110	-0.094	-0.104	-0.057	0.43	0.44	-0.27	-0.43	-0.37	-0.45	0.073
Mississippi	-0.014	-0.016	-0.007	-0.019	0.24	0.25	0.03	-0.11	-0.10	-0.09	-0.006	
Europe	Kalixaelven	0.004	-0.001	0.004	0.000	0.48	0.51	0.03	-0.13	-0.10	0.03	-0.125
	Thames	-0.009	-0.001	-0.022	-0.004	0.26	0.25	0.00	-0.20	-0.18	-0.06	-0.118
	Rhine	-0.011	-0.010	-0.015	-0.012	0.40	0.39	-0.06	-0.14	-0.12	-0.07	-0.043
	Danube	-0.010	-0.006	-0.017	-0.006	0.45	0.45	0.08	-0.09	-0.07	0.00	-0.063
	Volga	-0.015	-0.016	-0.015	-0.019	0.35	0.35	-0.02	-0.32	-0.27	-0.14	-0.133
Ebro	-0.032	-0.011	-0.075	-0.013	0.29	0.28	-0.07	-0.36	-0.29	-0.13	-0.167	
South America	Magdalena	-0.012	-0.008	-0.016	-0.008	0.21	0.21	0.01	0.00	-0.01	0.00	-0.003
	Amazon	-0.010	-0.009	-0.011	-0.009	0.19	0.19	0.02	-0.04	-0.04	-0.04	-0.005
	Araguaia	-0.021	-0.022	-0.013	-0.016	0.30	0.32	-0.03	-0.11	-0.11	-0.11	0.002
	Parana	-0.023	-0.027	-0.021	-0.031	0.27	0.29	-0.05	-0.19	-0.16	-0.18	0.015
Africa	Nile	-0.029	-0.033	-0.023	-0.035	0.38	0.39	0.12	-0.13	-0.12	-0.14	0.026
	Niger	0.000	-0.008	0.015	-0.006	0.27	0.28	0.28	-0.09	-0.06	-0.10	0.032
	Shabelle	-0.017	-0.018	-0.006	-0.006	0.23	0.24	0.27	-0.12	-0.12	-0.11	-0.013
	White-Volta	-0.005	-0.019	0.044	0.000	0.17	0.21	-0.08	-0.12	-0.10	-0.14	0.033
	Congo	-0.023	-0.024	-0.028	-0.034	0.28	0.28	0.05	-0.29	-0.24	-0.27	0.032
	Zambesi	-0.013	-0.007	-0.009	0.001	0.20	0.19	0.22	0.10	0.08	0.10	-0.020
	Cunene	-0.007	0.018	-0.028	0.036	0.22	0.18	0.21	0.16	0.14	0.19	-0.057
Orange	-0.036	-0.030	-0.064	-0.025	0.27	0.26	0.13	-0.54	-0.40	-0.36	-0.034	
South Asia	Brahmaputra	0.007	0.003	0.007	0.003	0.21	0.21	-0.05	-0.02	-0.02	-0.03	-0.010
	Ganges	0.009	0.004	0.011	0.007	0.14	0.14	-0.01	0.08	0.07	0.07	-0.002
	Godavari	0.009	0.006	0.014	0.014	0.05	0.05	-0.02	0.16	0.15	0.16	0.015
	Karnali	0.000	-0.007	0.003	-0.004	0.30	0.28	-0.01	0.04	0.04	0.02	-0.018
Australia	Murray	-0.020	-0.032	-0.032	-0.029	0.30	0.31	-0.28	-0.18	-0.14	-0.16	-0.028



3.3 Trends in precipitation, snowfall and 2m temperature

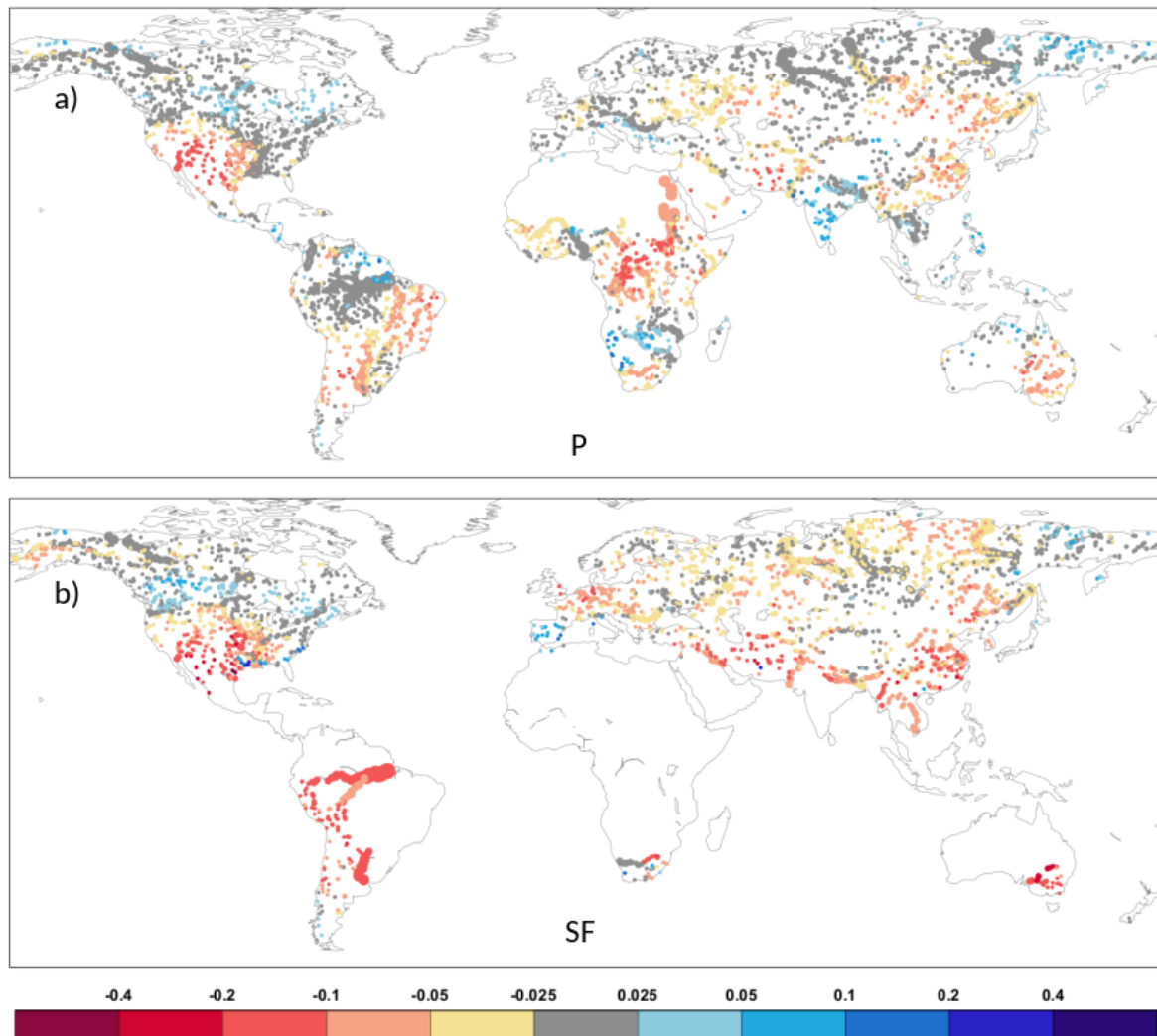


Figure 7. Raw linear trends (fraction/decade) at global river catchments for ERA5 a) Precipitation (P) and b) Snowfall (SF), based on the 1981-2018 period. The circles represent the catchment outlets, while their size the catchment area.

Precipitation shows the same trend signs to river discharge over much of the world (Figure 7a). The raw linear trend magnitudes are generally smaller than in river discharge, but a lot of the differences are in fact related to the larger M-term in Eq. 1, as precipitation is generally much larger than river discharge. The standardised linear trends highlight (see Table A1 for the selected global catchments in Appendix B) that in tropical and subtropical areas of the world, including Africa, Central and South America, South Asia and Australia, precipitation and river discharge trends are very similar, while over the Northern Extratropics river discharge trends tend to be more pronounced than precipitation.

The largest linear trends (both raw and standardised) in precipitation are for the Colorado and Rio Grande basins in the United States and also the Congo and upper Nile basins in Central Africa, where the negative raw trend is between -0.1 and -0.2 (10-20% decrease in just 10 years, see also the P column in Table 2; or over 0.5 standard deviation of the annual mean time series sample, see Table A1 with the standardised trends).

Although some of the tropical and subtropical basins, mainly the rivers downstream of the Andes in South America and areas in South Asia, show clearly more negative trends, the snowfall contribution to precipitation is usually very little in those areas (Figure 7b). On the other hand, in the more snow dominant higher latitude areas of the Northern Hemisphere, some areas such as Alaska, central parts of Europe or northern parts of Russia, there is a moderate tendency to more negative trends.

The main reason for the decreasing snowfall is very likely to be the generally increasing temperature. Figure A1 in the Appendix A highlights that the 2m temperature trend is positive almost everywhere. The largest positive trends, above 0.4 degree change in 10 years, are in the Nile basin in Africa, the southwest part of the USA, the eastern parts of Europe, the Middle-East and also many of the smaller rivers in the northern-most latitudes. Trends in ERA5 and ERA5-Land are generally similar, if anything, ERA5-Land tends to be slightly warmer (see the annual mean time series for the selected global river basins in Appendix C), but the trends are almost the same everywhere. These differences can originate from the snow cover and evaporation processes which can differ in coupled (ERA5) vs offline (ERA5-Land) systems.

These large global temperature increases in ERA5 are consistent with the scientific literature (e.g. Hansen et al., 2006; Parmesan and Yohe, 2003, IPCC, 2007 and 2014).

It is difficult to determine how realistic the identified ERA5 precipitation and snowfall trends are, due to the sparse precipitation observing network and the highly variable quality of the satellite derived precipitation data (Sun et al., 2018).

The AR4 (IPCC, 2007) and AR5 (IPCC, 2014) IPCC reports disagree on precipitation trends in many parts of the world, the worst being West Africa where significant positive (AR4) trends turn to significant negative (AR5). Part of the reason is the different periods (1979-2005 in AR4 - Figure 3.13 vs. 1951-2010 in AR5 - Figure 1.1), however, the shortness of the first period (through capturing more of the natural climate variability as trends) and the differences between the used data sets must have also contributed. The estimation uncertainties in precipitation changes were acknowledged in the AR5 report when it concluded that 'Confidence in precipitation change averaged over global land areas since 1901 is low prior to 1951 and medium afterwards'. In fact, neither of the two IPCC reports are similar to the ERA5 precipitation linear trends presented here. In particular, there is no clear sign of either of the two most prominent trend areas in ERA5. While the southwestern USA is represented in AR4, although with smaller negative values in AR4 than in ERA5 (3-10% vs. 10-20%), the large negative ERA5 trends in central Africa are not there in any of these two sources.

Nguyen et al. (2018) analysed precipitation trends with satellite derived data in the 1983-2015 period, which is directly comparable with our period. They concluded that although only few percent of the land mass show pixel-by-pixel significant trends, this increases by regional- or catchment-based analysis, but even on the large catchment-scale (over 200 large rivers), only a smaller fraction has significantly large trends. The catchment-scale precipitation trends in Nguyen et al. (2018) show a lot of similarities, at least in sign, to the ERA5 precipitation linear trends in Figure 7a. For example, the trend patterns are similar in most parts of Australia, Central and South Africa, South America, but also in Europe and large parts of Asia. Major differences are present mainly in Central America, around Canada and also Central Asia where the trends show mainly opposite signs between ERA5 (Figure 7a) and the satellite-derived precipitation in Nguyen et al. (2018).

The dominantly decreasing trend in ERA5 is not supported by either of GPCP or GPCP, two of the available global precipitation estimate data sets, as described in Hersbach et al. (2020; see Figure 23). ERA5 seems to produce more precipitation than either GPCP or GPCP, and the difference gets smaller from 2000. It seems, after the large decline around 2000-2002 (see also Figure 5), the ERA5 precipitation is more realistic in the 21st century, which could potentially come from some changes in the used satellite data in ERA5. Nevertheless, further analysis is going to be needed in the future to better understand the behaviour of the ERA5 precipitation changes.

3.4 Trends in runoff and snowmelt

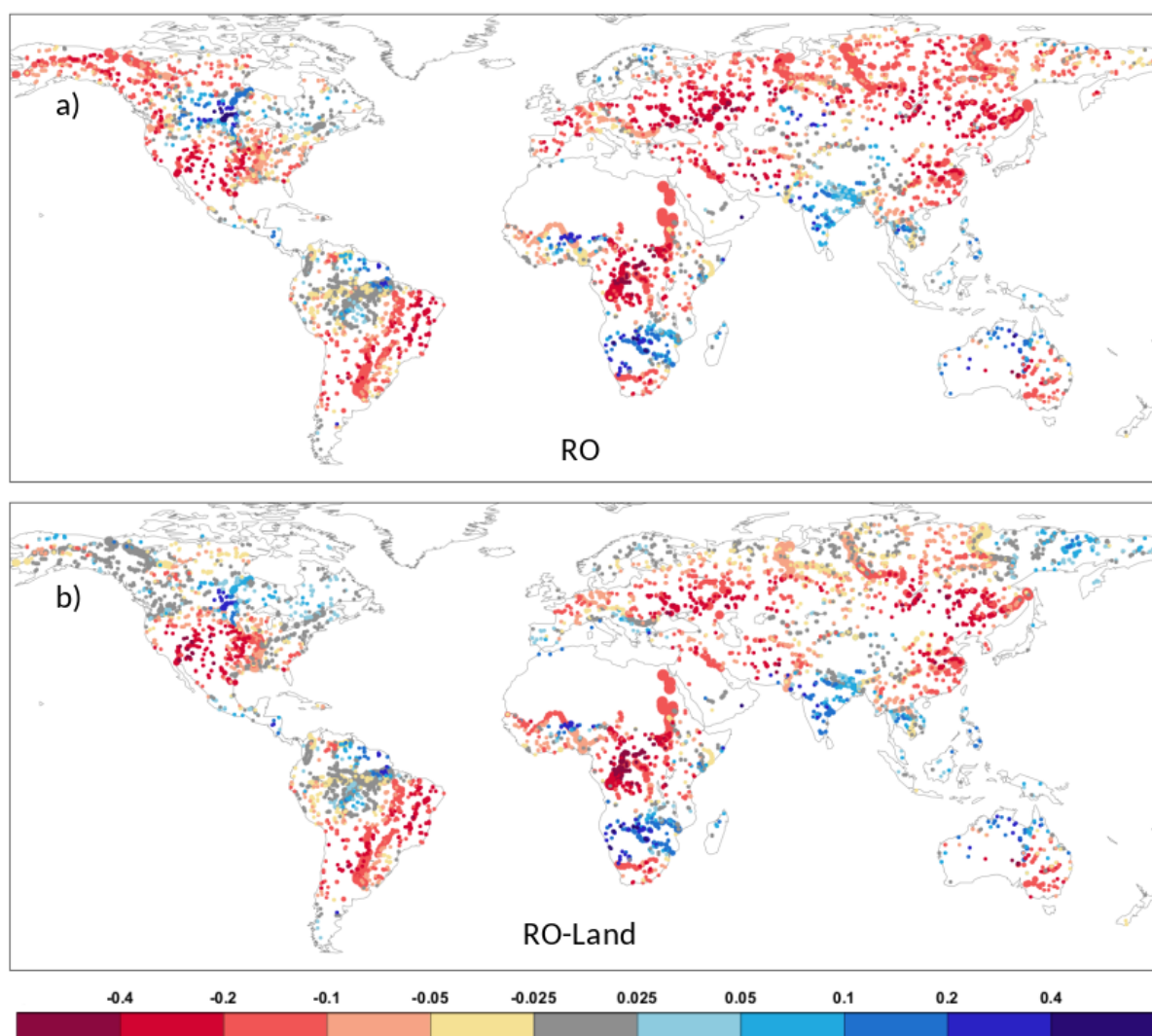


Figure 8. Raw linear trends (fraction/decade) at global river catchments for runoff in a) ERA5 (RO) and b) ERA5-Land (RO-Land), based on the 1981-2018 period. The circles represent the catchment outlets, while their size the catchment area.

The linear trends for runoff in ERA5 (Figure 8a) are almost identical to the GloFAS-ERA5 river discharge trends (Figure 6). This is expected, as the annual mean values of these two variables can usually differ only little, the river routing's time delay is averaged out by computing the mean over the whole year. However, the trends for runoff in ERA5-Land (figure 8b) are different from ERA5 in the

Northern Extratropics, namely the ERA5 trends are more negative in Alaska, western Canada and most of northern Eurasia. As the atmospheric forcing are the same in ERA5 and ERA5-Land, and the land-surface model is also mainly the same, differences in runoff and other surface variables will come from the missing coupling and land data assimilation and the much higher resolution and lapse-rate correction in ERA5-Land. The land data assimilation impact on the hydrological cycle can be substantial, considering both snow and soil moisture, as shown in Zsoter et al (2019), and the resolution change, through the different temperature conditions with the lapse rate correction, is also expected to have a potentially large impact.

As the ERA5 and ERA5-Land runoff trends are very similar in the tropics and subtropics (see Figure 8 and also the bottom half of Table 2 and A1), the likely culprit for the differences in the higher latitudes is the handling of the snow with the possible differences in snowmelt.

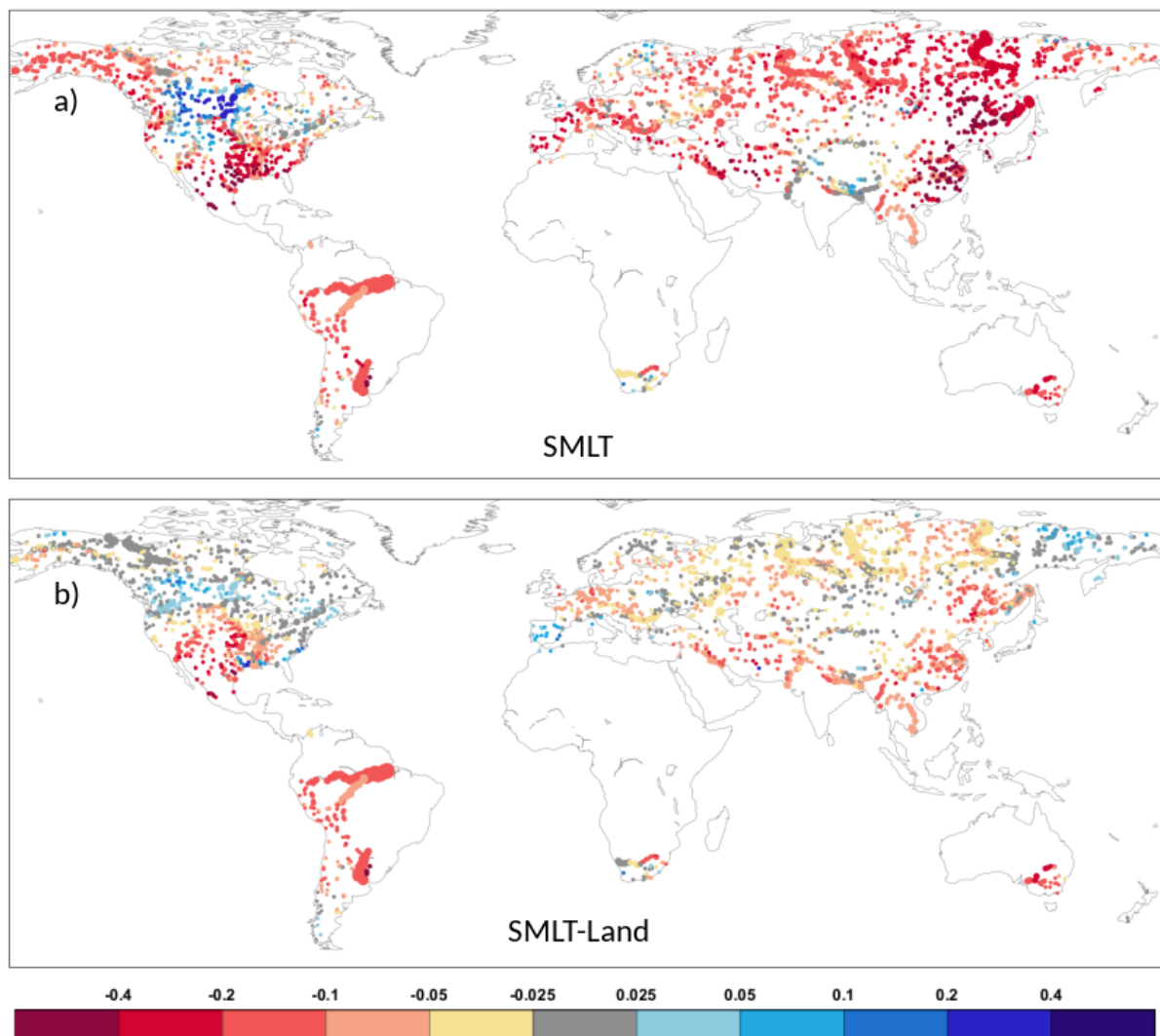


Figure 9. Raw linear trends (fraction/decade) at global river catchments for snowmelt in a) ERA5 (SMLT) and b) ERA5-Land (SMLT-Land), based on the 1981-2018 period. The circles represent the catchment outlets, while their size the catchment area

The runoff raw linear trend differences seem to come from snowmelt which are very different in ERA5 (Figure 9a) and ERA5-Land (Figure 9b). The snowmelt trends in ERA5 are much more negatively oriented in the Northern Extratropics such as the Lena, Amur (in Russia) or the Yukon (in Alaska) rivers. The exceptions are the central part of North America and some catchments in Northern Europe and near the Himalaya, where ERA5 has more positive trends (see the Churchill and Thames rivers in Table 2 and A1; SMLT columns), where snowmelt appears to have increased in the last ~40 years in ERA5. These ERA5 snowmelt linear trends can be partially explained by the changes in snowfall, i.e. the amount of snow available to melt, as the sign of the snowfall and snowmelt trends is the same over large parts of the world. However, the magnitude is clearly different in the Northern Hemisphere, with the snowmelt trends being lot more pronounced.

The scientific literature has documented trends in the snowpack related variables (snowfall, snow depth, snow cover) extensively. Studies are either based on available in situ observations, or satellite derived measurements. However, only snow cover extent (e.g. the IMS snow cover product used at ECMWF) seems to be reliable enough to be used quantitatively from satellites and snow water equivalent (SWE) and snowdepth (SD) have higher uncertainty and thus offer limited help (Hancock et al. 2013).

The 5th IPCC report states that there is very high confidence that the extent of Northern Hemisphere snow cover has decreased since the mid-20th century (IPCC, 2013, see Figure SPM.3). The declining snow cover is strongly related to the increasing global temperatures.

For example, Kunkel et al. (2016) provided a summary of several snow climatology studies and also found a strong decrease in maximum seasonal snow depth in the studied North America and Europe. Connolly et al. (2019) evaluated the snow cover extent trends in the Northern Hemisphere based on the Rutgers University snow cover dataset and found that the trend in the satellite-derived observations are poorly explained by the CMIP5 climate models, the models exhibiting a steadier decline during the 1967-2018 period. In our study no snow cover extent is analysed, however, both the snow water equivalent and snowmelt similarly show a steady decline over the global land areas in Figure 5, at least until 2004. Similarly, Knowles (2015) evaluated the trends in the GHCND climate observations for snow related variables in the 1950-2010 period for the United States. It was found that both snowfall and snow depth showed more negative than positive trends, which is in agreement with our analysis, even though the geographical distribution of their trends is different to the linear trends documented for snowfall and also for snowmelt in this study (Figure 7b and 9).

It can be concluded that the ERA5-Land runoff linear trends (the signs at least) are generally similar to the precipitation trends everywhere in the world. In ERA5, however, the runoff (and thus river discharge) trends seem to be dominated by precipitation in the tropics and subtropics, while the trends in higher latitudes resemble the snowmelt trends, as a consequence of the additional land data assimilation (see the SMLT and RO columns in Table 2 and A1). Note that the attribution of the ERA5/ERA5-Land trend differences to the observed and simulated trends in existing studies, and also the interpretation of these global and regional differences, were beyond the scope of this study, but would be a very important further piece of analysis.

3.5 Trends in evaporation, precipitation minus evaporation and soil moisture

The evaporation (E) and the two soil moisture variables (top 0-7 cm, SWV7 and top 0-100 cm, SWV100 layers) all show smaller raw linear trends for both ERA5 and ERA5-Land (Figure A2 and A4-5). The

smaller trend magnitudes mainly come from the much larger volume in these variables, thus a larger M term in Eq. 1 and thus a smaller trend magnitude (T) in relative terms. This is supported by Table A1 in Appendix B which shows that the standardised trends, defined by using the standardised variables, are generally in the same magnitude range as the other variables. More noticeable trends (both raw and standardised) are present e.g. in the Nile basin and Middle East regions or the southwestern United States area for evaporation and the soil water content variables.

The scientific literature agrees that during the last few decades the global land evaporation has generally increased (e.g. Jung et al. 2010; Zhang et al. 2016; Anabalon and Sharma et al. 2017). However, there seems to be evidence that this stopped in the 1998-2008 period (Jung et al. 2010), and then evaporation is relatively stable since (Javadian et al. 2020).

In contrast, the ERA5 and also ERA5-Land global land average evaporation trend (in Figure 5) is more positive than negative, somewhat contrary to the literature (showing slightly decreasing absolute values). However, the first period shows a small increase until 1998, followed by a marked decrease and then mainly no change in the last 10 years which is broadly similar to what is reported in the literature.

ERA5/ERA5-Land agrees with the large negative evaporation trends shown by Zhang et al. (2016) in the Middle East, western United States and the generally positive trends in the northern latitudes and also in Southeast Asia. However other areas show marked differences, especially parts of Africa and much of Australia.

Soil moisture has been shown to be generally decreasing in the last few decades by several studies (e.g. Feng and Zhang et al. 2016; Albergel et al 2013; Pan et al. 2019; Dorigo et al. 2012), agreeing with the dominantly negative trends documented in this study. About 30% of land is shown to have significant trend in these studies, a majority of being negative. However, there are large differences in the actual pattern depending on the data set used. For example, as shown in Albergel (2013), the ERAI-Land, MERRA-Land and SM-MW (a microwave-based multisatellite surface soil moisture dataset) all show marked differences in the trend patterns. Similarly, the ERA5 and ERA5-Land soil moisture trends show notable similarities to the SM-MW trends only in Central Asia, the Middle East, central South America, otherwise the match is poor.

The precipitation minus evaporation (P-E), i.e. the water source to the land-surface, and the two analysed soil moisture variables show roughly similar trend signs (see Figure A3-5). Moreover, ERA5 and ERA5-Land are broadly similar for all these four variables and only exhibit a few regional variations, most notably in Africa where they change noticeably in ERA5-Land. This happens over areas like the Niger, White-Volta and Cunene rivers, where evaporation even changes trend sign from negative to positive (Niger, White-Volta), which actually means decreasing amount of water leaving the land-surface through evaporation, as evaporation is dominantly negative over the world, or the Cunene river where evaporation changes from positive to negative, or the Nile river where the positive trend gets more pronounced, all these changes coinciding with also large swings in soil water content (see Table 2 and A1; the E, TP-E, SVW7 and SWV100 columns).

3.6 Trends in observed river discharge

The obvious question about the large trends in GloFAS-ERA5 river discharge is whether they are also present in the observations. Figure 10 highlights the match between the simulated and observed raw linear river discharge trends.

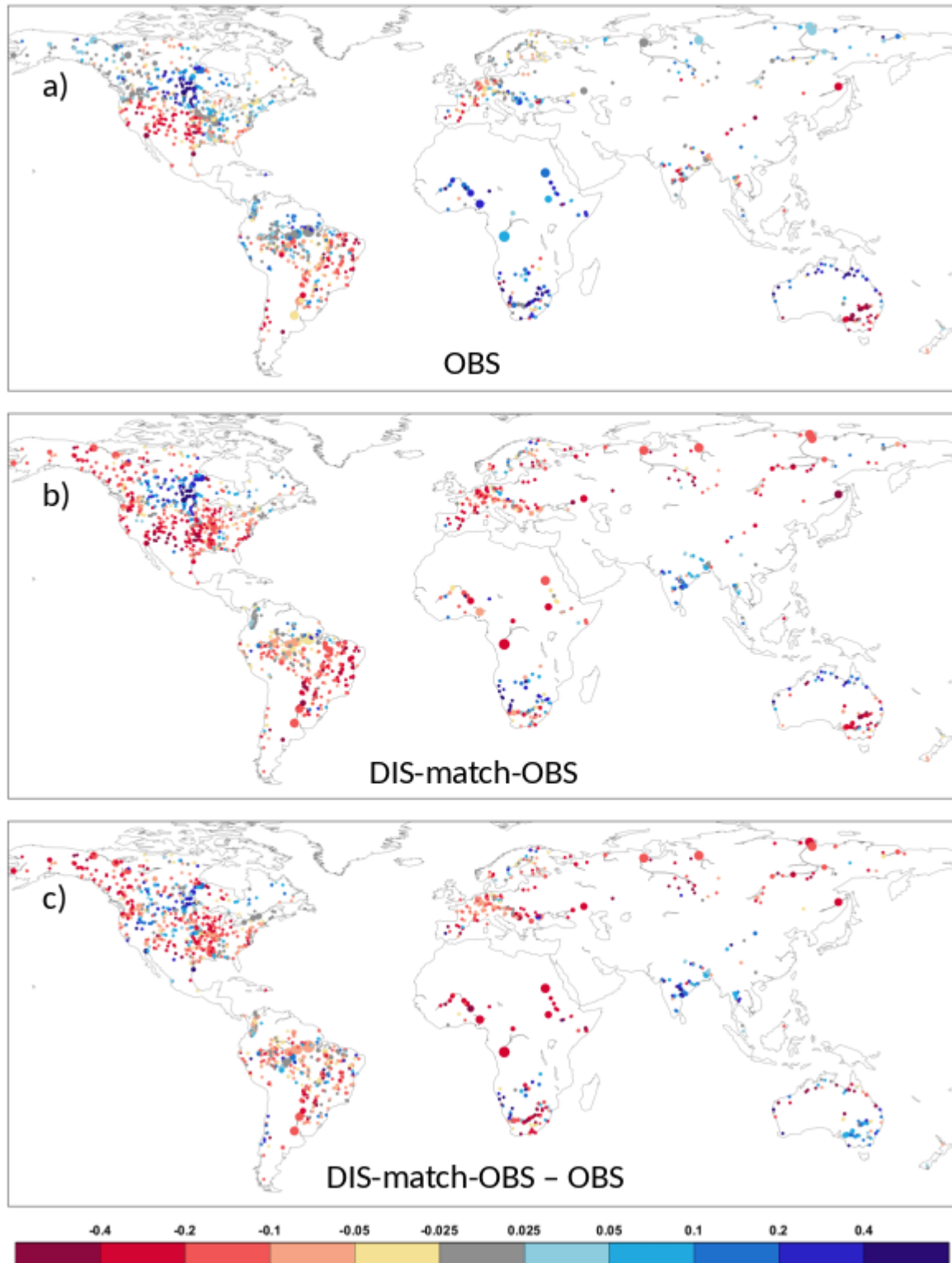


Figure 10. Raw linear trends (fraction/decade) at global river catchments for a) river discharge observations (OBS), b) GloFAS-ERA5 river discharge matching the available observations (DIS-match-OBS) and c) the difference (DIS-match-OBS minus OBS) catchments that have at least 16 years of available observations based on the 1981-2018 period. The circles represent the catchment outlets, while their size the catchment area.

The observed trends (Figure 10a) show a mixed picture with few more positive than negative changes. Almost all catchments show positive trends in Africa (Congo, Nile, Niger, Orange rivers), but also many in Russia, Canada, northern Australia and some in Amazonia (see for trend details in Table 2; OBS).

Other scientific studies, for example Su et al. (2018) or Dai et al. (2009) found similar results after analysing hundreds of the world's largest ocean-reaching rivers with mixed positive and negative trends. Although the main emphasis of their trends is shifted to generally more rivers showing negative than positive trends, this could likely be related to the different period (1948-2004) or the different geographical distribution of the analysed catchments.

In contrast, the GloFAS-ERA5 linear trends are dominantly negative, even though these trends are calculated over the exact same periods as for the observations. The observation-matched-period-based GloFAS-ERA5 raw linear trend (Figure 10b) can be quite different to the 38-year-based version in Figure 6, but the overall pattern is the same in both. The GloFAS-ERA5 trends are dominantly negative, while the observation trends are more positive than negative, therefore the difference between them is overwhelmingly negative (Figure 10c). This can be demonstrated by the rather different colours in Table 2 and A1 (columns of OBS and DIS-m as abbreviated from DIS-match-OBS), the simulation trend being dominantly orange (negative), while the observation trend is blue (positive). Clusters of positive differences (i.e. observations have a stronger tendency to increase) can mainly be seen in South-Asia, southern Australia and parts of central North America.

The trends in the GloFAS-ERA5 river discharge are thus only a poor match for the trends of the available observations. Apart from the likely reason of the unrealistic trends in the ERA5 forcing, some of this can be explained by the inadequate handling of the human influence in GloFAS-ERA5, which in some areas can have very large impact on river discharge, even though this is not necessarily will impact the sign of the trends. For example, see the Nile river in Appendix C, which has observed river discharge that is only a fraction of the GloFAS-ERA5 value. A large part of this comes from the fact that the river is highly regulated with also irrigation being important in the area.

3.7 Trend error comparison ERA5 vs ERA5-Land

It was shown earlier that the ERA5 and ERA5-Land snowmelt trends are markedly different in the Northern Hemisphere higher latitudes, which then directly influences the runoff trends. The error of ERA5 and ERA5-Land runoff raw linear trends, computed against the observed river discharge raw linear trends, are compared in Figure 11 (the raw trend values are shown in Table 2, while the standardised trends in A1 for selected catchments, with green and purple colours). It shows the difference of the absolute trend errors, with blue (green in Table 2 and A1) catchments showing where the ERA5 runoff trends are closer to the observed trends, while red (purple in Table 2 and A1) showing where the ERA5-Land trends are closer. It is clear that, due to the large difference in snowmelt, the ERA5-Land runoff linear trend is clearly closer to the observed trends in the higher latitudes (see the

dominantly green cells in Table 2 and A1, ROM/Imp column, over North Asia, North America and Europe). However, in the tropical and subtropical areas, and also in the central part of the United States, ERA5 is closer to the observations or the two have similar trends (see in Table 2 and A1 the slightly more purple colours over South America, Africa, South Asia and Australia).

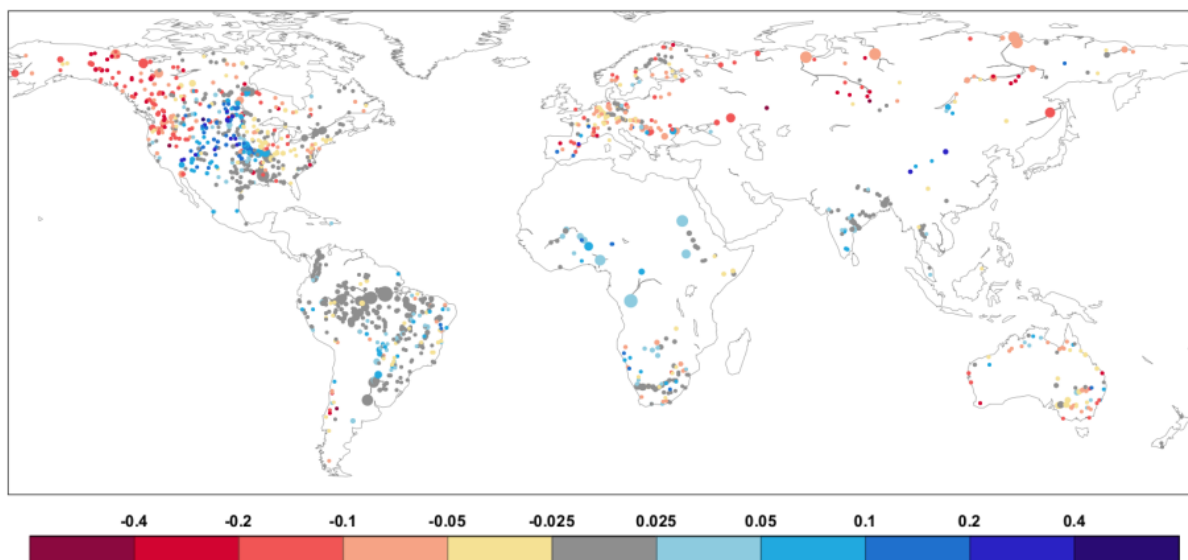


Figure 11. Difference between ERA5-Land and ERA5 absolute raw linear trend errors (simulated trend minus observed trend; fraction/decade) at catchments that have at least 16 years of available river discharge observations based on the 1981-2018 period. The circles represent the catchment outlets, while their size the catchment area.

3.8 ERA5 and ERA5-Land trends in 1981-2003 and 2004-2018

In this section the trend is compared in the two subperiods, 1981-2003 (period1, 23 years) and 2004-2018 (period2, 15 years), after removing the impact of the IMS satellite snow cover caused discontinuity in the time series.

The linear trends are generally different in the two periods, and usually larger for period2, although this shorter period would be expected to show larger random variability anyway. Figure 12 shows the raw linear trends for a few variables, while Table 3 highlights them for several variables for the selected global rivers, similarly to Table 2 and A1 (for location see Figure 4).

For precipitation, the rivers in southwestern United States, eastern South America, central Africa, the Middle East and eastern Australia stand out with their large negative trends in period1 (Figure 12a). In fact, these trends are very similar to the original 38-year trends in Figure 8a, for the majority of the world, especially for the stand-out negative areas. The second part of the 38-year period, on the other hand, does seem to show less stand-out geographical areas, the picture more mixed, even though the trend values are quite large, likely related to the shortness of the period. For snowmelt (Figure 12c-d) the same is valid.

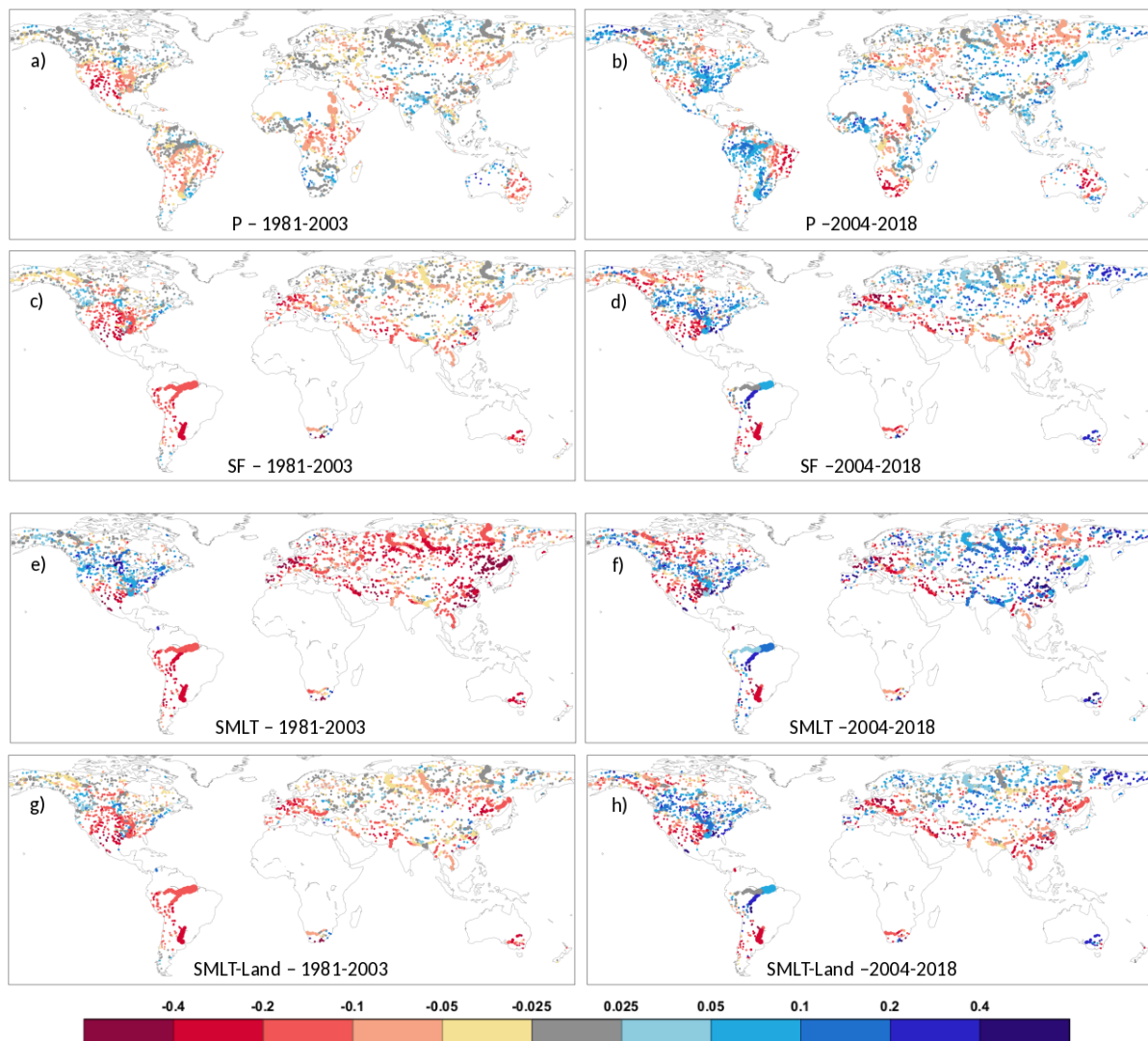
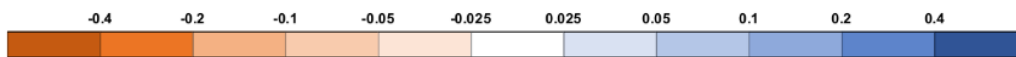


Figure 12. Raw linear trends (fraction/decade) at global river catchments for 1981-2003 (left column) and 2004-2018 (right column) for ERA5 precipitation (a-b), snowfall (c-d) and for ERA5 (e-f) and ERA5-Land (g-h) snowmelt. The circles represent the catchment outlets, while their size the catchment area.

Regarding snowmelt, the behaviour of ERA5 (Figure 12e-f) and ERA5-Land (Figure 12g-h) clearly differ, even after splitting the 38-year period in two. While period 2 behaves similarly for both (compare Figure 12f and 12h), the magnitude of the linear trends is in the same range, period1 shows larger differences between ERA5 and ERA5-Land (compare Figure 12e and 12g), Eurasia is more negative, while North America is somewhat more positive. This is also visible amongst the selected catchments in Table 3 (SMLT and SMLT-Land columns), where the 1981-2003 column for ERA5 is more orange than for ERA5-Land over Europe and North Asia, and generally more blue areas for North America. The pronounced differences between the ERA5 and ERA5-Land snowmelt for period1 suggests that the snow assimilation likely plays a role in producing the negative trends even before the introduction of the IMS snow product in 2004.

Table 3. Raw linear trends (fraction/decade) for selected catchments (see Figure 4) for two periods, 1981-2003 and 2004-2018, for GloFAS-ERA5 river discharge (DIS), runoff for ERA5 (RO) and ERA5-Land (RO-Land), precipitation (P), snowfall (SF) and snowmelt for ERA5 (SMLT) and ERA5-Land (SMLT-Land). Empty cells correspond to cases for which trend computation was not possible. Coloured cells indicate negative (orange) and positive (blue) trends. Where there is no raw linear trend, defined for absolute values less than 0.025, cells are not coloured. Darkening shades show increasing trend magnitudes. For location of the catchments see Figure 4.

Rivers		DIS		RO		RO-Land		P		SF		SMLT		SMLT-Land	
		1981-2003	2004-2018	1981-2003	2004-2018	1981-2003	2004-2018	1981-2003	2004-2018	1981-2003	2004-2018	1981-2003	2004-2018	1981-2003	2004-2018
North Asia	Ob	-0.13	0.01	-0.10	0.00	0.00	0.01	0.01	0.01	-0.03	0.04	-0.20	0.06	-0.03	0.03
	Yenisei	-0.13	-0.16	-0.12	-0.12	-0.06	-0.14	-0.02	-0.07	-0.04	0.00	-0.18	0.10	-0.05	0.02
	Lena	-0.18	-0.19	-0.13	-0.17	-0.07	-0.17	-0.01	-0.07	-0.01	-0.04	-0.14	-0.06	-0.02	-0.04
	Amur	-0.28	0.21	-0.23	0.15	-0.20	0.09	-0.06	0.06	-0.08	-0.16	-0.47	0.09	-0.14	-0.15
North America	Yukon	-0.03	0.07	-0.03	0.10	-0.04	0.12	-0.02	0.08	-0.03	-0.06	0.02	0.01	-0.03	-0.07
	Mackenzie	0.00	-0.27	0.00	-0.19	0.00	-0.08	0.00	-0.01	-0.04	-0.08	0.01	-0.15	-0.04	-0.05
	Churchill	0.65	-1.14	0.29	-0.53	0.04	-0.10	0.01	-0.02	-0.14	0.03	0.03	-0.17	-0.17	0.06
	Columbia	-0.02	0.14	-0.02	0.12	-0.07	0.17	-0.07	0.04	0.01	0.06	0.10	0.09	0.01	0.09
	Colorado	-0.62	-0.64	-0.56	-0.52	-0.68	-0.47	-0.27	-0.10	-0.22	-0.29	-0.20	-0.28	-0.22	-0.28
	Mississippi	0.01	0.13	-0.01	0.15	-0.12	0.22	-0.06	0.09	-0.12	0.07	0.08	0.03	-0.12	0.09
Europe	Kalixaelven	-0.27	0.61	-0.20	0.45	-0.03	0.12	-0.01	0.03	0.01	0.09	-0.13	0.55	0.01	0.19
	Thames	-0.07	0.39	-0.07	0.36	0.03	0.37	0.02	0.02	-0.67	0.21	-0.94	-0.09	-0.65	0.17
	Rhine	-0.11	0.16	-0.09	0.13	-0.07	0.04	-0.02	-0.03	-0.19	-0.18	-0.37	0.02	-0.18	-0.13
	Danube	-0.07	-0.04	-0.07	-0.08	-0.05	-0.11	0.01	-0.03	-0.09	-0.12	-0.15	-0.12	-0.10	-0.13
	Volga	-0.32	-0.11	-0.27	-0.10	-0.11	-0.11	-0.03	-0.06	0.01	0.05	-0.14	0.04	0.00	0.03
South America	Ebro	-0.21	0.52	-0.16	0.42	-0.14	0.33	-0.01	0.17	-0.06	0.12	-0.19	0.60	-0.08	0.14
	Magdalena	-0.03	-0.17	-0.04	-0.17	-0.05	-0.17	-0.03	-0.11						
	Amazon	-0.03	0.10	-0.03	0.10	-0.03	0.11	-0.02	0.06	-0.15	0.07	-0.17	0.10	-0.16	0.07
	Araguaia	-0.16	-0.33	-0.15	-0.29	-0.17	-0.28	-0.08	-0.09						
Africa	Parana	-0.12	0.11	-0.11	0.07	-0.12	0.09	-0.05	0.05	-0.21	-0.26	-0.23	-0.26	-0.21	-0.26
	Nile	-0.12	-0.01	-0.12	-0.04	-0.14	-0.05	-0.07	-0.07						
	Niger	-0.01	0.09	0.00	0.08	-0.02	0.08	0.00	0.08						
	Shabelle	-0.13	-0.04	-0.13	-0.04	-0.13	-0.05	-0.09	0.03						
	White-Volta	0.26	0.54	0.22	0.46	0.17	0.51	0.00	0.17						
	Congo	-0.24	-0.16	-0.20	-0.16	-0.23	-0.17	-0.08	-0.05						
	Zambesi	-0.05	0.30	-0.03	0.20	0.01	0.21	-0.02	0.01						
	Cunene	0.22	-0.31	0.20	-0.29	0.26	-0.16	0.10	-0.05						
South Asia	Orange	0.17	-0.53	0.08	-0.42	0.08	-0.43	0.00	-0.22	-0.07	-0.15	-0.09	-0.09	-0.07	-0.14
	Brahmaputra	0.01	0.03	0.01	0.03	0.01	0.01	0.00	0.01	-0.02	-0.06	-0.04	0.06	-0.02	-0.09
	Ganges	0.12	0.12	0.10	0.11	0.12	0.10	0.05	0.04	-0.03	-0.04	-0.04	0.18	-0.01	-0.03
	Godavari	0.07	0.10	0.07	0.09	0.10	0.11	0.06	0.01						
Australia	Karnali	0.07	0.11	0.07	0.11	0.06	0.10	0.04	0.05	-0.04	-0.09	-0.04	0.03	-0.03	-0.06
	Murray	-0.22	0.38	-0.17	0.19	-0.23	0.12	-0.10	-0.05	-0.19	0.21	-0.27	0.23	-0.19	0.22



4 Conclusions

This study has analysed the GloFAS-ERA5 river discharge reanalysis data set, the related ERA5 and ERA5-Land surface variables, and the available river discharge observations, for noticeable changes in the time series characterised by linear trends, in the 38-year period of 1981-2018, also including the 1981-2003 and 2004-2018 subperiods. It was found that the river discharge simulation shows a dominantly negative change across the world during 1981-2018, with some major world rivers having quite substantial decrease (Yenisei, Volga, Congo, Amur, Colorado, Yukon, Nile, Lena, Yellow, see Table 2 and A1).

The river discharge observations do not support such dominantly negative linear trends, and although varied, observations show overall more positive than negative changes in the 38-year period. The scientific literature generally documents a similar behaviour to the observational trend analysis

presented here, with mixed trends globally, but with slightly more major rivers showing negative than positive changes in river discharge during the period of 1948-2004 (Su et al., 2018; Dai et al., 2009).

The linear trends in GloFAS-ERA5 seem to be driven by changes in precipitation over the tropical and subtropical areas of the world, with the snowmelt changes showing a very strong influence in determining the river discharge trends in the northern latitudes of the Northern Hemisphere. The reason for this atypical behaviour in the northern latitudes is likely to be related to changes in the snowmelt producing processes, including the snow assimilation.

The snowmelt exhibits a pronounced negative linear trend in large parts of the world in ERA5, while this is not present in ERA5-Land. This suggests that the negative trends are, at least partially, related to the snow assimilation tendency to remove water from the water cycle as a consequence of the suboptimal snow scheme in HTESSEL (Zsoter et al. 2019). Some of the issues stem from the use of the IMS snow product from 2004 in the snow assimilation, which creates a discontinuity in the ERA5 time series (see Figure 5).

It has to be acknowledged that such discontinuity can make any trend analysis unreliable. However, as Figure 5 suggests, the snow evolution in ERA5 and ERA5-Land seems to be more complex than a single discontinuity in 2004, so linear trends can still deliver valuable information even on the whole 1981-2018 period.

After splitting the period into 1981-2003 and 2004-2018 and removing the impact of this discontinuity on the linear trends, it could still be shown, that even in the first subperiod of 1981-2003 there is a large area globally with significant negative snowmelt trends in ERA5, mainly in Asia and Europe, which is not present in ERA5-Land. This highlights that there should be other contributing factors in generating such negative trends in the ERA5 snowmelt, other than just the introduction of the IMS satellite product. Potentially the generally lower temperatures in mountains due to the higher orography in ERA5-Land could also contribute to this by decreasing the snowmelt amount compared with ERA5.

Two particularly interesting areas with the largest linear trends, that were highlighted by this study, are the central region of Africa (e.g. Congo and Nile river basins), and the southwestern part of the United States (e.g. Colorado river basin). Both these areas show very dominant and large negative trends both in precipitation and river discharge, but also in runoff by not just ERA5 but also equally by ERA5-Land. However, based on the limited analysis of the scientific literature, there was no indication of such strong precipitation trends in the explored studies, and similarly no such large trends were shown either in the river discharge observations available in this study.

It will require more work in the future to better identify the underlying reasons for these very dominant negative trends. Moreover, it would also be beneficial to repeat the analysis including an improved precipitation observation data set, preferably one that is high quality and merges several of the available gauge- and/or satellite-based data sets, such as the MSWEP (Beck et al., 2019), or the latest bias corrected ERA5 data set, WFDE5 (Cucchi et al. 2020). This would allow us to directly evaluate the quality of the ERA5 trends against the best available observation estimates.

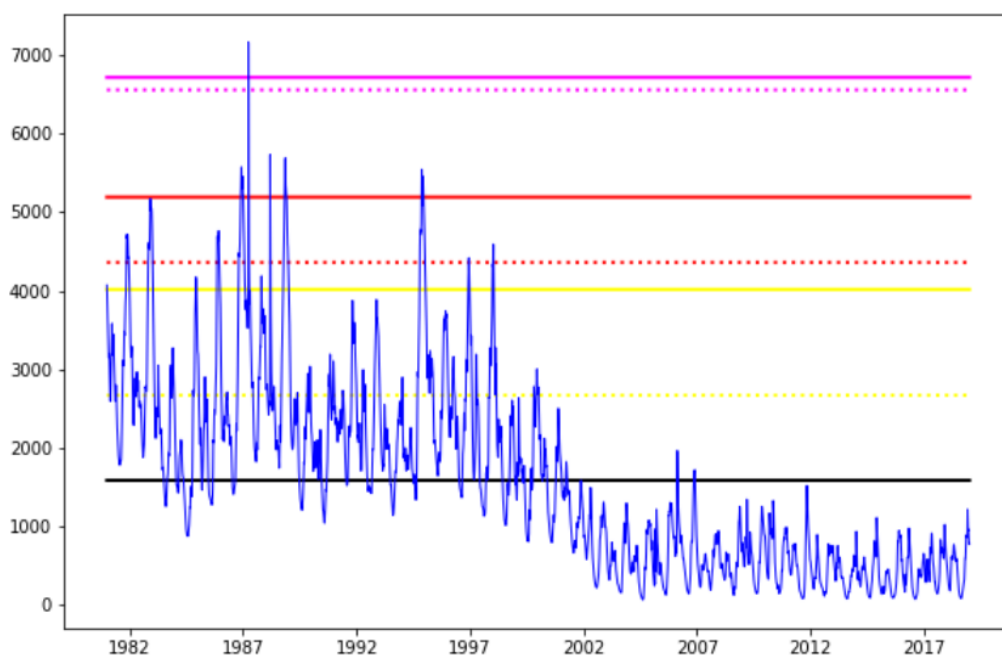


Figure 13. Example of the daily GloFAS-ERA5 river discharge (m^3/s) time series for an upstream catchment in the Congo river basin and the 2- (yellow lines), 5- (red lines) and 20-year (magenta lines) flood thresholds based on two different fitting methods. The dashed lines represent the flood thresholds fitted using all annual maxima, while the solid lines were produced using only annual maxima over the sample mean discharge shown by the black line.

A potential driver of the exposed ERA5 trends is the method of production: ERA5 is produced in several streams that were later merged into one consolidated data set. These streams have a year overlap to allow for long enough spin-up. According to Hersbach et al. (2020), in the deep soil, where spin-up can take several years, discontinuities could be observed. The deep soil can certainly impact on the runoff through the sub-surface runoff, which can impact on river discharge, however, it is not expected to have any noticeable impact on variables such as precipitation or evaporation which vary on a significantly shorter timescale.

The GloFAS-ERA5 linear trends, presented here, have a direct impact on the quality of the GloFAS flood warnings through the use of the flood thresholds. The presence of significant trends, or a very substantial regime change, such as in the example provided in Figure 13, makes it difficult to produce flood thresholds that correctly represent the extreme event behaviour in the forecasts. In the provided example, the river discharge level collapses to less than a third after 2000. Thus, the thresholds will be much too high and represent only the first half of the period. In this case, the real time GloFAS forecast will likely be similar to the latter part of the reanalysis period and will hardly ever exceed these flood thresholds, making the flood warnings very unreliable.

In other catchments, where the river discharge is significantly increasing, the situation is the opposite. In such catchments the real time forecasts will be mostly similar to the latter part of the reanalysis and the flood thresholds will be biased towards the lower earlier years. In this case, the thresholds will be

little too low and the real time GloFAS forecasts are expected to show too frequent flood events, making the forecasts unreliable again.

The example in Figure 13 is a very extreme one from the upstream part of the Congo basin. However, it is not an isolated case causing problems, as areas where the linear trend shows at least ~20% change in the ~40-year period, extreme value fitting to compute the flood thresholds is likely to provide us with difficulties. There is no scientific basis for this 20% minimum value (equivalent to ~0.05 raw linear trend magnitude), further tests would be needed to identify the expected forecast reliability loss due to such trends in the reanalysis time series. Based on the current reanalysis period, as used in GloFAS, at least 50% of land areas show raw linear trends higher (lower) than 0.05 (-0.05) (see Figure 6 and also Table 2) causing a significant issue in the operational running of GloFAS.

The extension of ERA5 back to 1950 (Hersbach et al., 2020) will provide an increase in the period used in the flood thresholds computation. However, it is strongly recommended that hydrological trends, with any potential discontinuities or regime changes due to merging different streams in the ERA5 production, should be analysed in that extended data set before making any change in GloFAS.

In addition, it will be important to explore ways to better derive the flood thresholds for catchments that are impacted by large trends in the GloFAS-ERA5 river discharge. An option could be to limit the period for the flood threshold computation to most recent decades, on a case by case basis (for single catchments, or maybe whole regions) selecting the period length that provides historical time series with low enough trend magnitudes. Based on this study, and the current ERA5 reanalysis, this could be as short as the last 15-17 years from ~2004, which although not ideal for estimating longer return periods, may provide improvements to make the GloFAS flood warnings more reliable in the future.

Zsoter et al. 2020 recommends that river discharge ensemble reforecasts should be used to compute flood thresholds instead of reanalysis, which would help to create more reliable flood warnings especially at longer lead times. The use of the reforecasts would be beneficial, as although they are initialised from GloFAS-ERA5 and are thus bound to inherit any trend problems that are present in this reanalysis, they are only generated on the most recent 20-year period (currently 1999-2018), which would undoubtedly lessen the trend impact documented in this study.

Finally, the documented river discharge linear trends in the GloFAS-ERA5 dataset are large enough to warrant further investigation of the underlying causes to the general behaviour of the water cycle variables in ERA5. This is crucial in order to provide improvements in hydrological variables such as river discharge, especially in the context of any future version of ECWMF reanalysis data sets, such as ERA6.

References

- Anabalón A., and A. Sharma, 2017: On the divergence of potential and actual evapotranspiration trends: An assessment across alternate global datasets. *Earth's Future*, **5**, 905–917.
- Albergel C., and Coauthors, 2013: Skill and Global Trend Analysis of Soil Moisture from Reanalyses and Microwave Remote Sensing. *J. Hydrometeor.*, **14**, 1259–1277, <https://doi.org/10.1175/JHM-D-12-0161.1>.

- Balsamo G., A. Beljaars, K. Scipal, P. Viterbo, B. van den Hurk, M. Hirschi, and A. K. Betts, 2009: A Revised Hydrology for the ECMWF Model: Verification from Field Site to Terrestrial Water Storage and Impact in the Integrated Forecast System. *J. Hydrometeorol.*, **10**, 623–643. <http://dx.doi.org/10.1175/2008JHM1068.1>.
- Beck H. E., E. F. Wood, M. Pan, and C. K. Fisher, 2019: MSWEP V2 global 3-hourly 0.1° precipitation: methodology and quantitative assessment. *Bull. Amer. Meteor. Soc.* **100**, 473–500, <https://doi.org/10.1175/BAMS-D-17-0138.1>.
- Connolly R., M. Connolly, W. Soon, D. R. Legates, R. G. Cionco, and H. V. M. Velasco Herrera, 2019: Northern Hemisphere Snow-Cover Trends (1967–2018): A Comparison between Climate Models and Observations. *Geosciences*, **9**, 135. <https://doi.org/10.3390/geosciences9030135>.
- Cucchi M., G. P. Weedon, A. Amici, N. Bellouin, S. Lange, H. M. Schmied, H. Hersbach, and C. Buontempo, 2020: WFDE5: bias adjusted ERA5 reanalysis data for impact studies, *Earth Syst. Sci. Data Discuss.*, <https://doi.org/10.5194/essd-2020-28>, in review, 2020.
- Dai A., T. Qian, K. E. Trenberth, and J. D. Milliman, 2009: Changes in continental freshwater discharge from 1948 to 2004. *Journal of Climate*, **22**(10), 2773–2792. <https://doi.org/10.1175/2008JCLI2592.1>.
- Dorigo W., R. de Jeu, D. Chung, R. Parinussa, Y. Liu, W. Wagner, and D. Fernández-Prieto, 2012: Evaluating global trends (1988–2010) in harmonized multi-satellite surface soil moisture. *Geophys. Res. Lett.*, **39** (18), 10.1029/2012GL052988.
- Drusch M., D. Vasiljevic, and P. Viterbo, 2004: ECMWF's Global Snow Analysis: Assessment and Revision Based on Satellite Observations. *J. Appl. Meteor.*, **43**, 1282–1294, [https://doi.org/10.1175/1520-0450\(2004\)043<1282:EGSAAA>2.0.CO;2](https://doi.org/10.1175/1520-0450(2004)043<1282:EGSAAA>2.0.CO;2).
- Dutra E., P. Viterbo, P. M. A. Miranda, and G. Balsamo, 2012: Complexity of Snow Schemes in a Climate Model and Its Impact on Surface Energy and Hydrology. *J. Hydrometeorol.*, **13**, 521–538, <https://doi.org/10.1175/JHM-D-11-072.1>.
- Feng H., and M. Zhang, 2016: Global land moisture trends: drier in dry and wetter in wet over land. *Sci Rep*, **5**, 18018. <https://doi.org/10.1038/srep18018>.
- Hansen J., S. Makiko, R. Ruedy, K. Lo, D. W. Lea, and M. Medina-Elizade. 2006: Global temperature change. *PNAS*, **6**, 14288-14293; <https://doi.org/10.1073/pnas.0606291103>.
- Hancock S., R. Baxter, J. Evans, and B. Huntley, 2013: Evaluating global snow water equivalent products for testing land surface models. *Remote Sens. Environ.*, **128**, 107–117, <https://doi.org/10.1016/j.rse.2012.10.004>.
- Harrigan S., E. Zsoter, L. Alfieri, C. Prudhomme, P. Salamon, F. Wetterhall, H. Cloke, and F. Pappenberger, 2020: GloFAS-ERA5 operational global river discharge reanalysis 1979–present, *Earth Syst. Sci. Data*, <https://doi.org/10.5194/essd-12-2043-2020>.
- Hersbach H., & Coauthors, 2020: The ERA5 Global Reanalysis. *Q. J. R. Meteorol. Soc.*, <https://doi.org/10.1002/qj.3803>.
- IPCC AR4 report, 2007, https://www.ipcc.ch/site/assets/uploads/2018/05/ar4_wg1_full_report-1.pdf.

- IPCC AR5 report WG1 contribution, 2013, https://www.ipcc.ch/site/assets/uploads/2018/02/WG1AR5_all_final.pdf.
- IPCC AR5 report, 2014, https://www.ipcc.ch/site/assets/uploads/2018/05/SYR_AR5_FINAL_full_wcover.pdf.
- Javadian M., A. Behrangi, W. K. Smith, and J. B. Fisher, 2020: Global Trends in Evapotranspiration Dominated by Increases across Large Cropland Regions. *Remote Sens.*, **12**(7), <https://doi.org/10.3390/rs12071221>.
- Jung M., M. Reichstein, and P. Ciais, 2020: Recent decline in the global land evapotranspiration trend due to limited moisture supply. *Nature*, **467**, 951–954, <https://doi.org/10.1038/nature09396>.
- Knowles N., 2015: Trends in Snow Cover and Related Quantities at Weather Stations in the Conterminous United States. *J. Climate*, **28**, 7518–7528, <https://doi.org/10.1175/JCLI-D-15-0051.1>.
- Kunkel K. E., D. A. Robinson, and S. Champion, 2016: Trends and Extremes in Northern Hemisphere Snow Characteristics. *Curr Clim Change Rep*, **2**, 65–73, <https://doi.org/10.1007/s40641-016-0036-8>.
- Lavers D., S. Harrigan, E. Andersson, D. S. Richardson, C. Prudhomme, and F. Pappenberger, 2019: A vision for improving global flood forecasting, *Environ. Res. Lett.*, doi:10.1088/1748-9326/ab52b2.
- Nguyen P., A. Thorstensen, S. Sorooshian, K. Hsu, A. Aghakouchak, H. Ashouri, H. Tran, and D. Braithwaite, 2018: Global precipitation trends across spatial scales using satellite observations. *Bull. Amer. Meteor. Soc.*, **99**, 689–697, <https://doi.org/10.1175/BAMS-D-17-0065.1>.
- Pan N., S. Wand, Y. Liu, W. Zhao, and B. Fu, 2019: Global Surface Soil Moisture Dynamics in 1979–2016 Observed from ESA CCI SM Dataset. *Water*, **11**(5), 883; <https://doi.org/10.3390/w11050883>.
- Parnesan C., and G. Yohe, 2003: Globally coherent fingerprint of climate change impacts across natural systems. *Nature*, **421**, 37–42, <https://doi.org/10.1038/nature01286>.
- Pavelsky T.M., M. T. Durand, K. M. Andreadis, R. E. Beighley, R. C. D. Paiva, G. H. Allen, and Z. F. Miller, 2014: Assessing the potential global extent of SWOT river discharge observations. *Journal of Hydrology*, **519** (PB), 1516–1525. <https://doi.org/10.1016/j.jhydrol.2014.08.044>.
- Rodda J. C., S. A. Pieyns, N. S. Sehmi, and G. Matthews, 1993: Towards a world hydrological cycle observing system *Hydrol. Sci. J.* **38**, 373–378. <https://doi.org/10.1080/026266693099492687>.
- de Rosnay P., L. Isaksen, and M., Dahoui, 2015: Snow data assimilation at ECMWF. *ECMWF newsletter*, 143, <https://www.ecmwf.int/sites/default/files/elibrary/2015/17328-snow-data-assimilation-ecmwf.pdf>.
- de Rosnay P., G. Balsamo, and C. Albergel, 2014: Initialisation of Land Surface Variables for Numerical Weather Prediction. *Surv Geophys*, **35**, 607–621, <https://doi.org/10.1007/s10712-012-9207-x>.

- Stahl K., L. M. Tallaksen, J. Hannaford, and H. A. J. van Lanen, 2012: Filling the white space on maps of European runoff trends: estimates from a multi-model ensemble. *Hydrology Earth System Sciences*, **16** (7), 2035–2047.
- Su L., C. Miao, D. Kong, Q. Duan, X. Lei, Q. Hou, and H. Li, 2018: Long-term trends in global river flow and the causal relationships between river flow and ocean signals. *Journal of Hydrology*. <https://doi.org/10.1016/j.jhydrol.2018.06.058>.
- Sun Q., C. Miao, Q. Duan, H. Ashouri, S. Sorooshian, and K. L. Hsu, 2018: A review of global precipitation datasets: Data sources, estimation, and intercomparisons. *Rev. Geophys.*, **56**, 79–107, <https://doi.org/10.1002/2017RG000574>.
- van der Knijff J. M., J. Younis, and A. P. J. de Roo, 2010: LISFLOOD: A GIS-based distributed model for river basin scale water balance and flood simulation. *Int. J. Geogr. Inf. Sci.*, **24**, 189–212, <https://doi.org/10.1080/13658810802549154>.
- Zhang Y., J. Peña-Arancibia, and T. McVicar, 2016: Multi-decadal trends in global terrestrial evapotranspiration and its components. *Sci Rep*, **6**, 19124, <https://doi.org/10.1038/srep19124>.
- Zsoter E., H. Cloke, E. Stephens, P. de Rosnay, J. Muñoz-Sabater, C. Prudhomme, and F. Pappenberger, 2019: How well do operational Numerical Weather Prediction setups represent hydrology? *J. Hydrometeorol.*, **14**, 1533–1552, <https://doi.org/10.1175/JHM-D-18-0086.1>.
- Zsoter E., C. Prudhomme, E. Stephens, F. Pappenberger and H. Cloke, 2020: Using ensemble reforecasts to generate flood thresholds for improved global flood forecasting. *J. Flood Risk Management*, <https://doi.org/10.1111/jfr3.12658>.

Appendix A: ERA5 and ERA5-Land trends for some additional surface variables

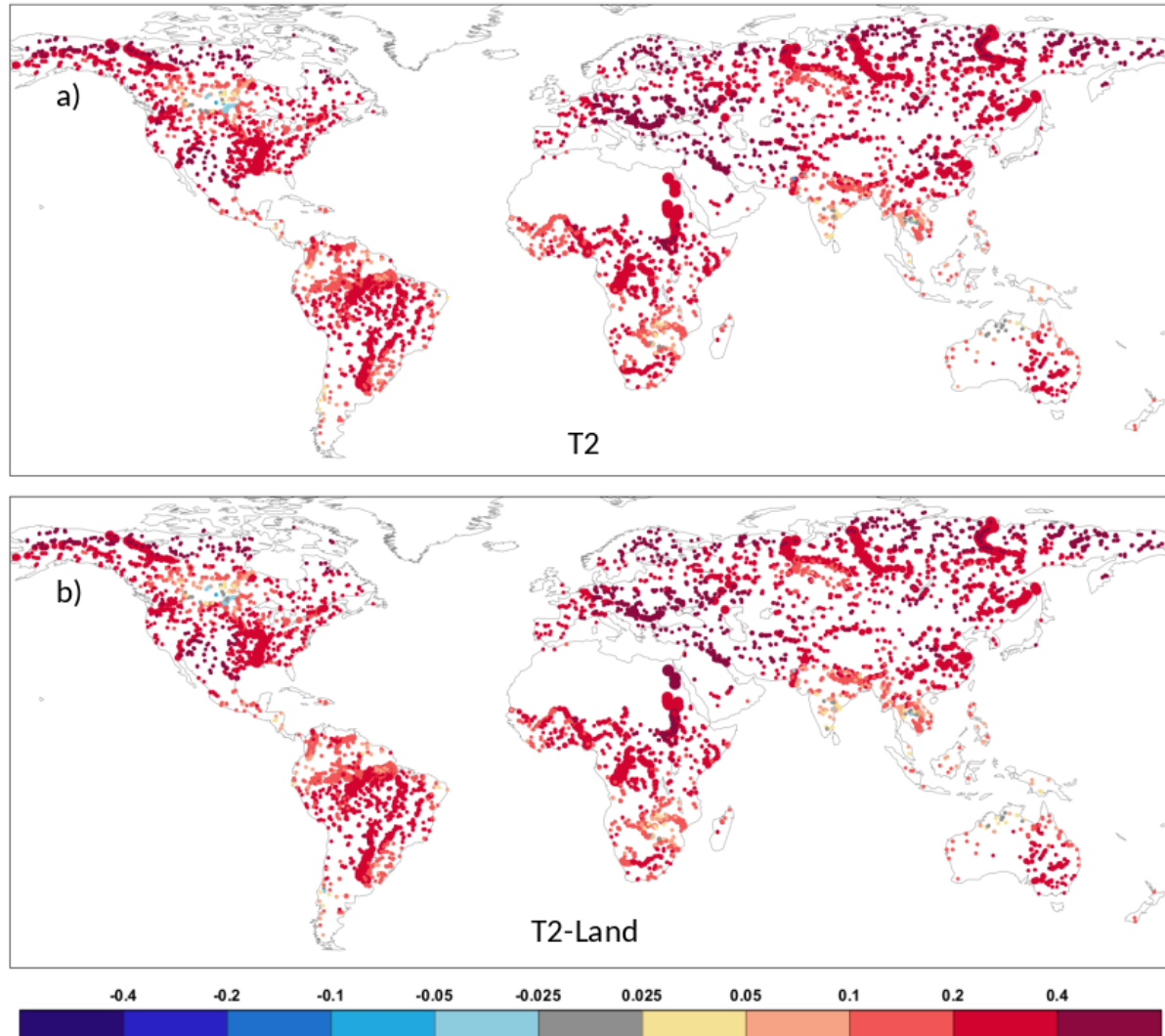


Figure A1. Raw linear trend (K) for global river catchments for ERA5 (a) and ERA5-Land (b) 2m temperature, based on the 1981-2018 period. The circles represent the catchment outlets, while their size the catchment area.

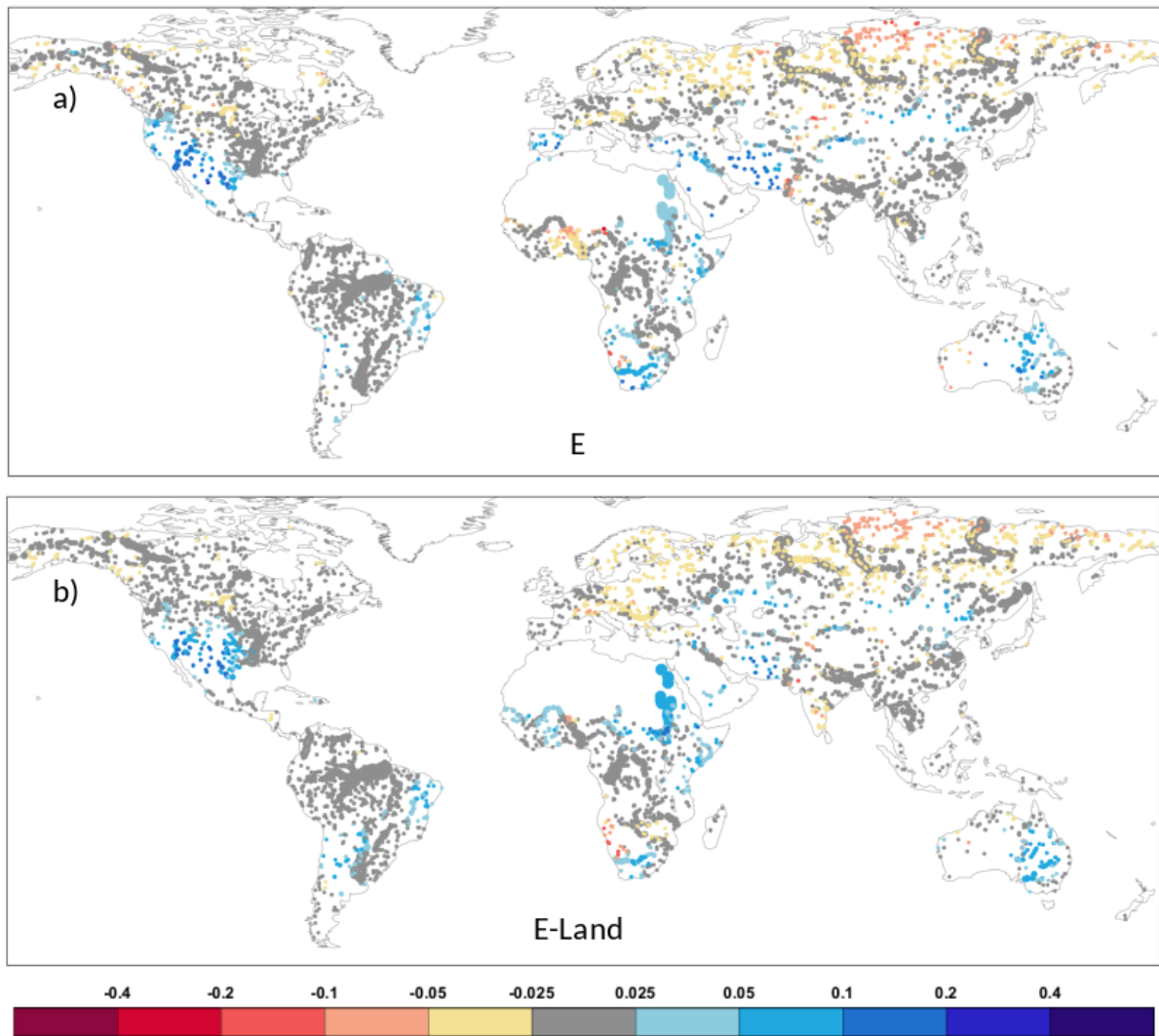


Figure A2. Raw linear trend (fraction/decade) for global river catchments for ERA5 (a) and ERA5-Land (b) evaporation, based on the 1981-2018 period. The circles represent the catchment outlets, while their size the catchment area.

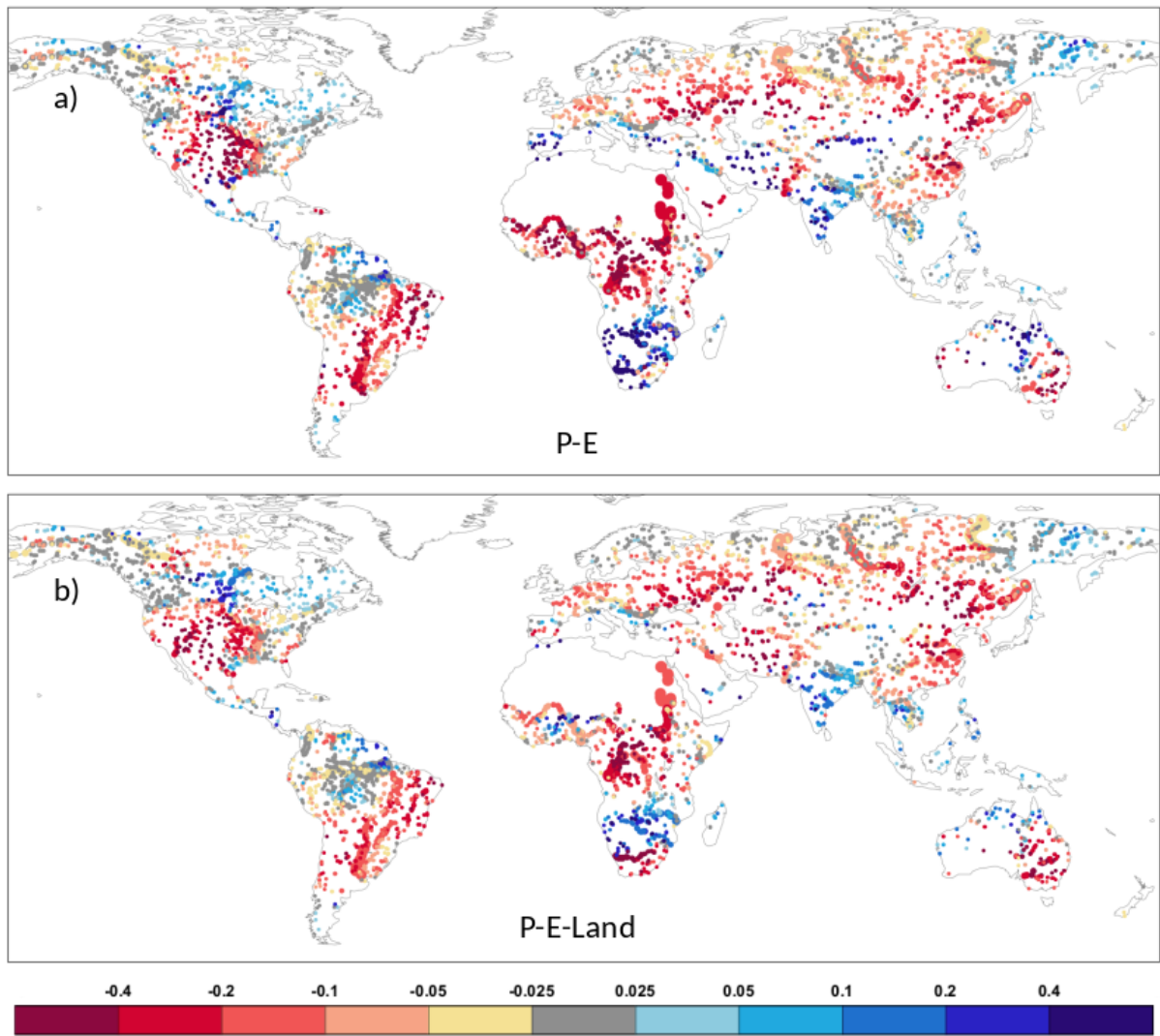


Figure A3. Raw linear trend (fraction/decade) for global river catchments for ERA5 (a) and ERA5-Land (b) evaporation, based on the 1981-2018 period. The circles represent the catchment outlets, while their size the catchment area.

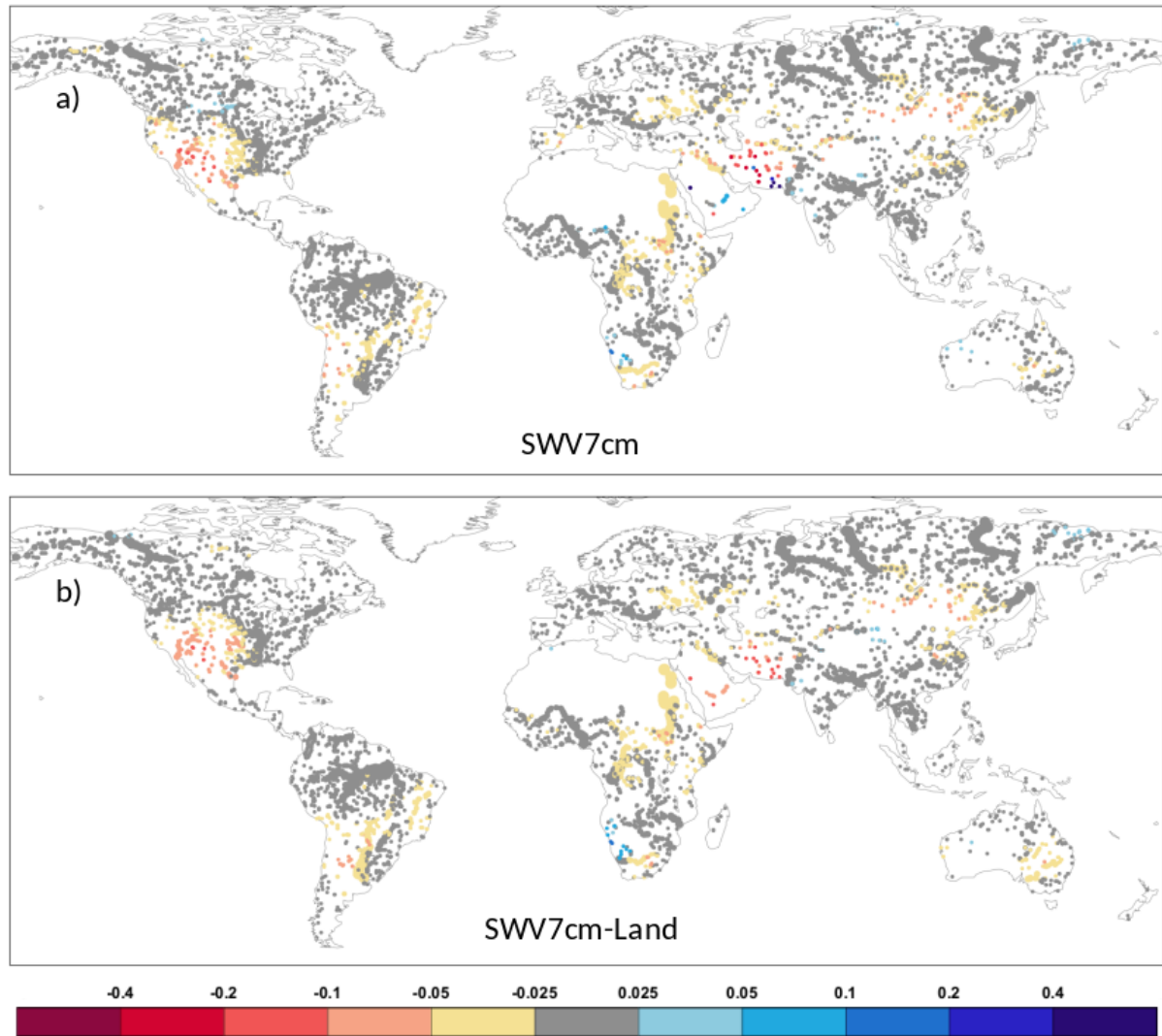


Figure A4. Raw linear trend (fraction/decade) for global river catchments for ERA5 (a) and ERA5-Land (b) soil moisture in the top 0-7 cm layer of the soil, based on the 1981-2018 period. The circles represent the catchment outlets, while their size the catchment area.

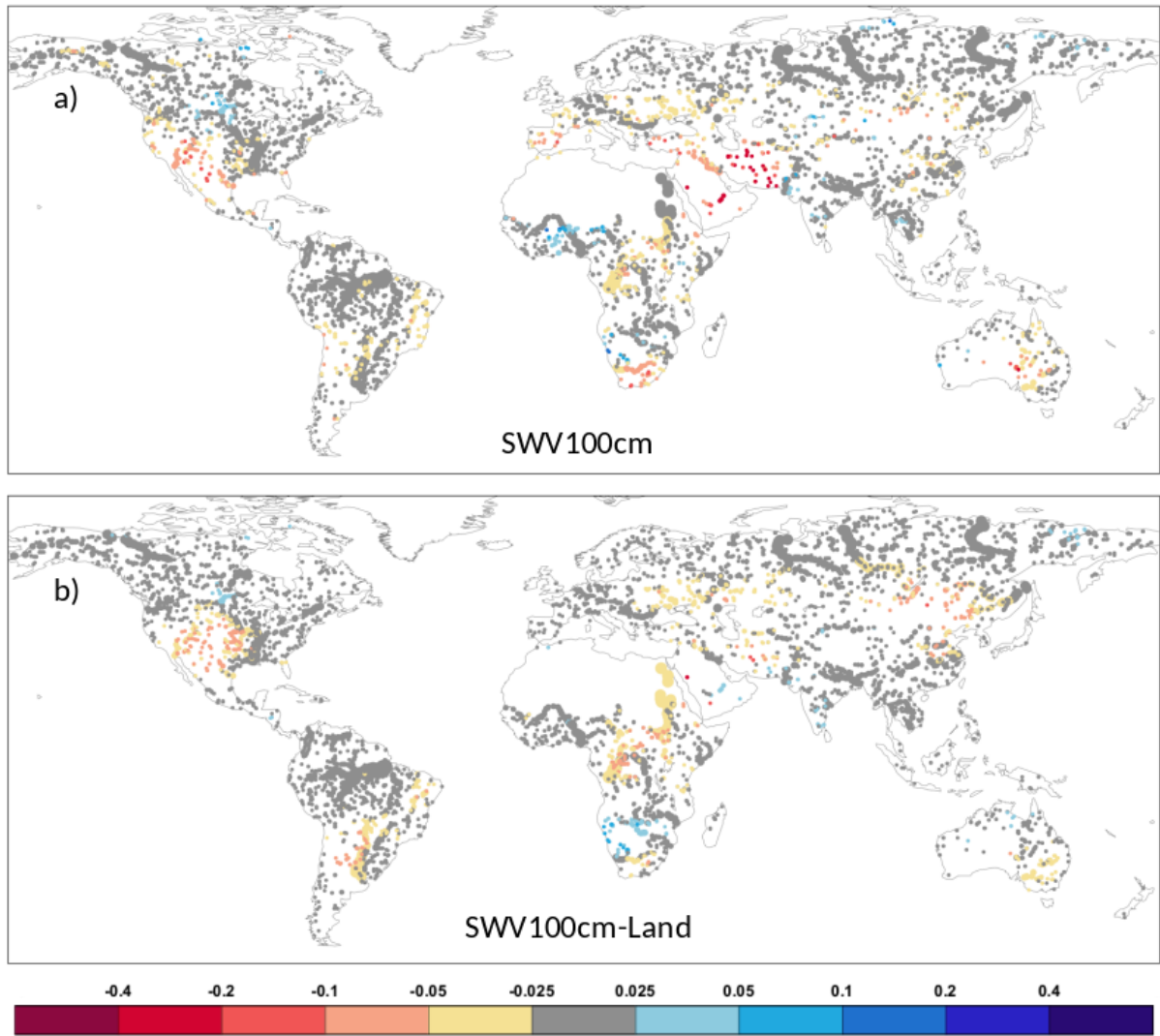


Figure A5. Raw linear trend (fraction/decade) for global river catchments for ERA5 (a) and ERA5-Land (b) soil moisture in the top 0-100 cm layer of the soil, based on the 1981-2018 period. The circles represent the catchment outlets, while their size the catchment area.

Appendix B: Standardised trend magnitudes for selected global catchments

Table A1. Standardised linear trends (fraction of standard deviation / decade) for selected catchments (see Figure 4) for 1981-2018, for GloFAS-ERA5 river discharge (DIS), ERA5 precipitation (P) and snowfall (SF) and both ERA5 and ERA5-Land snowmelt (SMLT), runoff (RO), evaporation (E), precipitation minus evaporation (P-E), soil moisture in the top 0-7 cm (SWV7) and 0-100 cm (SWV100) and 2m temperature (T2). Raw linear trends are also provided for observed river discharge (OBS) and the observation availability matched GloFAS-ERA5 river discharge (DISm) and ERA5 and ERA5-Land runoff (ROm). Differences in the absolute raw linear trend errors between ERA5-Land and ERA5 are also indicated in the last column (Imp). Empty cells correspond to cases for which trend computation was not possible. Coloured cells indicate negative (orange), positive (blue) trends and also decreasing (green) and increasing (purple) trend errors in ERA5 (Imp column). Where there is no raw linear trend, defined for absolute values less than 0.025, cells are not coloured. Darkening shades show increasing trend magnitudes.

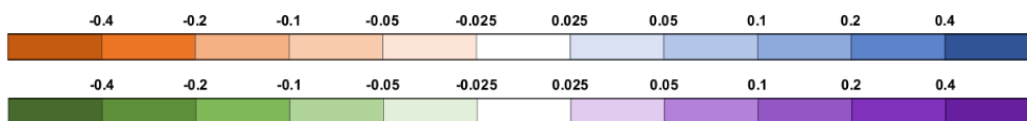
Rivers		DIS	P	SF	SMLT		RO		E		P-E	
		ERA5	ERA5	ERA5	ERA5	ERA5-Land	ERA5	ERA5-Land	ERA5	ERA5-Land	ERA5	ERA5-Land
North Asia	Ob	-0.50	-0.07	-0.30	-0.70	-0.25	-0.58	-0.40	-0.58	-0.45	-0.28	-0.23
	Yenisei	-0.81	-0.30	-0.29	-0.99	-0.22	-0.82	-0.49	-0.47	-0.49	-0.44	-0.44
	Lena	-0.57	-0.07	-0.36	-1.11	-0.21	-0.69	-0.27	-0.49	-0.63	-0.21	-0.26
	Amur	-0.63	-0.44	-0.33	-0.98	-0.26	-0.70	-0.63	-0.24	-0.14	-0.48	-0.46
North America	Yukon	-0.60	-0.10	-0.21	-0.65	-0.18	-0.73	-0.22	-0.03	-0.27	-0.10	-0.21
	Mackenzie	-0.54	-0.03	-0.06	-0.43	-0.04	-0.75	-0.13	-0.22	-0.23	-0.11	-0.12
	Churchill	0.12	0.27	0.15	0.30	0.10	0.19	0.37	-0.19	-0.20	0.22	0.22
	Columbia	-0.38	-0.15	0.04	-0.30	0.06	-0.39	-0.06	0.65	0.34	0.04	-0.06
	Colorado	-0.62	-0.58	-0.44	-0.39	-0.44	-0.69	-0.66	0.66	0.61	-0.06	-0.18
	Mississippi	-0.28	-0.21	-0.34	-0.32	-0.32	-0.31	-0.31	-0.17	0.19	-0.28	-0.17
Europe	Kalixaelven	0.04	0.24	0.10	-0.26	0.12	0.04	0.22	-0.44	-0.48	0.17	0.17
	Thames	-0.25	0.06	-0.14	0.11	-0.13	-0.24	0.00	0.06	-0.30	0.09	-0.02
	Rhine	-0.40	-0.23	-0.26	-0.50	-0.32	-0.41	-0.40	-0.48	-0.59	-0.33	-0.35
	Danube	-0.41	0.12	-0.18	-0.46	-0.24	-0.44	-0.21	-0.51	-0.72	0.00	-0.06
	Volga	-0.68	-0.37	-0.22	-0.59	-0.18	-0.69	-0.53	-0.65	-0.36	-0.53	-0.46
	Ebro	-0.44	0.02	0.13	-0.49	0.11	-0.53	-0.06	0.66	-0.03	0.42	0.01
South America	Magdalena	-0.25	-0.23				-0.28	-0.25	0.09	-0.56	-0.22	-0.26
	Amazon	-0.18	-0.07	-0.47	-0.50	-0.42	-0.18	-0.11	-0.11	-0.43	-0.08	-0.12
	Araguaia	-0.53	-0.52				-0.56	-0.54	0.12	0.43	-0.48	-0.42
	Parana	-0.45	-0.55	-0.57	-0.62	-0.54	-0.50	-0.59	0.17	0.70	-0.59	-0.44
Africa	Nile	-0.59	-0.70				-0.67	-0.78	0.49	0.88	-0.76	-0.51
	Niger	-0.28	-0.20				-0.32	-0.45	-0.62	0.15	-0.61	-0.18
	Shabelle	-0.21	-0.17				-0.23	-0.17	0.19	0.22	-0.12	-0.08
	White-Volta	0.24	-0.20				0.27	0.17	-0.62	0.46	-0.69	0.09
	Congo	-0.71	-0.81				-0.87	-0.91	0.38	0.61	-0.83	-0.80
	Zambesi	0.17	0.09				0.28	0.33	0.70	0.31	0.31	0.19
	Cunene	0.27	0.33				0.24	0.40	0.50	-0.51	0.79	0.09
	Orange	-0.22	-0.32	-0.03	-0.05	-0.04	-0.30	-0.37	0.63	0.33	0.24	-0.18
South Asia	Brahmaputra	-0.12	-0.19	-0.50	-0.05	-0.50	-0.12	-0.20	-0.45	-0.25	-0.21	-0.20
	Ganges	0.30	0.25	-0.34	0.12	-0.32	0.32	0.29	-0.39	-0.18	0.17	0.21
	Godavari	0.24	0.27				0.26	0.29	-0.36	-0.26	0.20	0.22
	Karnali	0.23	0.11	-0.38	-0.25	-0.38	0.23	0.09	-0.40	-0.25	0.06	0.07
Australia	Murray	-0.13	-0.30	-0.29	-0.42	-0.21	-0.26	-0.33	0.28	0.35	-0.25	-0.15



(continues on next page)

Table A1. Standardised linear trends (fraction of standard deviation / decade) for selected catchments (see Figure 4) for 1981-2018 (continued)

Rivers		SWV 0-7		SWV 0-100		T2		OBS	DISm	ROm		
		ERA5	ERA5-Land	ERA5	ERA5-Land	ERA5	ERA5-Land	-	ERA5	ERA5	ERA5-Land	Imp
North Asia	Ob	-0.25	-0.28	-0.27	-0.39	0.26	0.25	0.16	-0.70	-0.83	-0.34	-0.49
	Yenisei	-0.51	-0.55	-0.31	-0.72	0.38	0.37	0.43	-1.14	-1.20	-0.49	-0.72
	Lena	-0.27	-0.06	-0.16	-0.04	0.43	0.42	0.30	-0.82	-0.88	-0.43	-0.46
	Amur	-0.70	-0.56	-0.34	-0.70	0.46	0.44	-1.36	-2.05	-2.27	-1.93	-0.34
North America	Yukon	-0.40	-0.11	-0.61	-0.06	0.41	0.40	0.20	-1.05	-1.28	-0.40	-0.88
	Mackenzie	-0.34	-0.14	-0.39	-0.15	0.35	0.34	0.39	-0.67	-0.95	-0.11	-0.84
	Churchill	0.08	0.18	0.18	0.22	0.12	0.11	0.63	0.26	0.36	0.37	-0.01
	Columbia	-0.62	-0.35	-0.66	-0.28	0.45	0.43	-0.10	-0.52	-0.53	-0.21	-0.32
	Colorado	-0.59	-0.58	-0.77	-0.48	0.56	0.56	-0.21	-0.95	-1.04	-1.01	-0.03
	Mississippi	-0.34	-0.40	-0.16	-0.46	0.31	0.32	0.15	-0.38	-0.44	-0.51	0.07
Europe	Kalixaelven	0.10	-0.01	0.09	0.01	0.51	0.53	0.24	-0.23	-0.24	0.11	-0.35
	Thames	-0.17	-0.02	-0.43	-0.07	0.42	0.42	-0.01	-0.43	-0.40	-0.14	-0.26
	Rhine	-0.28	-0.26	-0.38	-0.32	0.53	0.52	-0.30	-0.57	-0.57	-0.46	-0.12
	Danube	-0.25	-0.15	-0.40	-0.14	0.62	0.62	0.56	-0.44	-0.41	-0.03	-0.37
	Volga	-0.47	-0.50	-0.46	-0.58	0.41	0.41	-0.08	-1.22	-1.25	-0.87	-0.38
	Ebro	-0.48	-0.17	-1.02	-0.20	0.53	0.50	-0.26	-0.86	-1.06	-0.48	-0.59
South America	Magdalena	-0.48	-0.34	-0.63	-0.35	0.51	0.50	0.03	-0.03	-0.06	-0.03	-0.03
	Amazon	-0.67	-0.62	-0.73	-0.62	0.60	0.60	0.25	-0.46	-0.46	-0.40	-0.07
	Araguaia	-0.68	-0.68	-0.46	-0.52	0.64	0.69	-0.14	-0.62	-0.70	-0.67	-0.03
	Parana	-0.58	-0.69	-0.52	-0.80	0.67	0.70	-0.20	-0.82	-0.94	-1.10	0.16
Africa	Nile	-0.66	-0.78	-0.54	-0.87	0.75	0.78	0.19	-1.46	-1.59	-1.88	0.29
	Niger	-0.01	-0.25	0.49	-0.19	0.64	0.66	1.35	-0.52	-0.54	-0.79	0.24
	Shabelle	-0.23	-0.24	-0.12	-0.11	0.63	0.64	0.32	-0.97	-1.06	-0.85	-0.21
	White-Volta	-0.09	-0.35	0.87	0.01	0.48	0.59	-0.28	-0.13	-0.14	-0.20	-0.06
	Congo	-0.71	-0.73	-0.85	-1.04	0.75	0.76	0.27	-1.59	-1.89	-1.99	0.10
	Zambesi	-0.35	-0.20	-0.27	0.04	0.53	0.50	0.48	0.33	0.53	0.61	0.08
	Cunene	-0.09	0.25	-0.42	0.55	0.52	0.41	0.40	0.40	0.39	0.54	0.14
	Orange	-0.34	-0.29	-0.61	-0.25	0.45	0.43	0.17	-0.78	-0.95	-0.97	0.02
South Asia	Brahmaputra	0.44	0.22	0.46	0.23	0.45	0.45	-0.32	-0.12	-0.12	-0.20	-0.08
	Ganges	0.29	0.12	0.37	0.23	0.36	0.35	-0.03	0.45	0.48	0.45	-0.02
	Godavari	0.23	0.15	0.38	0.37	0.15	0.16	-0.04	0.41	0.44	0.48	0.04
	Karnali	0.01	-0.24	0.09	-0.15	0.50	0.46	-0.05	0.29	0.29	0.14	-0.14
Australia	Murray	-0.22	-0.34	-0.40	-0.33	0.49	0.52	-0.25	-0.39	-0.64	-0.74	0.10

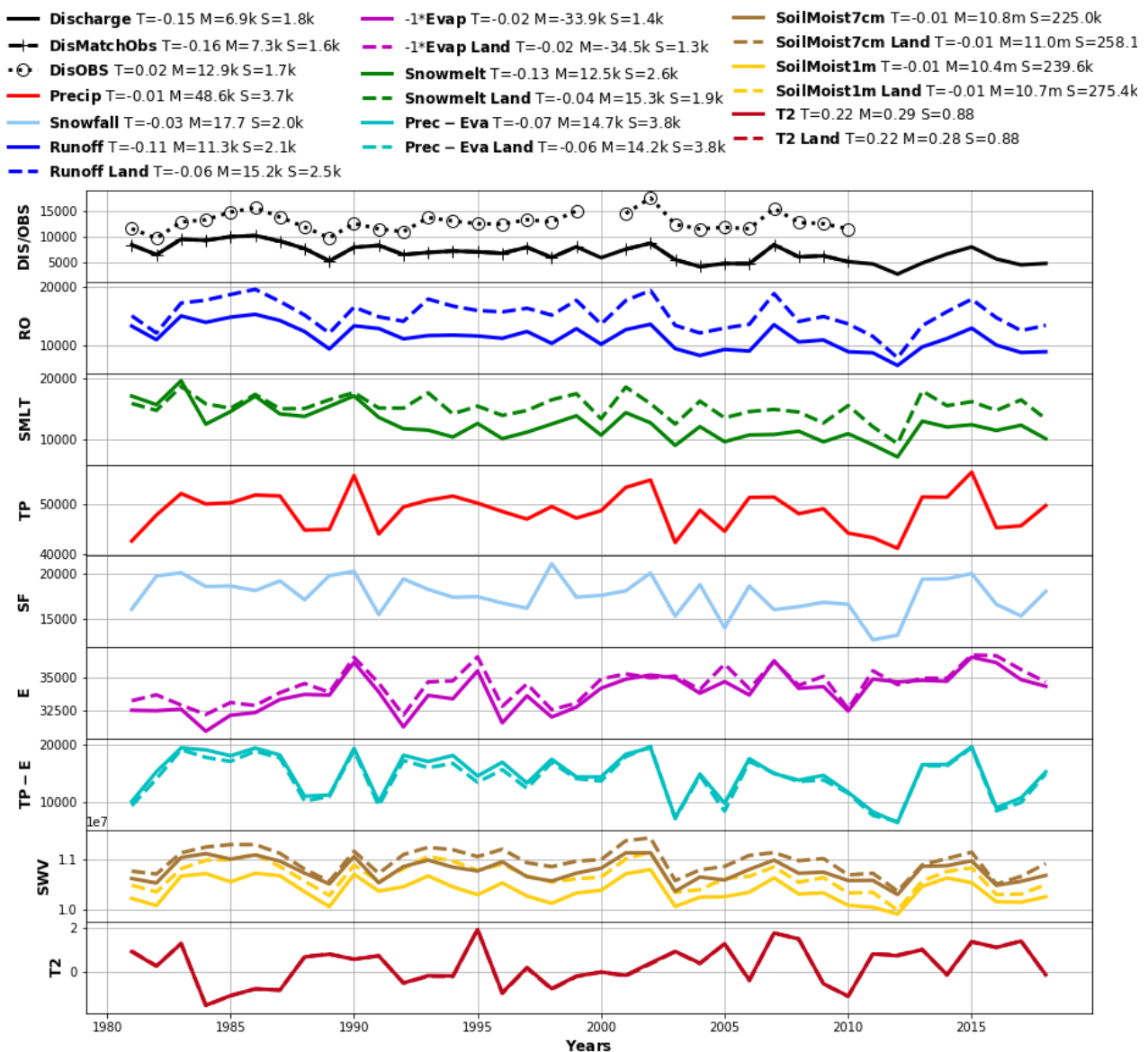


Appendix C: Trend hydrographs for selected global catchments

Annual mean time series diagrams with all the analysed variables (Table 1) are provided for several world rivers (33 in total), grouped into continents (see Figure 4 for the locations). These graphs include in the line legends also the trend magnitudes and the mean and the standard deviation values of the annual mean time series in the 38-year period for each variable (other than the observed river discharge which includes trend values only if at least 16 years were available).

North Asia - No.1

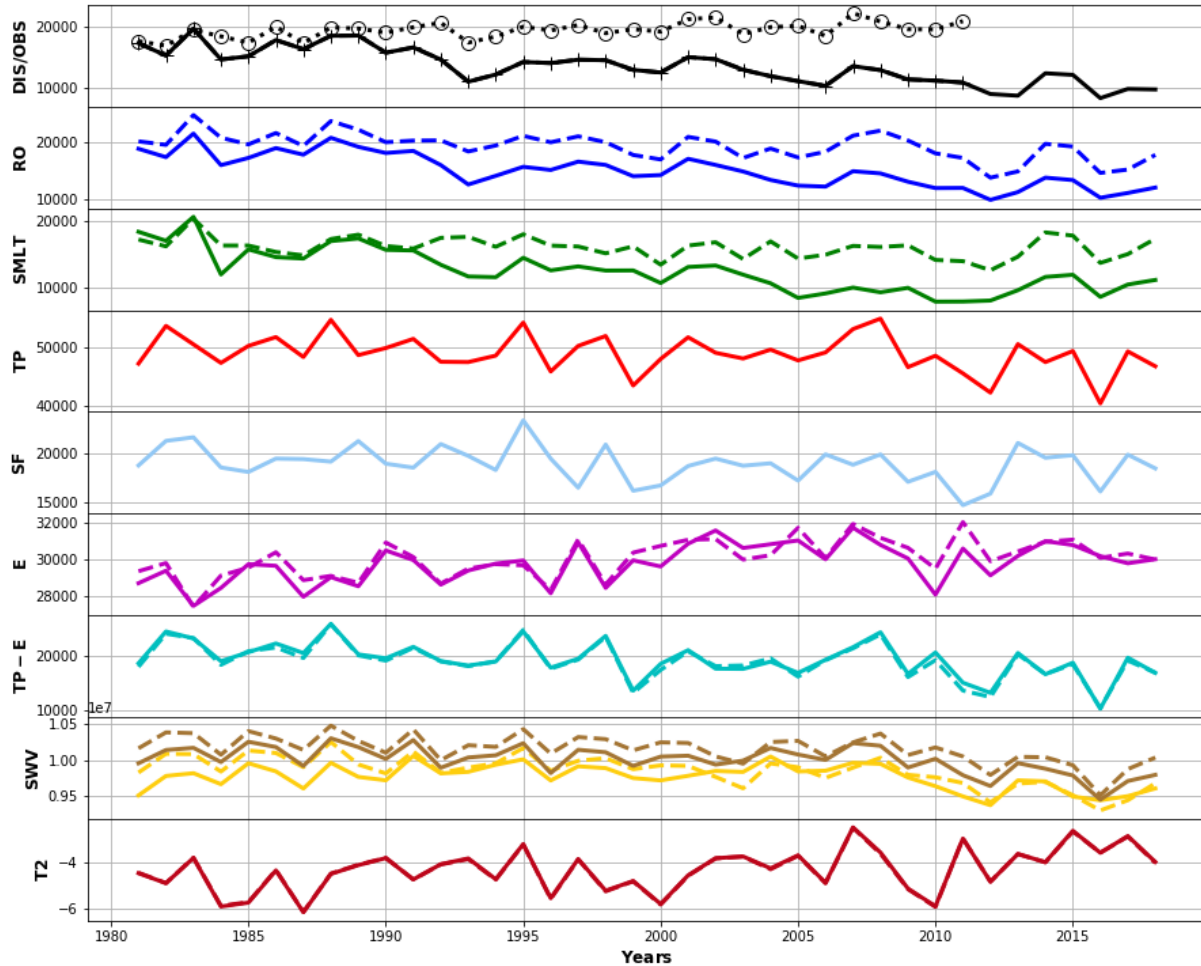
River: Ob, Outlet: [66.55N; 66.45E], Area: 2541170 km²



North Asia - No.2

River: Yenisei, Outlet: [67.45N; 86.45E], Area: 2651150 km2

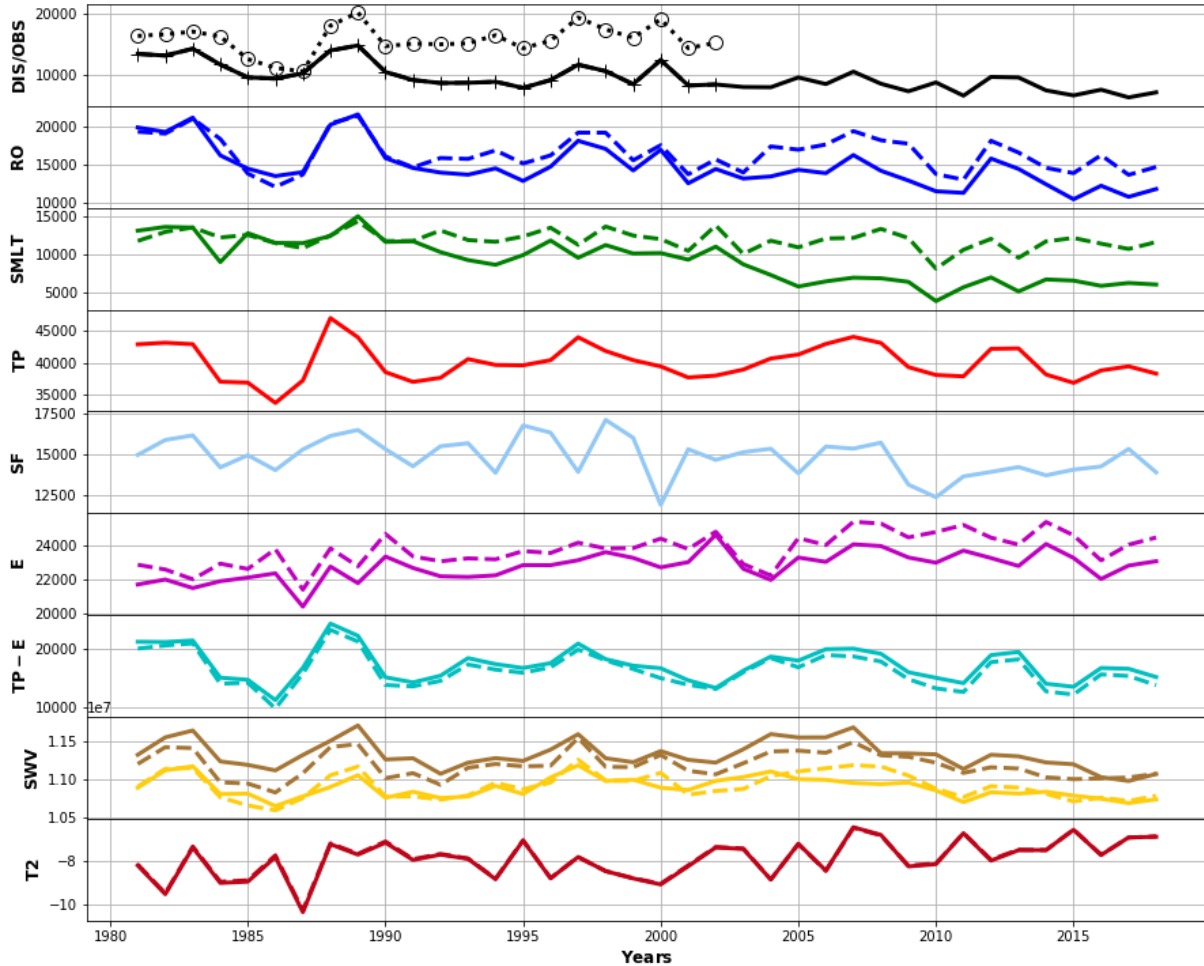
- **Discharge** T=-0.16 M=13.5k S=2.9k
- **DisMatchObs** T=-0.15 M=14.3k S=2.5k
- **DisOBS** T=0.04 M=19.5k S=1.3k
- **Precip** T=-0.02 M=49.0k S=3.2k
- **Snowfall** T=-0.03 M=19.0 S=1.8k
- **Runoff** T=-0.15 M=15.1k S=2.9k
- **Runoff Land** T=-0.07 M=19.3k S=2.3k
- **-1*Evap** T=-0.02 M=-29.7k S=1.0k
- **-1*Evap Land** T=-0.02 M=-30.0k S=1.0k
- **Snowmelt** T=-0.18 M=12.5k S=3.1k
- **Snowmelt Land** T=-0.03 M=16.1k S=1.5k
- **Prec - Eva** T=-0.07 M=19.3k S=3.2k
- **Prec - Eva Land** T=-0.08 M=19.0k S=3.3k
- **SoilMoist7cm** T=-0.01 M=10.0m S=186.5k
- **SoilMoist7cm Land** T=-0.01 M=10.2m S=194.0
- **SoilMoist1m** T=-0.01 M=9.8m S=171.6k
- **SoilMoist1m Land** T=-0.01 M=9.9m S=211.6k
- **T2** T=0.36 M=-4.30 S=0.94
- **T2 Land** T=0.35 M=-4.31 S=0.94



North Asia - No.3

River: Lena, Outlet: [72.25N; 126.75E], Area: 2443690 km2

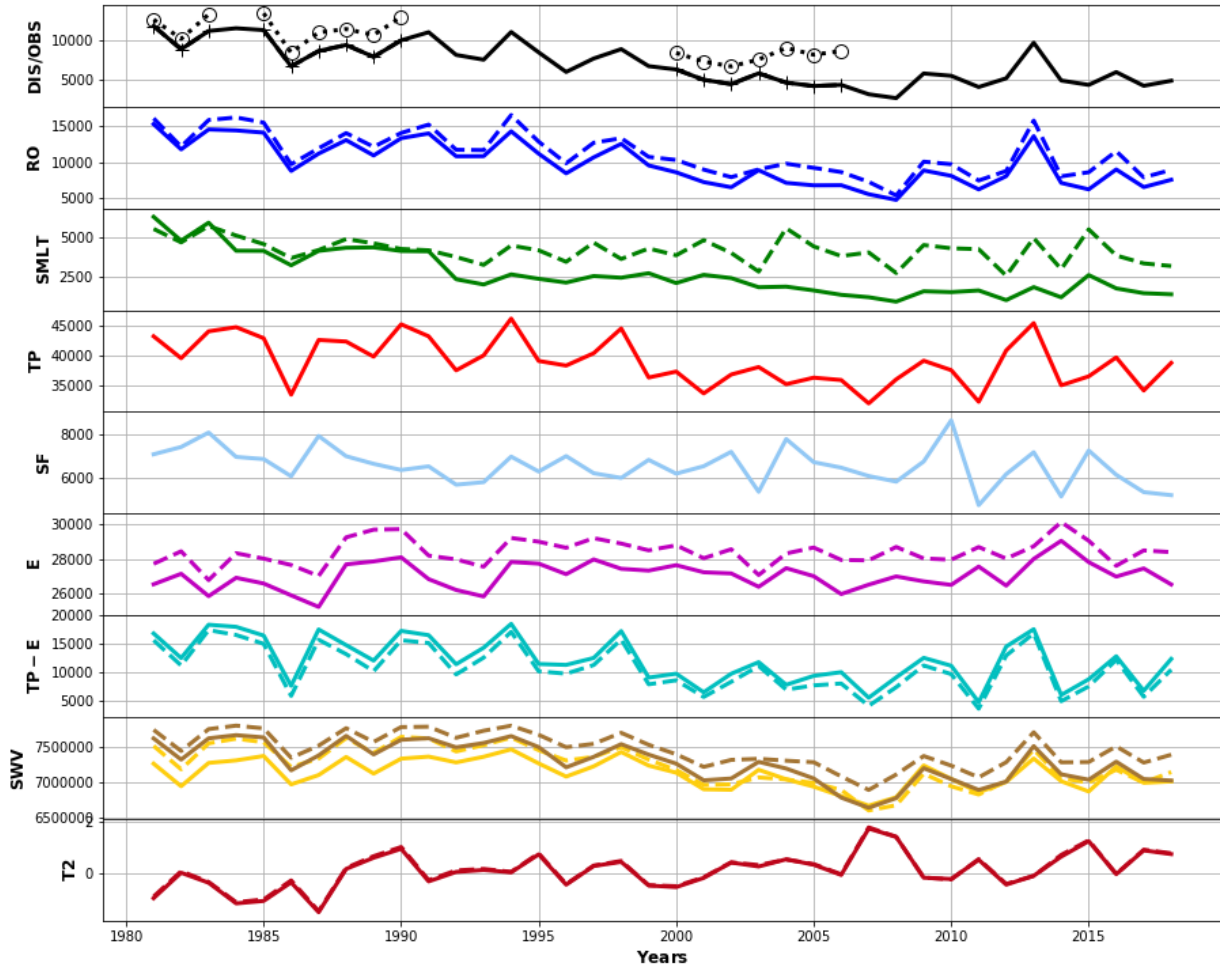
- Discharge T=-0.14 M=9.7k S=2.2k
- DisMatchObs T=-0.17 M=10.7k S=2.1k
- DisOBS T=0.04 M=15.8k S=2.3k
- Precip T=-0.00 M=40.0k S=2.7k
- Snowfall T=-0.03 M=14.9 S=1.2k
- Runoff T=-0.11 M=14.9k S=2.8k
- Runoff Land T=-0.04 M=16.6k S=2.3k
- -1*Evap T=-0.02 M=-22.8k S=812
- -1*Evap Land T=-0.02 M=-23.8k S=950
- Snowmelt T=-0.24 M=9.2k S=2.8k
- Snowmelt Land T=-0.04 M=11.9k S=1.2k
- Prec - Eva T=-0.04 M=17.3k S=2.8k
- Prec - Eva Land T=-0.05 M=16.3k S=2.9k
- SoilMoist7cm T=-0.00 M=11.3m S=180.7k
- SoilMoist7cm Land T=-0.00 M=11.2m S=171.9
- SoilMoist1m T=-0.00 M=10.9m S=133.7k
- SoilMoist1m Land T=-0.00 M=10.9m S=169.6k
- T2 T=0.37 M=-7.93 S=0.87
- T2 Land T=0.36 M=-7.91 S=0.86



North Asia - No.4

River: Amur, Outlet: [50.55N; 137.15E], Area: 1846250 km2

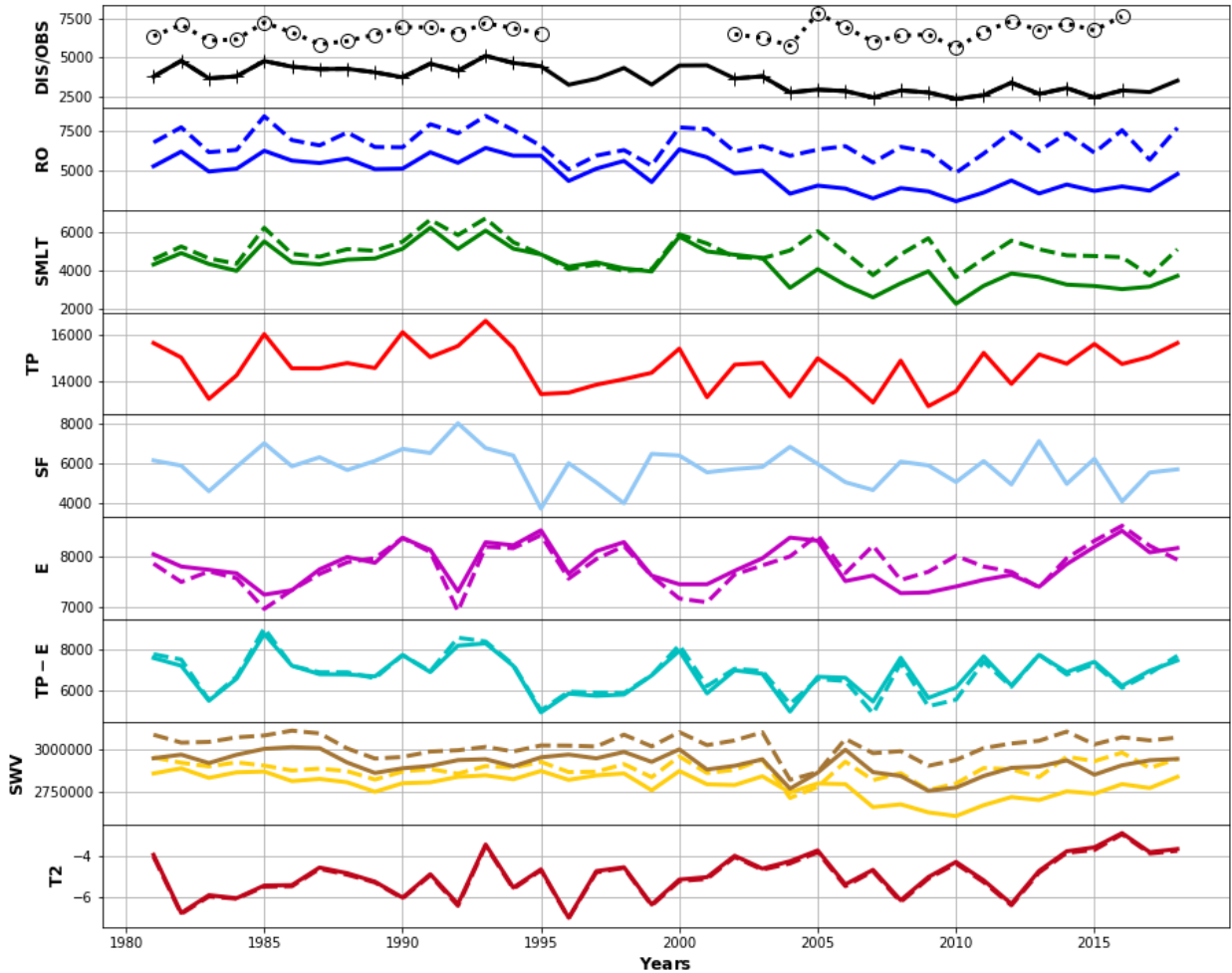
- Discharge T=-0.26 M=7.0k S=2.6k
- DisMatchObs T=-0.65 M=7.5k S=2.6k
- DisOBS T=-0.33 M=9.9k S=2.2k
- Precip T=-0.04 M=39.1k S=3.9k
- Snowfall T=-0.04 M=6.5 S=857
- Runoff T=-0.20 M=9.8k S=3.0k
- Runoff Land T=-0.16 M=11.2k S=2.9k
- -1*Evap T=-0.01 M=-27.0k S=774
- -1*Evap Land T=-0.00 M=-28.4k S=732
- Snowmelt T=-0.39 M=2.6k S=1.3k
- Snowmelt Land T=-0.07 M=4.2k S=782
- Prec - Eva T=-0.16 M=12.1k S=3.9k
- Prec - Eva Land T=-0.17 M=10.7k S=3.9k
- SoilMoist7cm T=-0.02 M=7.3m S=277.9k
- SoilMoist7cm Land T=-0.02 M=7.5m S=239.5k
- SoilMoist1m T=-0.01 M=7.1m S=199.9k
- SoilMoist1m Land T=-0.02 M=7.2m S=280.9k
- T2 T=0.32 M=0.08 S=0.69
- T2 Land T=0.31 M=0.11 S=0.69



North America - No.1

River: Yukon, Outlet: [61.85N; -162.85W], Area: 865451 km²

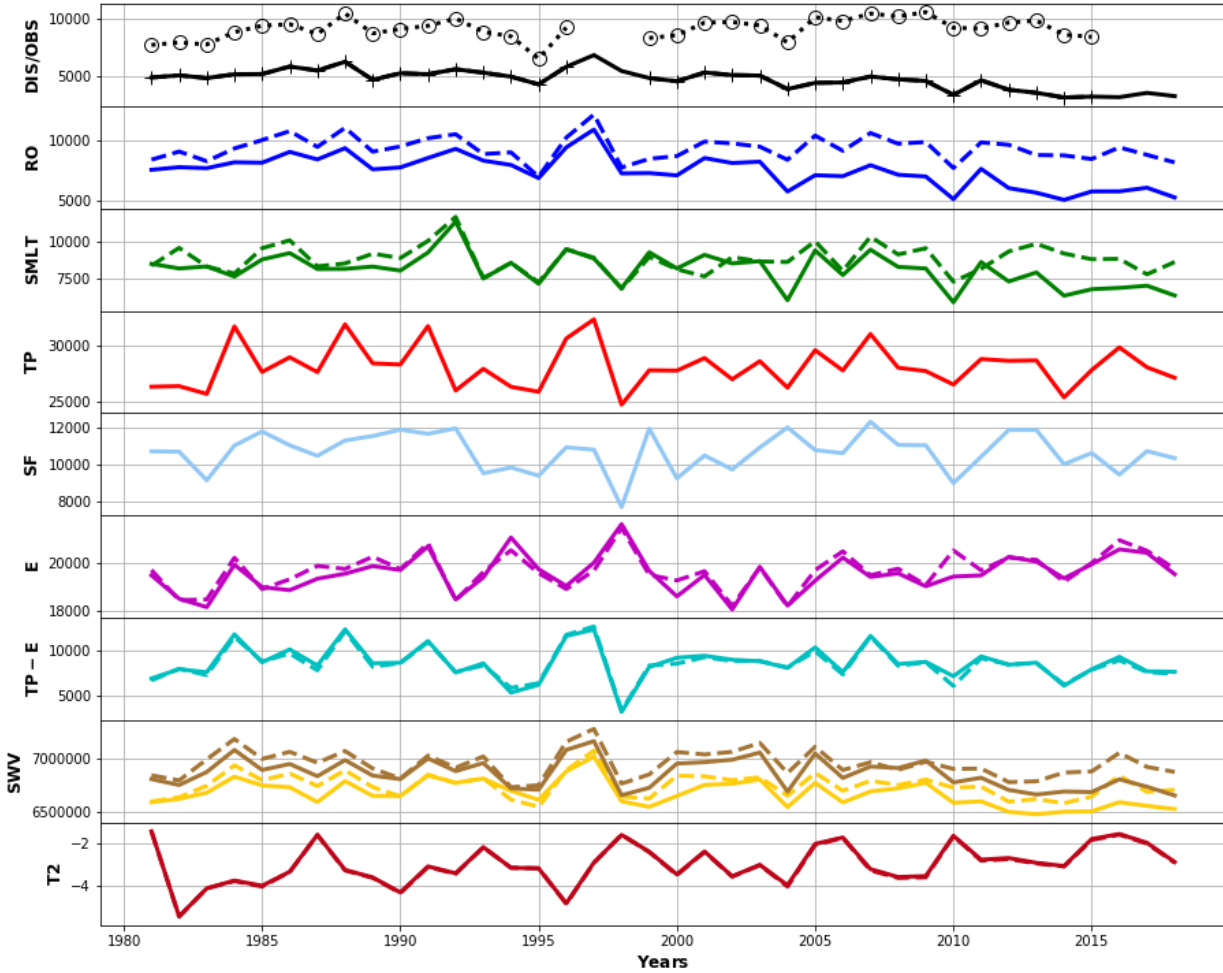
- Discharge T=-0.14 M=3.6k S=781
- DisMatchObs T=-0.20 M=3.6k S=819
- DisOBS T=0.02 M=6.7k S=534
- Precip T=-0.01 M=14.6k S=894
- Snowfall T=-0.03 M=5.8 S=889
- Runoff T=-0.13 M=4.8k S=956
- Runoff Land T=-0.03 M=6.7k S=857
- -1*Evap T=-0.00 M=-7.8k S=373
- -1*Evap Land T=-0.01 M=-7.8k S=401
- Snowmelt T=-0.13 M=4.2k S=933
- Snowmelt Land T=-0.03 M=5.0k S=750
- Prec - Eva T=-0.01 M=6.8k S=905
- Prec - Eva Land T=-0.03 M=6.8k S=979
- SoilMoist7cm T=-0.01 M=2.9m S=63.4k
- SoilMoist7cm Land T=-0.00 M=3.0m S=64.7k
- SoilMoist1m T=-0.01 M=2.8m S=70.6k
- SoilMoist1m Land T=-0.00 M=2.9m S=56.2k
- T2 T=0.40 M=-4.95 S=0.98
- T2 Land T=0.39 M=-5.02 S=0.97



North America - No.2

River: Mackenzie, Outlet: [67.45N; -133.65W], Area: 1726490 km²

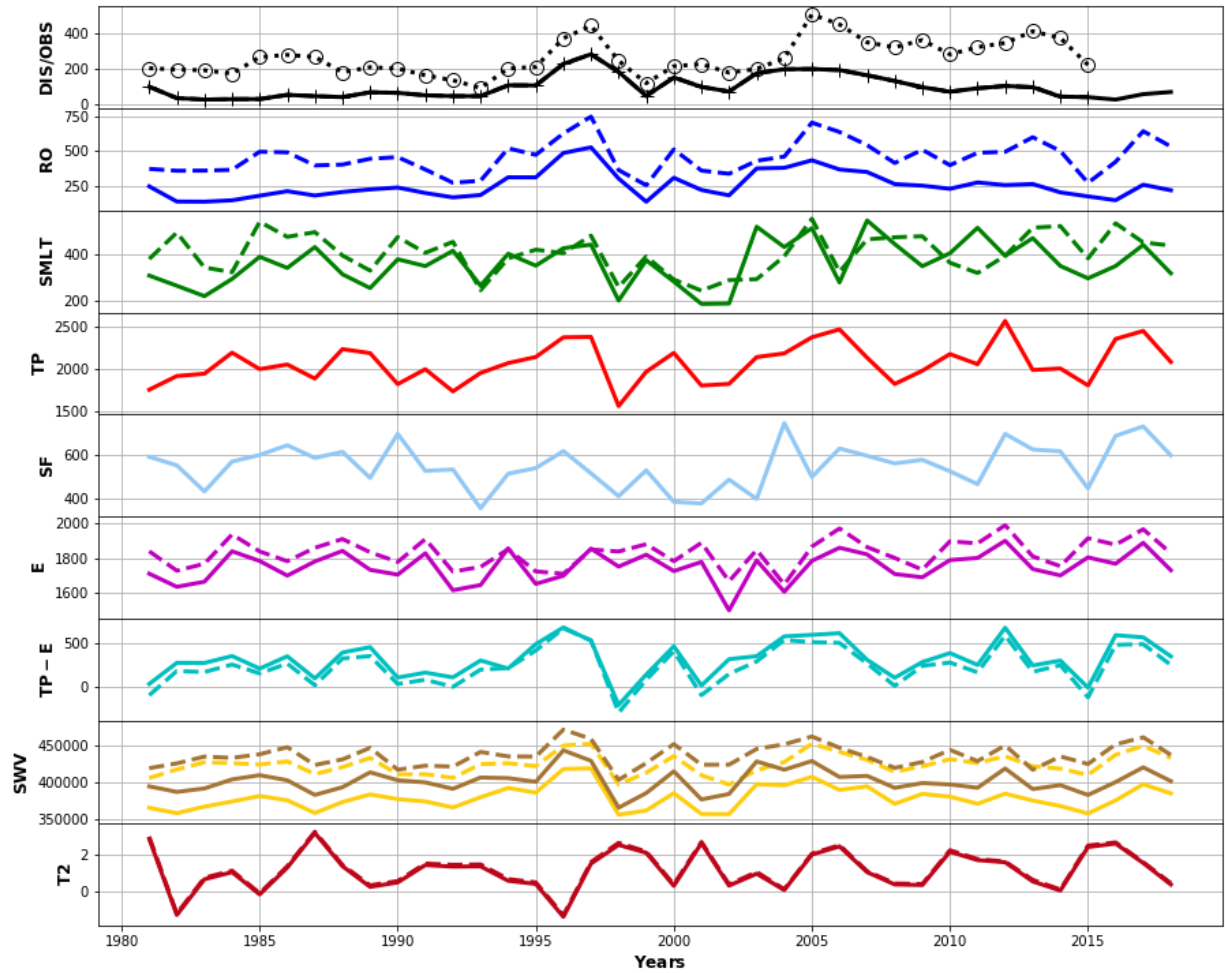
- Discharge T=-0.12 M=4.7k S=877
- DisMatchObs T=-0.12 M=4.8k S=743
- DisOBS T=0.04 M=9.1k S=907
- Precip T=-0.00 M=28.1k S=1.8k
- Snowfall T=-0.01 M=10.7 S=1.0k
- Runoff T=-0.11 M=7.4k S=1.3k
- Runoff Land T=-0.02 M=9.3k S=1.0k
- -1*Evap T=-0.01 M=-19.5k S=755
- -1*Evap Land T=-0.01 M=-19.7k S=738
- Snowmelt T=-0.05 M=8.1k S=1.1k
- Snowmelt Land T=-0.00 M=8.8k S=946
- Prec - Eva T=-0.02 M=8.6k S=1.9k
- Prec - Eva Land T=-0.03 M=8.5k S=1.8k
- SoilMoist7cm T=-0.01 M=6.9m S=136.3k
- SoilMoist7cm Land T=-0.00 M=6.9m S=128.4k
- SoilMoist1m T=-0.01 M=6.7m S=121.2k
- SoilMoist1m Land T=-0.00 M=6.7m S=112.4k
- T2 T=0.34 M=-2.97 S=0.96
- T2 Land T=0.33 M=-3.00 S=0.96



North America - No.3

River: Churchill, Outlet: [55.65N; -104.75W], Area: 120999 km²

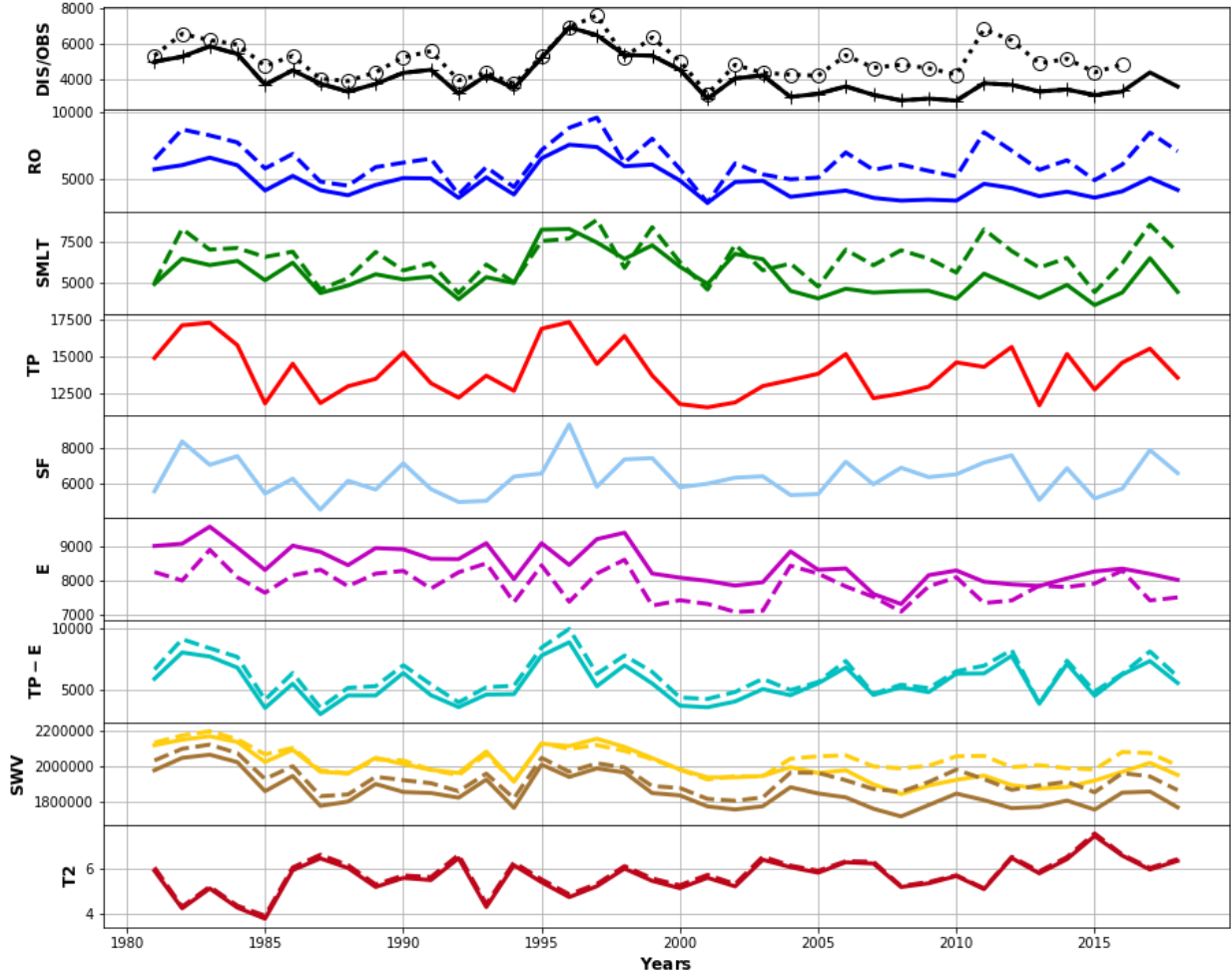
- Discharge T=0.12 M=95 S=64
- DisMatchObs T=0.22 M=99 S=65
- DisOBS T=0.20 M=262 S=98
- Precip T=0.03 M=2.1k S=227
- Snowfall T=0.03 M=554 S=97
- Runoff T=0.07 M=259 S=93
- Runoff Land T=0.07 M=457 S=115
- -1*Evap T=-0.01 M=-1.7k S=85
- -1*Evap Land T=-0.01 M=-1.8k S=81
- Snowmelt T=0.07 M=360 S=93
- Snowmelt Land T=0.02 M=406 S=86
- Prec - Eva T=0.15 M=315 S=200
- Prec - Eva Land T=0.19 M=237 S=211
- SoilMoist7cm T=0.00 M=401.8k S=15.8k
- SoilMoist7cm Land T=0.01 M=436.1k S=14.7k
- SoilMoist1m T=0.01 M=379.0k S=15.9k
- SoilMoist1m Land T=0.01 M=424.2k S=13.9k
- T2 T=0.13 M=1.14 S=1.09
- T2 Land T=0.12 M=1.22 S=1.09



North America - No.4

River: Columbia, Outlet: [45.65N; -121.25W], Area: 612077 km2

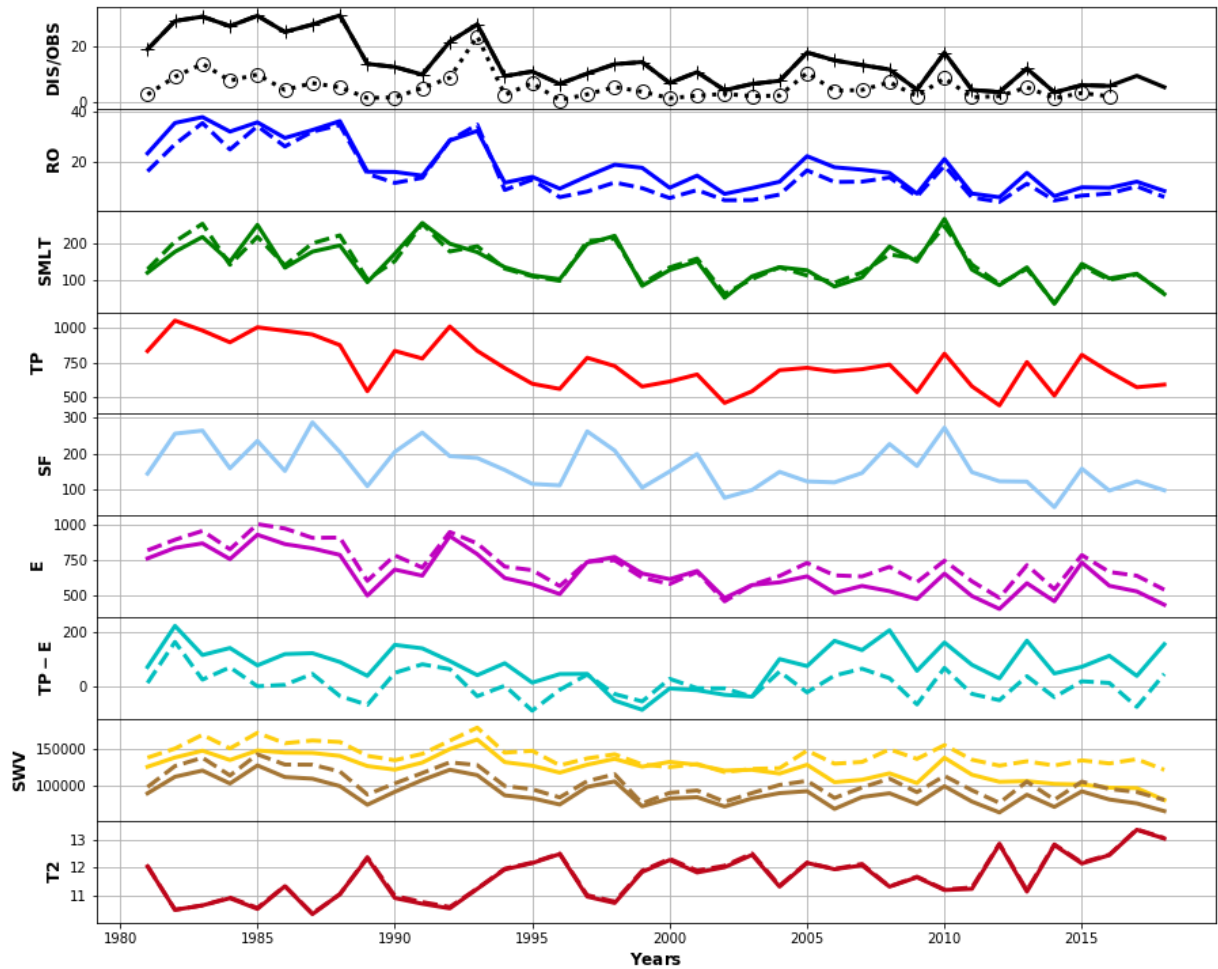
- Discharge T=-0.11 M=4.1k S=1.0k
- DisMatchObs T=-0.13 M=4.1k S=1.1k
- DisOBS T=-0.02 M=5.1k S=971
- Precip T=-0.02 M=14.0k S=1.7k
- Snowfall T=0.01 M=6.4 S=1.0k
- Runoff T=-0.10 M=4.8k S=1.1k
- Runoff Land T=-0.01 M=6.4k S=1.4k
- -1*Evap T=0.04 M=-8.5k S=522
- -1*Evap Land T=0.02 M=-7.9k S=462
- Snowmelt T=-0.06 M=5.4k S=1.2k
- Snowmelt Land T=0.01 M=6.4k S=1.2k
- Prec - Eva T=0.01 M=5.5k S=1.4k
- Prec - Eva Land T=-0.01 M=6.1k S=1.5k
- SoilMoist7cm T=-0.03 M=1.9m S=89.4k
- SoilMoist7cm Land T=-0.01 M=1.9m S=78.1k
- SoilMoist1m T=-0.03 M=2.0m S=87.4k
- SoilMoist1m Land T=-0.01 M=2.0m S=68.2k
- T2 T=0.34 M=5.64 S=0.75
- T2 Land T=0.32 M=5.74 S=0.75



North America - No.5

River: Colorado, Outlet: [36.15N; -111.75W], Area: 68780 km2

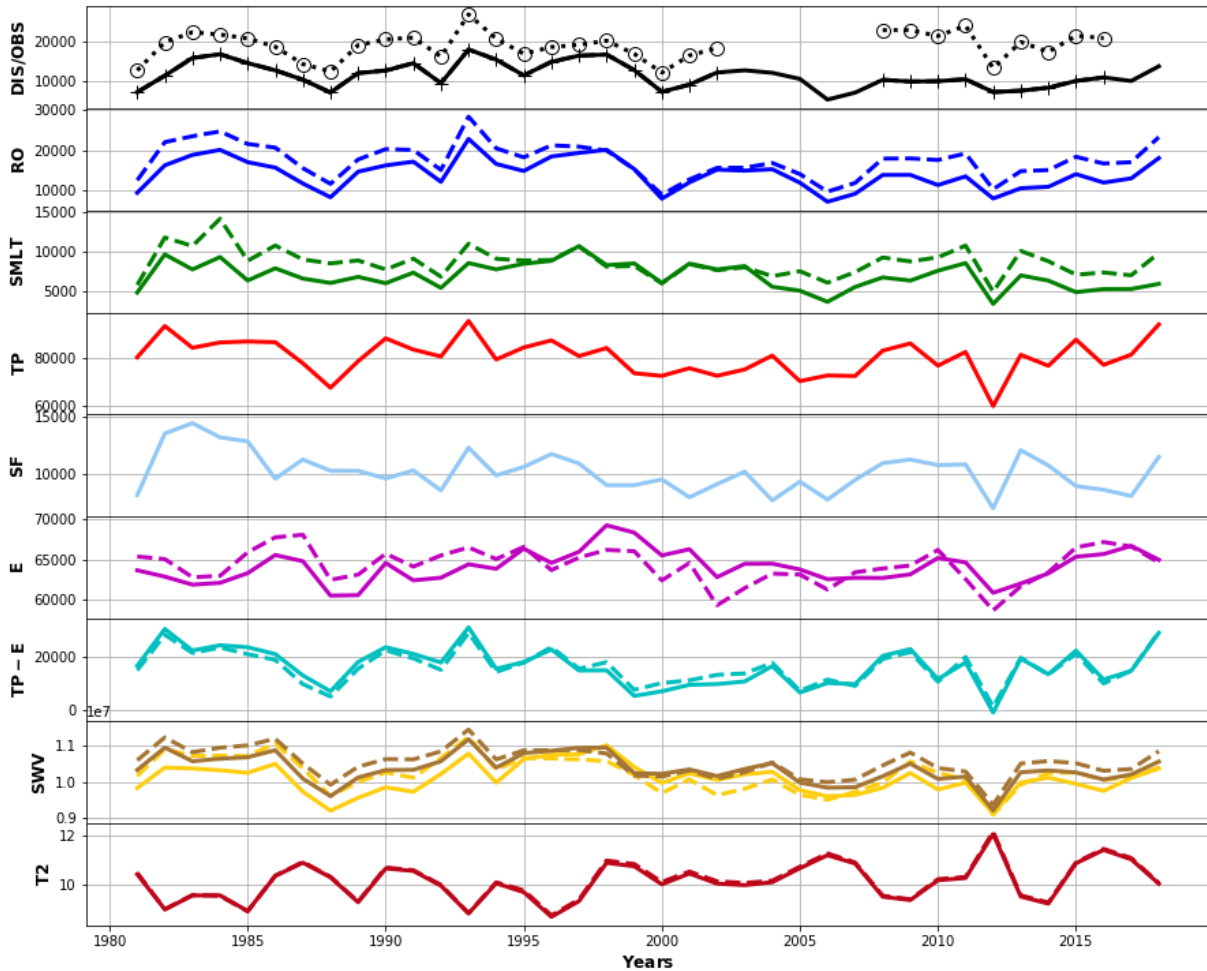
- Discharge T=-0.42 M=14 S= 8
- DisMatchObs T=-0.43 M=14 S= 8
- DisOBS T=-0.27 M= 5 S= 4
- Precip T=-0.13 M=724 S=165
- Snowfall T=-0.16 M=165 S=58
- Runoff T=-0.36 M=17 S= 9
- Runoff Land T=-0.43 M=14 S= 9
- -1*Evap T=0.14 M=-645 S=141
- -1*Evap Land T=0.12 M=-714 S=140
- Snowmelt T=-0.15 M=144 S=54
- Snowmelt Land T=-0.16 M=146 S=53
- Prec - Eva T=-0.05 M=79 S=69
- Prec - Eva Land T=-1.05 M=10 S=50
- SoilMoist7cm T=-0.11 M=89.8k S=16.7k
- SoilMoist7cm Land T=-0.09 M=102.7k S=17.9k
- SoilMoist1m T=-0.10 M=123.5k S=17.7k
- SoilMoist1m Land T=-0.06 M=140.8k S=14.9k
- T2 T=0.43 M=11.64 S=0.78
- T2 Land T=0.44 M=11.67 S=0.78



North America - No.6

River: Mississippi, Outlet: [32.15N; -91.05W], Area: 2963330 km²

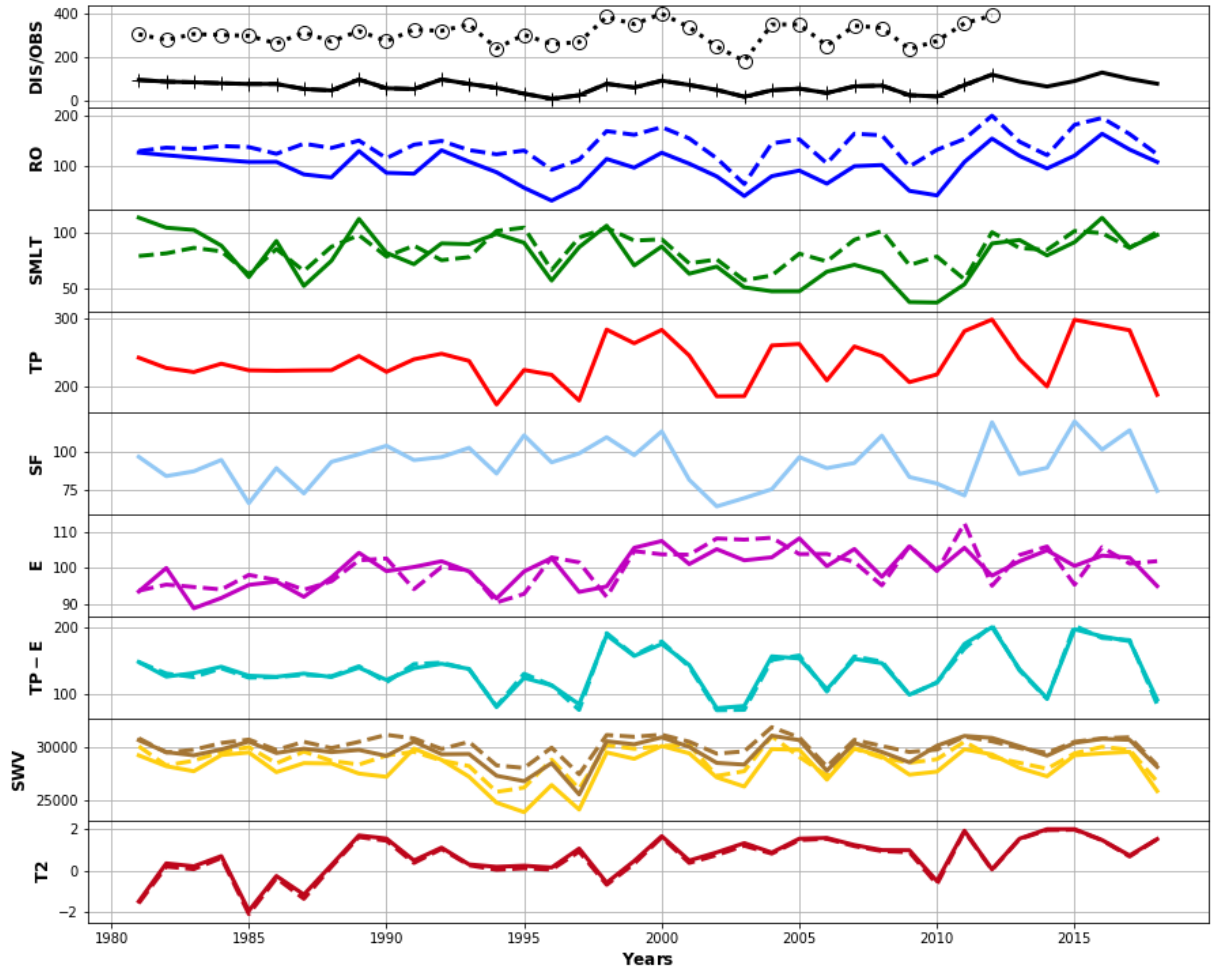
- Discharge T=-0.09 M=11.4k S=3.1k
- DisMatchObs T=-0.11 M=11.7k S=3.1k
- DisOBS T=0.03 M=18.9k S=3.4k
- Precip T=-0.02 M=80.6k S=7.4k
- Snowfall T=-0.06 M=10.2 S=1.7k
- Runoff T=-0.08 M=14.2k S=3.7k
- Runoff Land T=-0.07 M=17.5k S=4.2k
- -1*Evap T=-0.01 M=-64.1k S=1.9k
- -1*Evap Land T=0.01 M=-64.3k S=2.2k
- Snowmelt T=-0.08 M=6.8k S=1.7k
- Snowmelt Land T=-0.06 M=8.6k S=1.8k
- Prec - Eva T=-0.12 M=16.5k S=7.3k
- Prec - Eva Land T=-0.07 M=16.3k S=6.5k
- SoilMoist7cm T=-0.01 M=10.4m S=395.4k
- SoilMoist7cm Land T=-0.02 M=10.5m S=407.4
- SoilMoist1m T=-0.01 M=10.1m S=417.2k
- SoilMoist1m Land T=-0.02 M=10.2m S=458.5k
- T2 T=0.24 M=10.11 S=0.77
- T2 Land T=0.25 M=10.16 S=0.78



Europe - No.1

River: Kalixaelven, Outlet: [66.15N; 22.85E], Area: 10996 km2

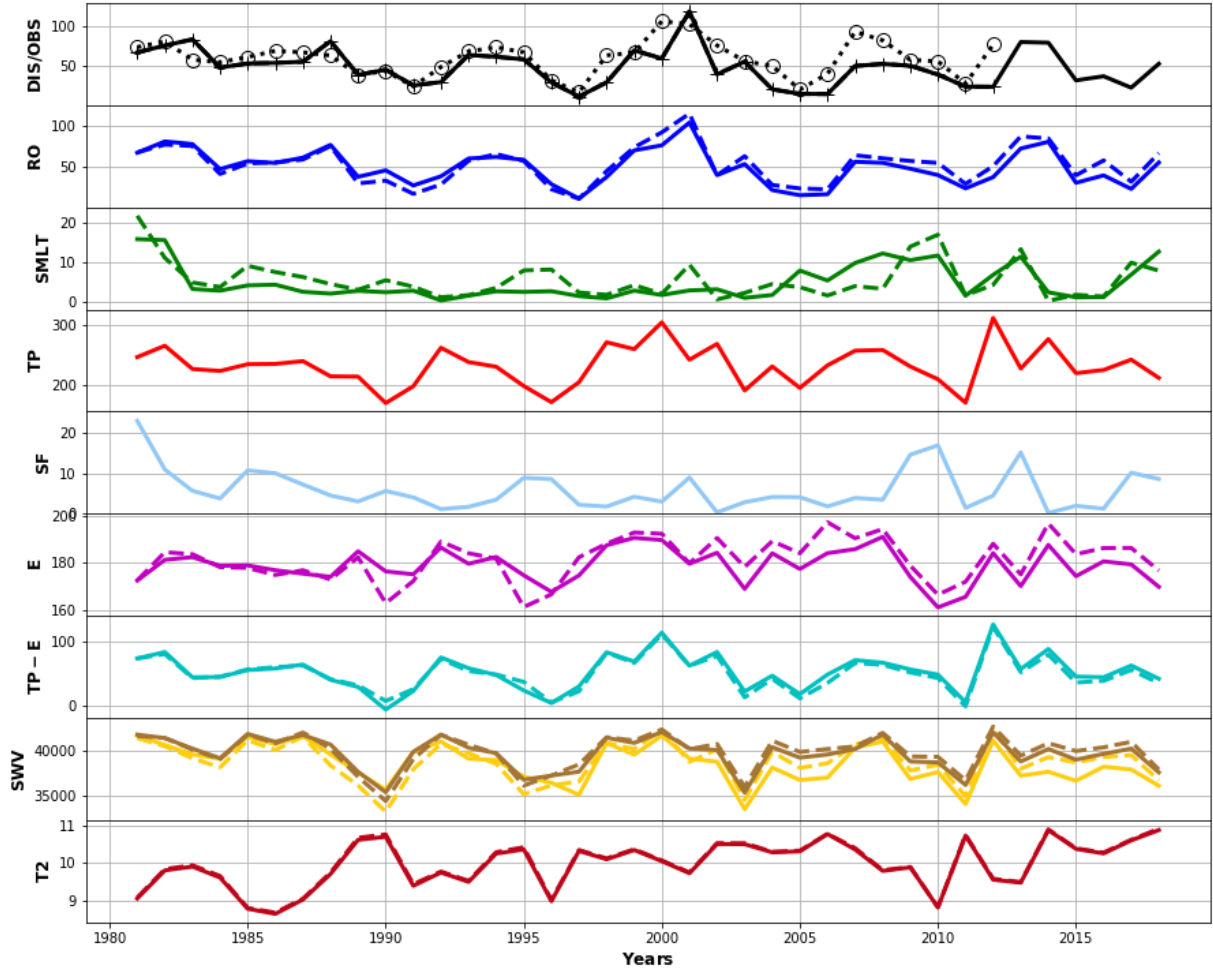
- | | | |
|----------------------------------|-------------------------------------|---|
| — Discharge T=0.02 M=69 S=27 | — -1*Evap T=-0.02 M=-99 S= 4 | — SoilMoist7cm T=0.00 M=29.6k S=1.2k |
| — DisMatchObs T=-0.13 M= 64 S=26 | — -1*Evap Land T=-0.02 M=-100 S= 5 | — SoilMoist7cm Land T=-0.00 M=30.1k S=992 |
| • DisOBS T=0.03 M=307 S=48 | — Snowmelt T=-0.06 M=78 S=20 | — SoilMoist1m T=0.00 M=28.2k S=1.6k |
| — Precip T=0.03 M=236 S=33 | — Snowmelt Land T=0.02 M=83 S=13 | — SoilMoist1m Land T=0.00 M=28.9k S=1.3k |
| — Snowfall T=0.02 M=92 S=14 | — Prec - Eva T=0.04 M=136 S=31 | — T2 T=0.48 M=0.68 S=0.93 |
| — Runoff T=0.01 M=96 S=30 | — Prec - Eva Land T=0.04 M=136 S=33 | — T2 Land T=0.51 M=0.59 S=0.96 |
| — Runoff Land T=0.05 M=139 S=27 | | |



Europe - No.2

River: Thames, Outlet: [51.35N; -0.45W], Area: 9926 km2

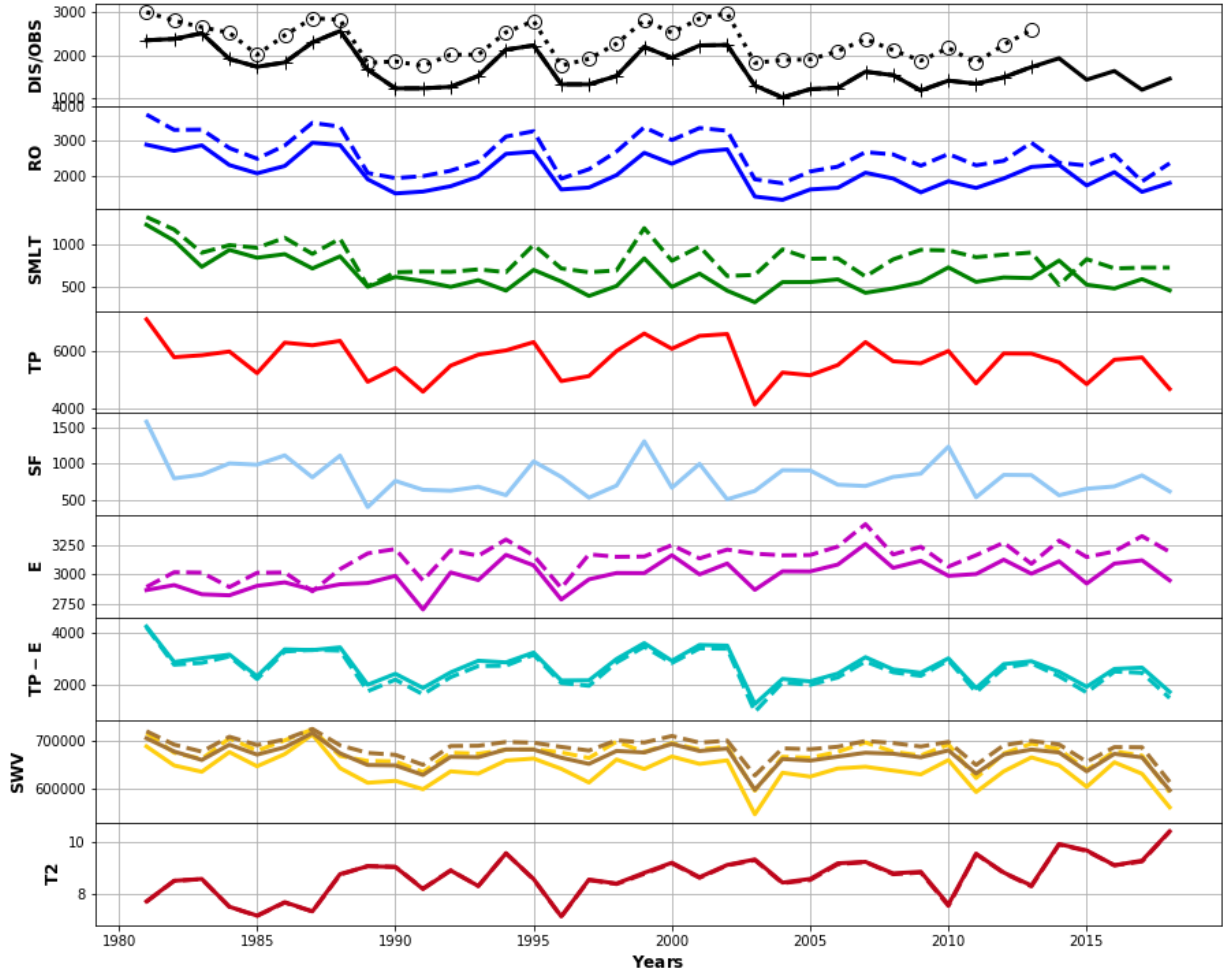
- Discharge T=-0.11 M=49 S=22
- DisMatchObs T=-0.20 M=48 S=23
- DisOBS T=-0.00 M=60 S=21
- Precip T=0.01 M=231 S=32
- Snowfall T=-0.12 M= 5 S= 5
- Runoff T=-0.11 M=50 S=21
- Runoff Land T=-0.00 M=53 S=23
- -1*Evap T=0.00 M=-178 S= 7
- -1*Evap Land T=-0.01 M=-181 S= 8
- Snowmelt T=0.10 M= 4 S= 4
- Snowmelt Land T=-0.10 M= 5 S= 4
- Prec - Eva T=0.05 M=52 S=28
- Prec - Eva Land T=-0.01 M=50 S=27
- SoilMoist7cm T=-0.01 M=39.6k S=1.8k
- SoilMoist7cm Land T=-0.00 M=39.9k S=1.9k
- SoilMoist1m T=-0.02 M=38.6k S=2.2k
- SoilMoist1m Land T=-0.00 M=38.8k S=2.2k
- T2 T=0.26 M=9.97 S=0.61
- T2 Land T=0.25 M=9.99 S=0.61



Europe - No.3

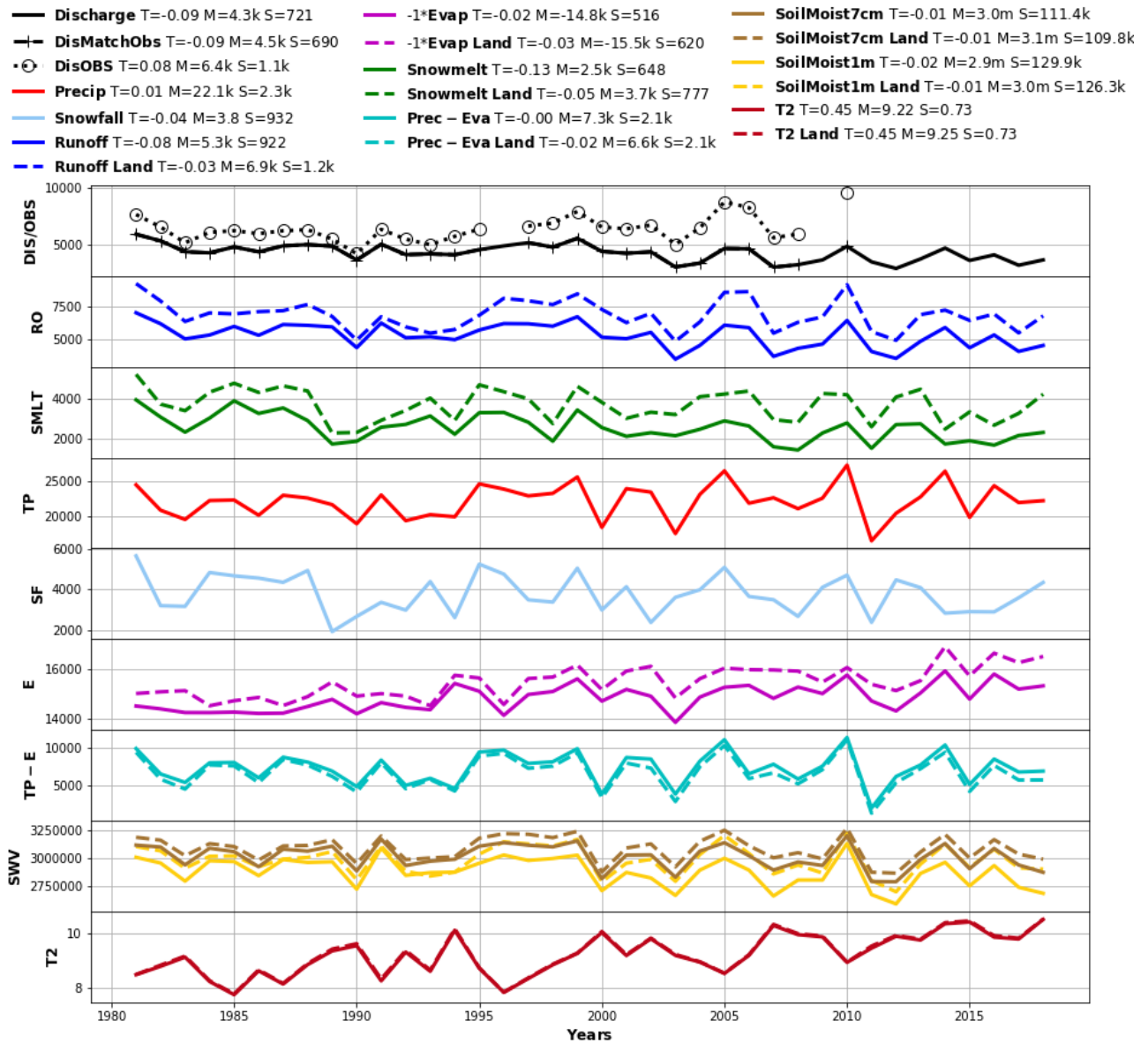
River: Rhine, Outlet: [51.85N; 6.15E], Area: 163315 km²

- Discharge T=-0.12 M=1.7k S=432
- DisMatchObs T=-0.14 M=1.7k S=448
- DisOBS T=-0.06 M=2.3k S=406
- Precip T=-0.03 M=5.7k S=636
- Snowfall T=-0.08 M=811 S=237
- Runoff T=-0.10 M=2.1k S=492
- Runoff Land T=-0.08 M=2.6k S=550
- -1*Evap T=-0.02 M=-3.0k S=113
- -1*Evap Land T=-0.02 M=-3.1k S=125
- Snowmelt T=-0.15 M=626 S=190
- Snowmelt Land T=-0.07 M=832 S=185
- Prec - Eva T=-0.08 M=2.7k S=610
- Prec - Eva Land T=-0.09 M=2.6k S=656
- SoilMoist7cm T=-0.01 M=667.5k S=24.0k
- SoilMoist7cm Land T=-0.01 M=687.1k S=22.0k
- SoilMoist1m T=-0.02 M=639.8k S=31.2k
- SoilMoist1m Land T=-0.01 M=673.3k S=27.2k
- T2 T=0.40 M=8.67 S=0.74
- T2 Land T=0.39 M=8.65 S=0.74



Europe - No.4

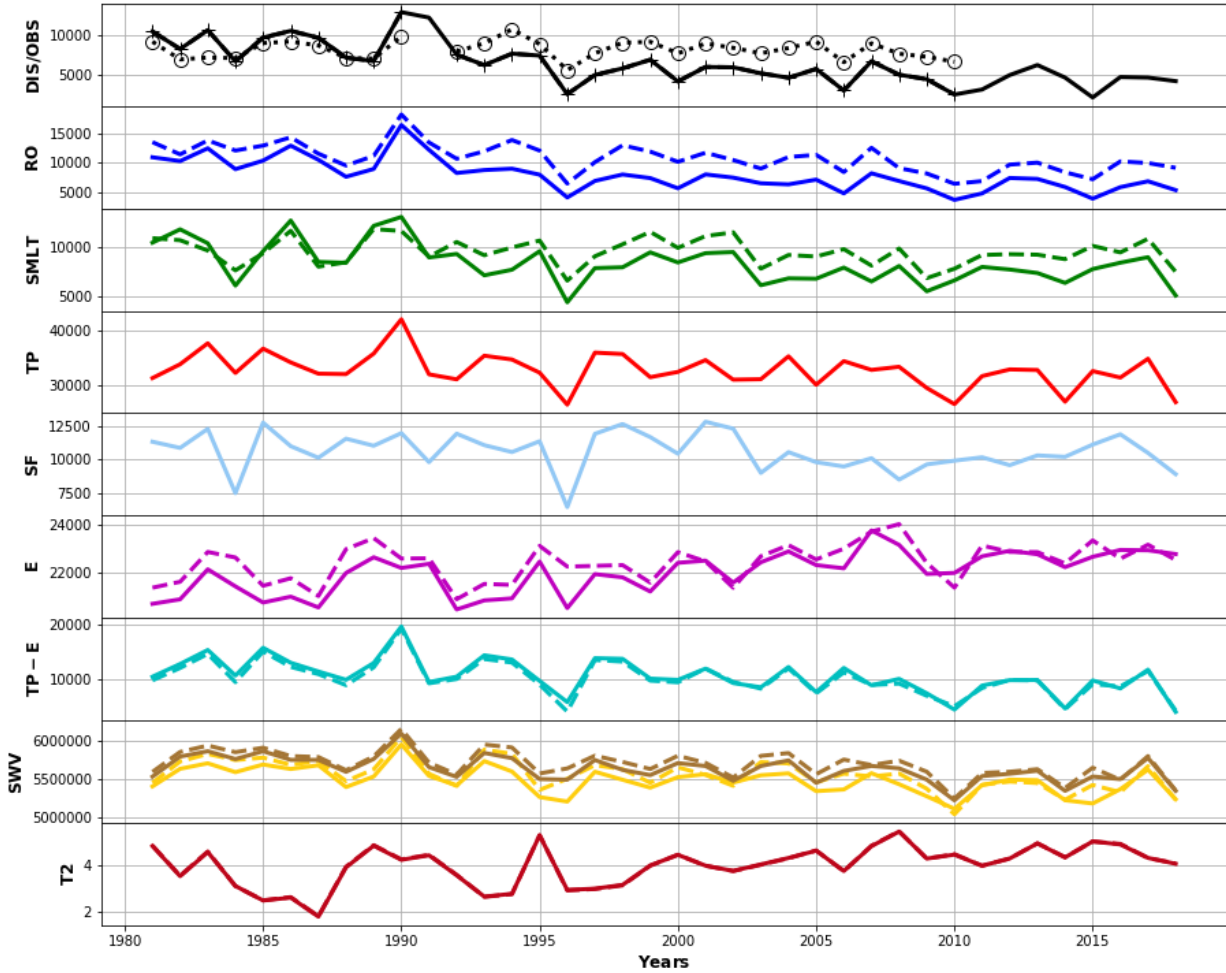
River: Danube, Outlet: [45.25N; 28.75E], Area: 788003 km2



Europe - No.5

River: Volga, Outlet: [48.85N; 44.65E], Area: 1445620 km²

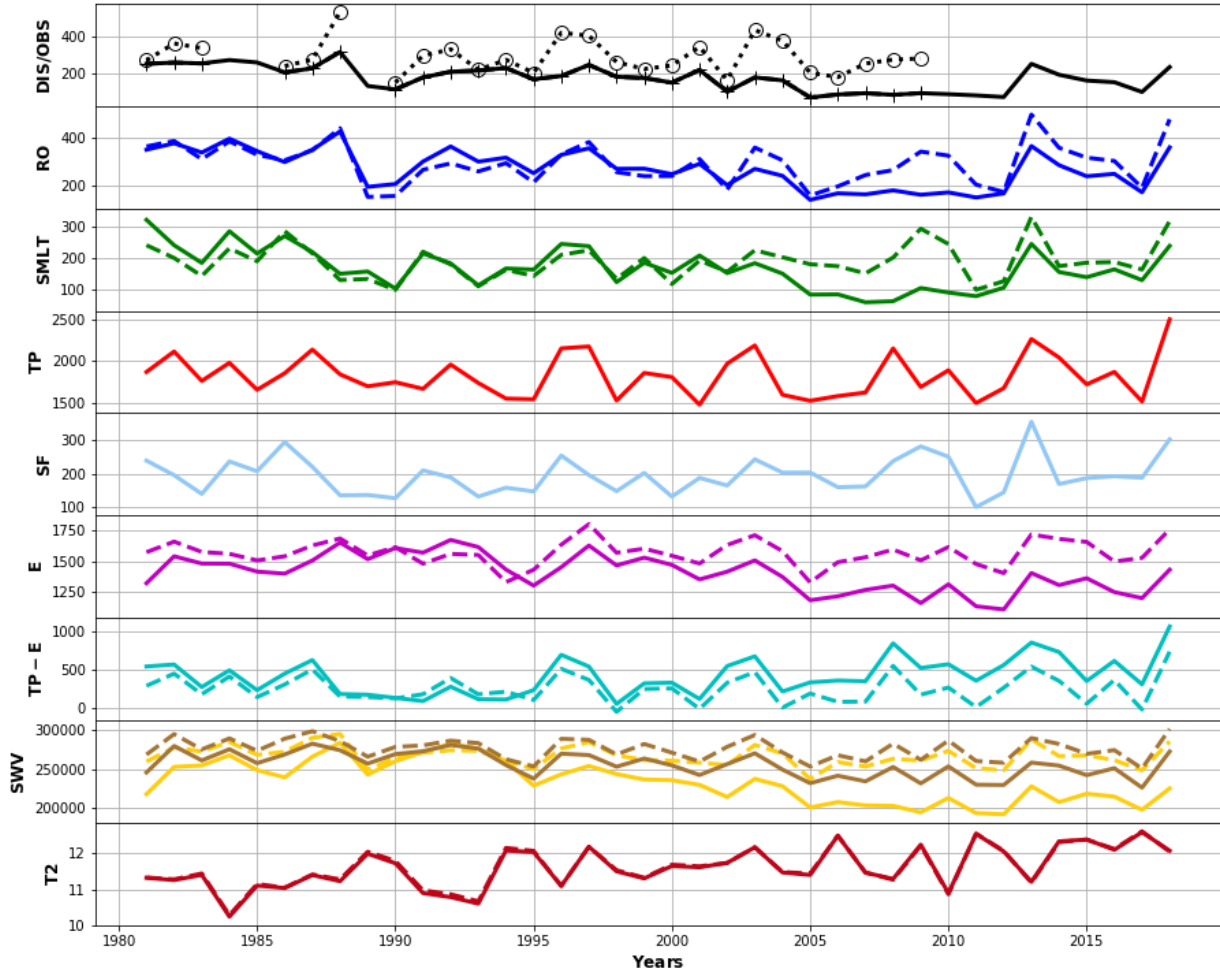
- **Discharge** T=-0.27 M=6.4k S=2.6k
- **DisMatchObs** T=-0.32 M=6.7k S=2.5k
- **DisOBS** T=-0.02 M=8.1k S=1.1k
- **Precip** T=-0.03 M=32.7k S=3.1k
- **Snowfall** T=-0.03 M=10.6 S=1.4k
- **Runoff** T=-0.22 M=7.8k S=2.7k
- **Runoff Land** T=-0.13 M=10.8k S=2.4k
- **-1*Evap** T=-0.02 M=-22.0k S=849
- **-1*Evap Land** T=-0.01 M=-22.4k S=759
- **Snowmelt** T=-0.12 M=8.3k S=2.0k
- **Snowmelt Land** T=-0.03 M=9.5k S=1.4k
- **Prec - Eva** T=-0.16 M=10.7k S=3.2k
- **Prec - Eva Land** T=-0.14 M=10.2k S=3.1k
- **SoilMoist7cm** T=-0.01 M=5.6m S=167.0k
- **SoilMoist7cm Land** T=-0.02 M=5.7m S=178.1k
- **SoilMoist1m** T=-0.02 M=5.5m S=175.9k
- **SoilMoist1m Land** T=-0.02 M=5.6m S=200.6k
- **T2** T=0.35 M=3.97 S=0.84
- **T2 Land** T=0.35 M=3.97 S=0.85



Europe - No.6

River: Ebro, Outlet: [40.85N; 0.55E], Area: 85737 km²

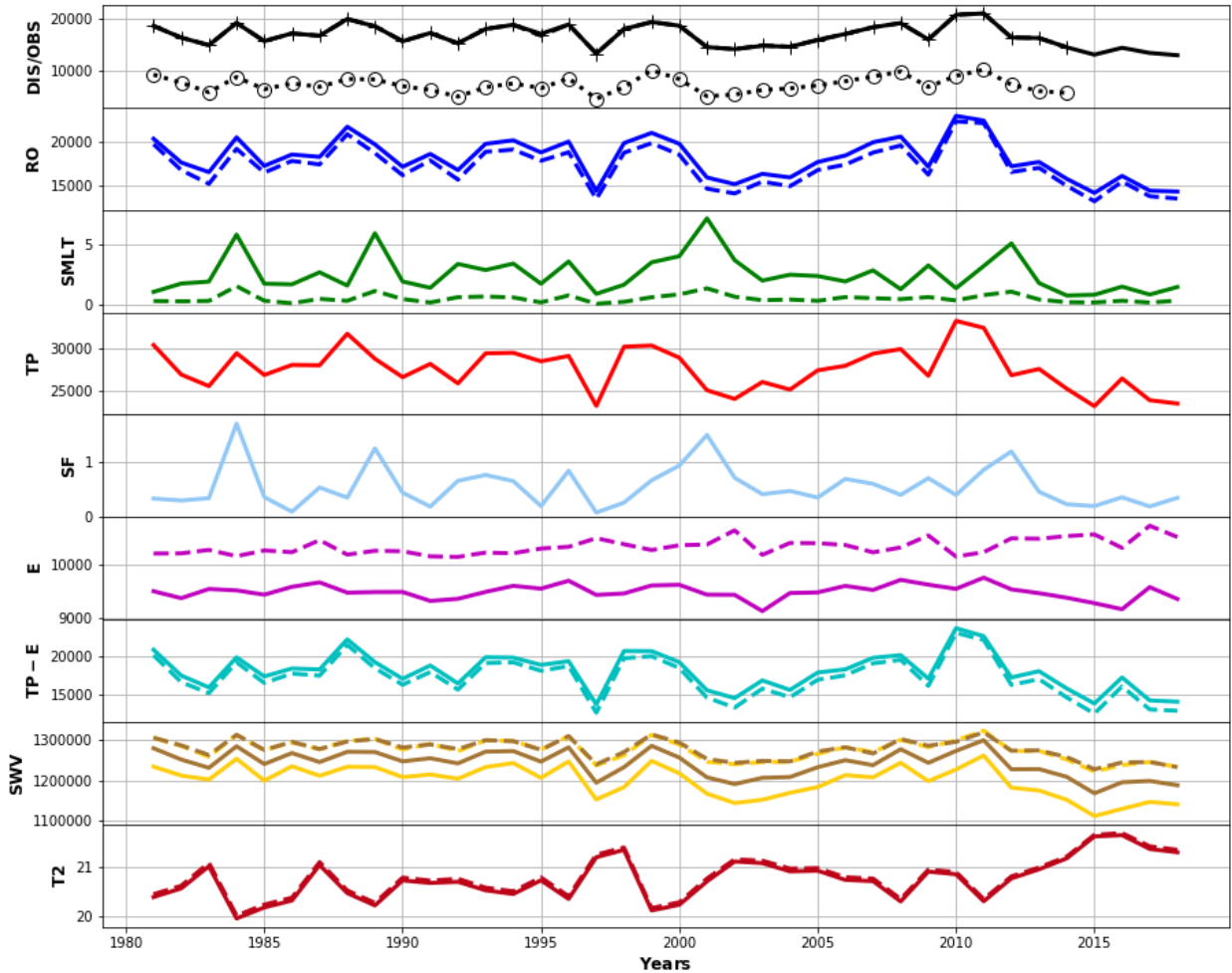
- | | | |
|----------------------------------|--------------------------------------|--|
| — Discharge T=-0.20 M=176 S=65 | — -1*Evap T=0.06 M=-1.4k S=147 | — SoilMoist7cm T=-0.03 M=256.2k S=16.0k |
| — DisMatchObs T=-0.36 M=180 S=63 | — -1*Evap Land T=-0.00 M=-1.6k S=102 | — SoilMoist7cm Land T=-0.01 M=276.2k S=13.4k |
| • DisOBS T=-0.07 M=290 S=88 | — Snowmelt T=-0.17 M=168 S=63 | — SoilMoist1m T=-0.08 M=233.5k S=26.3k |
| — Precip T=0.00 M=1.8k S=249 | — Snowmelt Land T=0.04 M=189 S=55 | — SoilMoist1m Land T=-0.01 M=267.1k S=13.2k |
| — Snowfall T=0.04 M=195 S=54 | — Prec - Eva T=0.21 M=422 S=237 | — T2 T=0.29 M=11.59 S=0.56 |
| — Runoff T=-0.15 M=268 S=80 | — Prec - Eva Land T=0.00 M=258 S=182 | — T2 Land T=0.28 M=11.61 S=0.55 |
| — Runoff Land T=-0.02 M=292 S=86 | | |



South America - No.1

River: Magdalena, Outlet: [10.15N; -74.95W], Area: 259487 km2

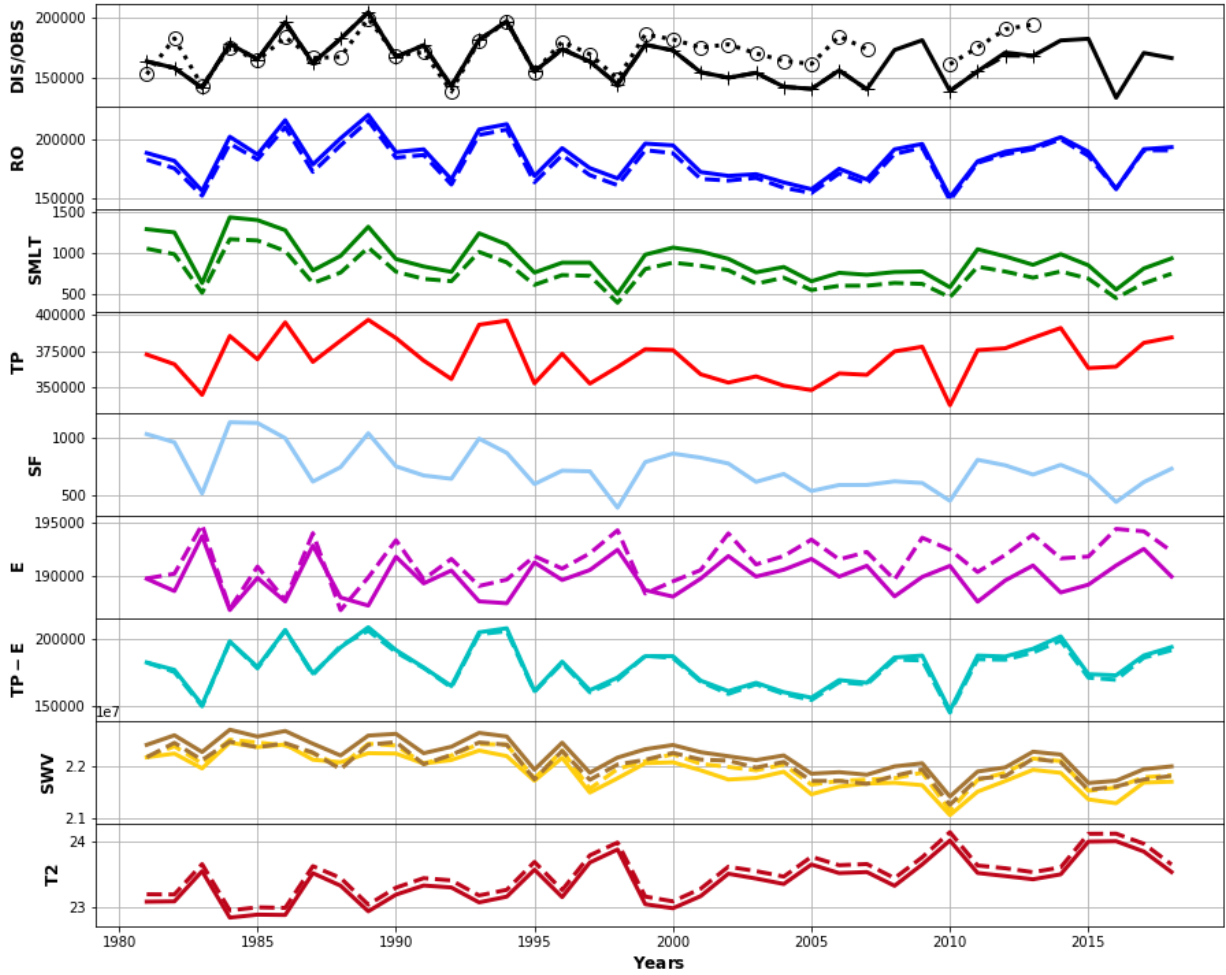
- Discharge T=-0.03 M=16.7k S=2.2k
- DisMatchObs T=-0.00 M=17.1k S=2.0k
- DisOBS T=0.01 M=7.4k S=1.4k
- Precip T=-0.02 M=27.6k S=2.5k
- Snowfall T=nan M= 0 S= 0
- Runoff T=-0.04 M=18.1k S=2.3k
- Runoff Land T=-0.03 M=17.2k S=2.4k
- -1*Evap T=0.00 M=-9.5k S=134
- -1*Evap Land T=-0.01 M=-10.3k S=147
- Snowmelt T=-0.08 M= 2 S= 1
- Snowmelt Land T=-0.04 M= 0 S= 0
- Prec - Eva T=-0.03 M=18.1k S=2.4k
- Prec - Eva Land T=-0.04 M=17.2k S=2.5k
- SoilMoist7cm T=-0.01 M=1.2m S=32.2k
- SoilMoist7cm Land T=-0.01 M=1.3m S=24.1k
- SoilMoist1m T=-0.02 M=1.2m S=37.9k
- SoilMoist1m Land T=-0.01 M=1.3m S=25.5k
- T2 T=0.21 M=20.76 S=0.42
- T2 Land T=0.21 M=20.81 S=0.41



South America - No.2

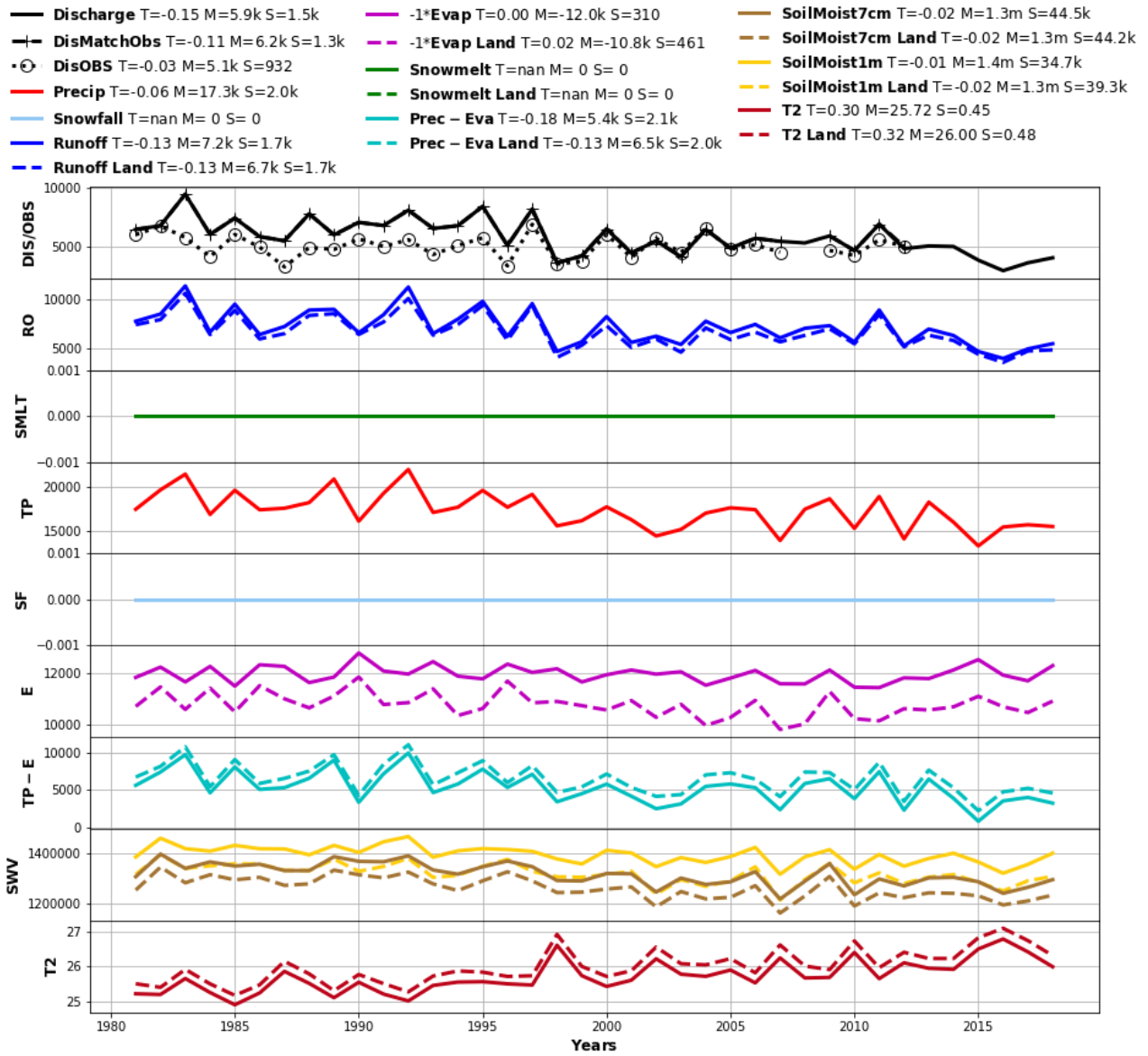
River: Amazon, Outlet: [-1.95S; -55.55W], Area: 4664200 km²

- Discharge T=-0.02 M=165.1k S=17.1k
- DisMatchObs T=-0.04 M=163.9k S=17.2k
- DisOBS T=0.02 M=172.4k S=14.5k
- Precip T=-0.00 M=370.3k S=15.0k
- Snowfall T=-0.12 M=737 S=184
- Runoff T=-0.02 M=184.7k S=17.1k
- Runoff Land T=-0.01 M=180.5k S=16.8k
- -1*Evap T=-0.00 M=-189.9k S=1.7k
- -1*Evap Land T=-0.00 M=-191.4k S=2.1k
- Snowmelt T=-0.12 M=920 S=232
- Snowmelt Land T=-0.12 M=746 S=189
- Prec - Eva T=-0.01 M=180.4k S=16.1k
- Prec - Eva Land T=-0.01 M=178.9k S=16.0k
- SoilMoist7cm T=-0.01 M=22.2m S=317.9k
- SoilMoist7cm Land T=-0.01 M=22.0m S=306.6
- SoilMoist1m T=-0.01 M=21.9m S=336.0k
- SoilMoist1m Land T=-0.01 M=22.0m S=317.8k
- T2 T=0.19 M=23.39 S=0.32
- T2 Land T=0.19 M=23.50 S=0.32



South America - No.3

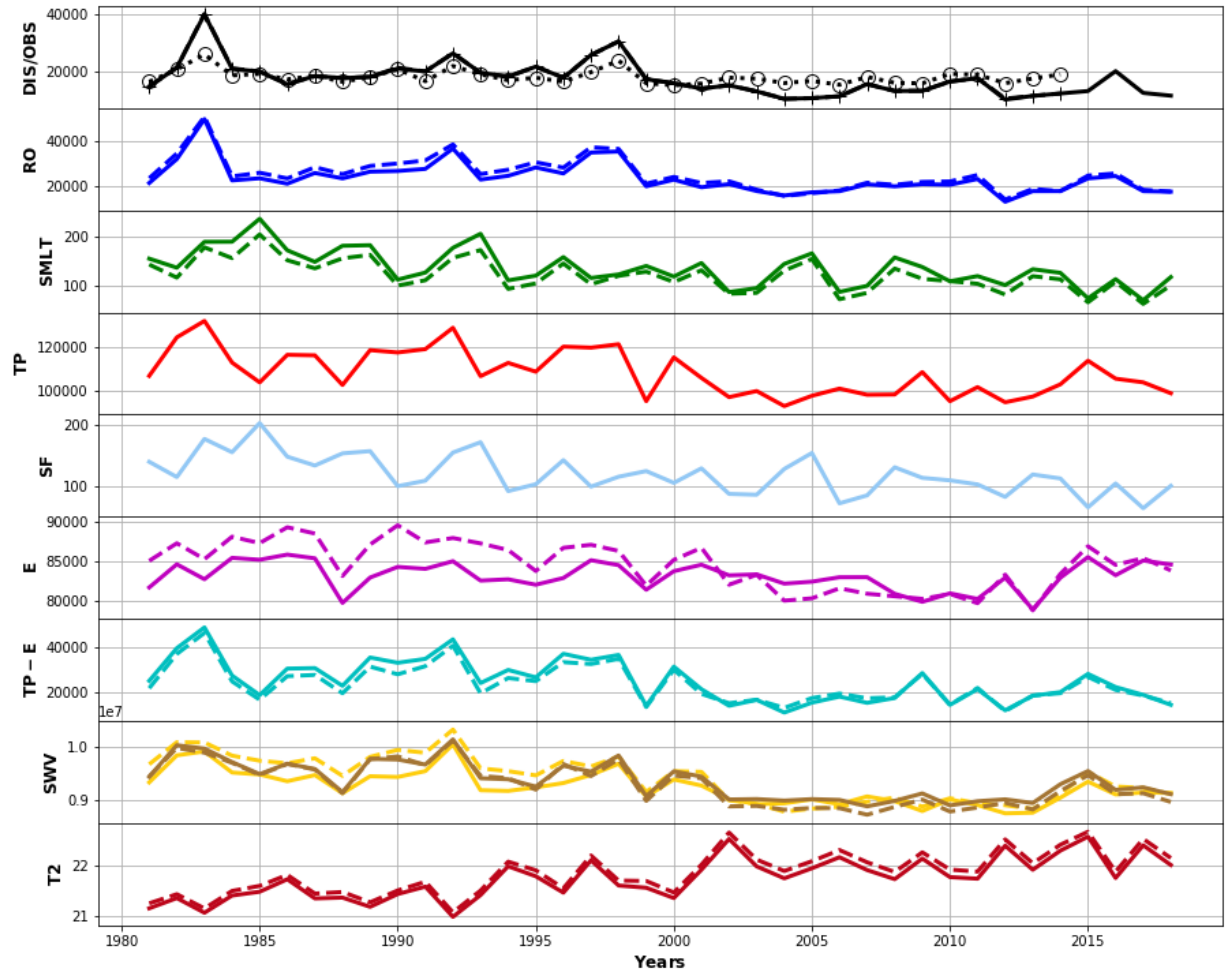
River: Araguaia, Outlet: [-8.35S; -49.25W], Area: 319643 km2



South America - No.4

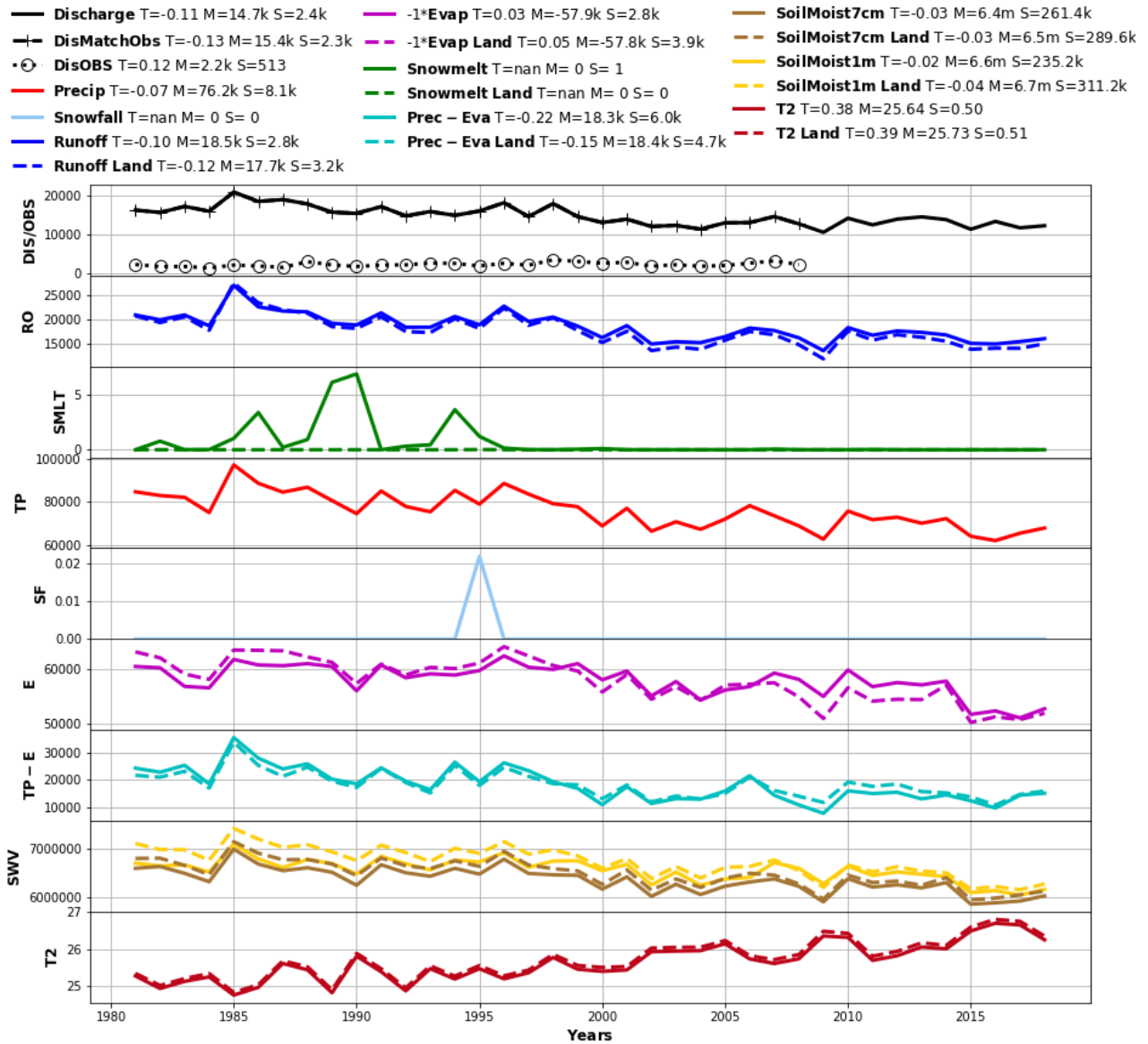
River: Parana, Outlet: [-32.75S; -60.75W], Area: 2430030 km2

- Discharge T=-0.17 M=17.5k S=5.9k
- DisMatchObs T=-0.19 M=17.9k S=6.0k
- DisOBS T=-0.05 M=18.2k S=2.4k
- Precip T=-0.05 M=108.1k S=10.2k
- Snowfall T=-0.15 M=119 S=32
- Runoff T=-0.14 M=23.6k S=6.8k
- Runoff Land T=-0.16 M=25.1k S=7.2k
- -1*Evap T=0.00 M=-83.2k S=1.7k
- -1*Evap Land T=0.02 M=-84.6k S=2.9k
- Snowmelt T=-0.16 M=136 S=37
- Snowmelt Land T=-0.16 M=120 S=32
- Prec - Eva T=-0.21 M=24.9k S=9.5k
- Prec - Eva Land T=-0.17 M=23.5k S=8.2k
- SoilMoist7cm T=-0.02 M=9.4m S=344.5k
- SoilMoist7cm Land T=-0.03 M=9.3m S=388.1k
- SoilMoist1m T=-0.02 M=9.2m S=307.0k
- SoilMoist1m Land T=-0.03 M=9.4m S=419.7k
- T2 T=0.27 M=21.74 S=0.40
- T2 Land T=0.29 M=21.86 S=0.41



Africa - No.1

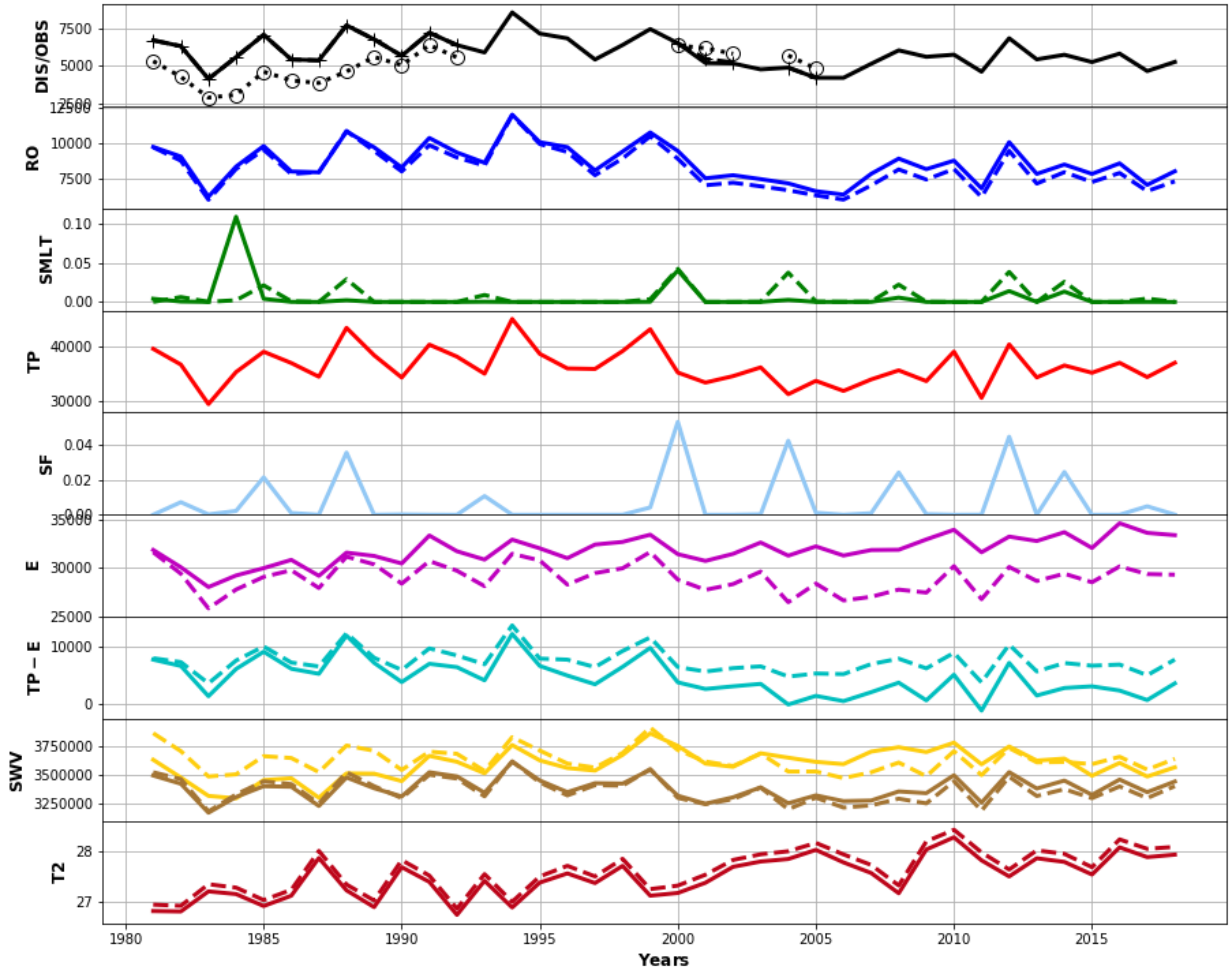
River: Nile, Outlet: [19.15N; 30.45E], Area: 2586140 km2



Africa - No.2

River: Niger, Outlet: [7.75N; 6.75E], Area: 2094830 km²

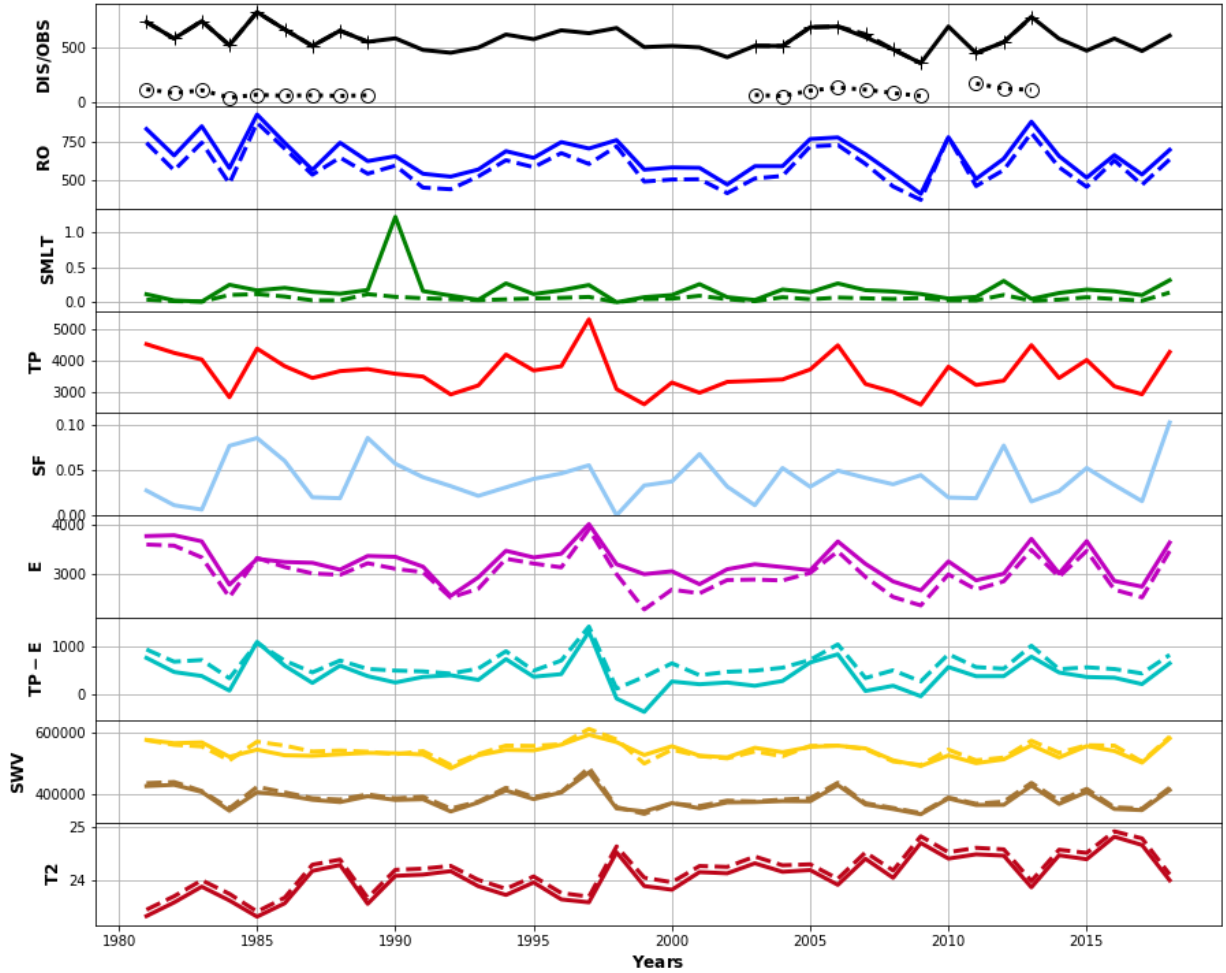
- Discharge T=-0.06 M=5.9k S=1.0k
- DisMatchObs T=-0.09 M=5.9k S=997
- DisOBS T=0.28 M=4.9k S=1.0k
- Precip T=-0.02 M=36.4k S=3.4k
- Snowfall T=nan M= 0 S= 0
- Runoff T=-0.05 M=8.6k S=1.3k
- Runoff Land T=-0.07 M=8.2k S=1.4k
- -1*Evap T=-0.03 M=-31.8k S=1.4k
- -1*Evap Land T=0.01 M=-29.0k S=1.5k
- Snowmelt T=nan M= 0 S= 0
- Snowmelt Land T=nan M= 0 S= 0
- Prec - Eva T=-0.35 M=4.6k S=3.1k
- Prec - Eva Land T=-0.06 M=7.4k S=2.1k
- SoilMoist7cm T=-0.00 M=3.4m S=98.7k
- SoilMoist7cm Land T=-0.01 M=3.4m S=108.6k
- SoilMoist1m T=0.02 M=3.6m S=129.1k
- SoilMoist1m Land T=-0.01 M=3.6m S=106.5k
- T2 T=0.27 M=27.49 S=0.41
- T2 Land T=0.28 M=27.63 S=0.42



Africa - No.3

River: Shabelle, Outlet: [3.85N; 45.55E], Area: 210122 km²

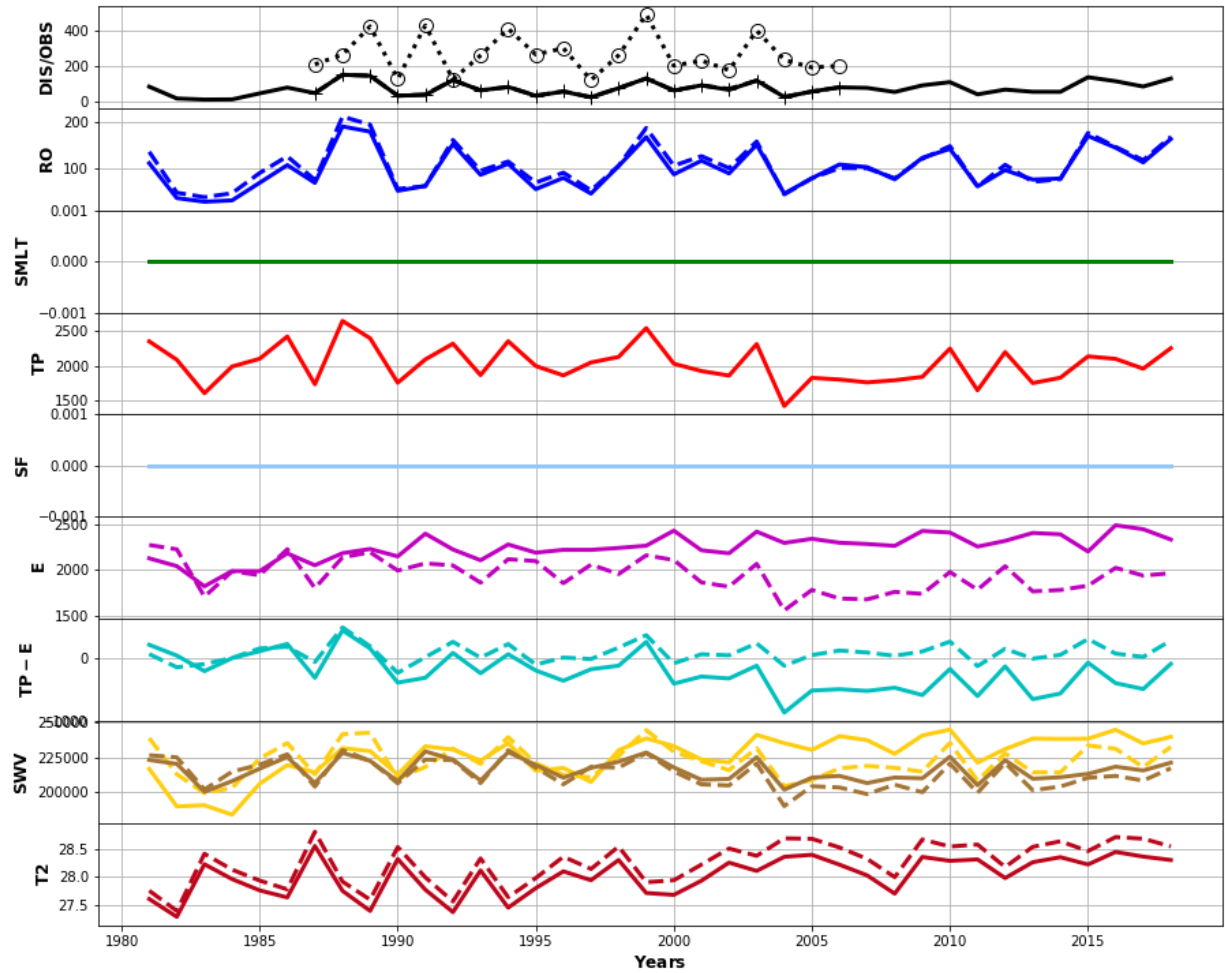
- Discharge T=-0.04 M=579 S=104
- DisMatchObs T=-0.12 M=604 S=119
- DisOBS T=0.27 M=91 S=33
- Precip T=-0.03 M=3.6k S=588
- Snowfall T=nan M= 0 S= 0
- Runoff T=-0.04 M=651 S=117
- Runoff Land T=-0.03 M=585 S=119
- -1*Evap T=0.02 M=-3.2k S=349
- -1*Evap Land T=0.03 M=-3.0k S=379
- Snowmelt T=nan M= 0 S= 0
- Snowmelt Land T=nan M= 0 S= 0
- Prec - Eva T=-0.08 M=392 S=308
- Prec - Eva Land T=-0.03 M=603 S=249
- SoilMoist7cm T=-0.02 M=384.3k S=29.8k
- SoilMoist7cm Land T=-0.02 M=390.7k S=32.1k
- SoilMoist1m T=-0.01 M=539.9k S=24.6k
- SoilMoist1m Land T=-0.01 M=544.2k S=26.7k
- T2 T=0.23 M=24.06 S=0.37
- T2 Land T=0.24 M=24.18 S=0.37



Africa - No.4

River: White-Volta, Outlet: [9.75N; -0.95W], Area: 93343 km2

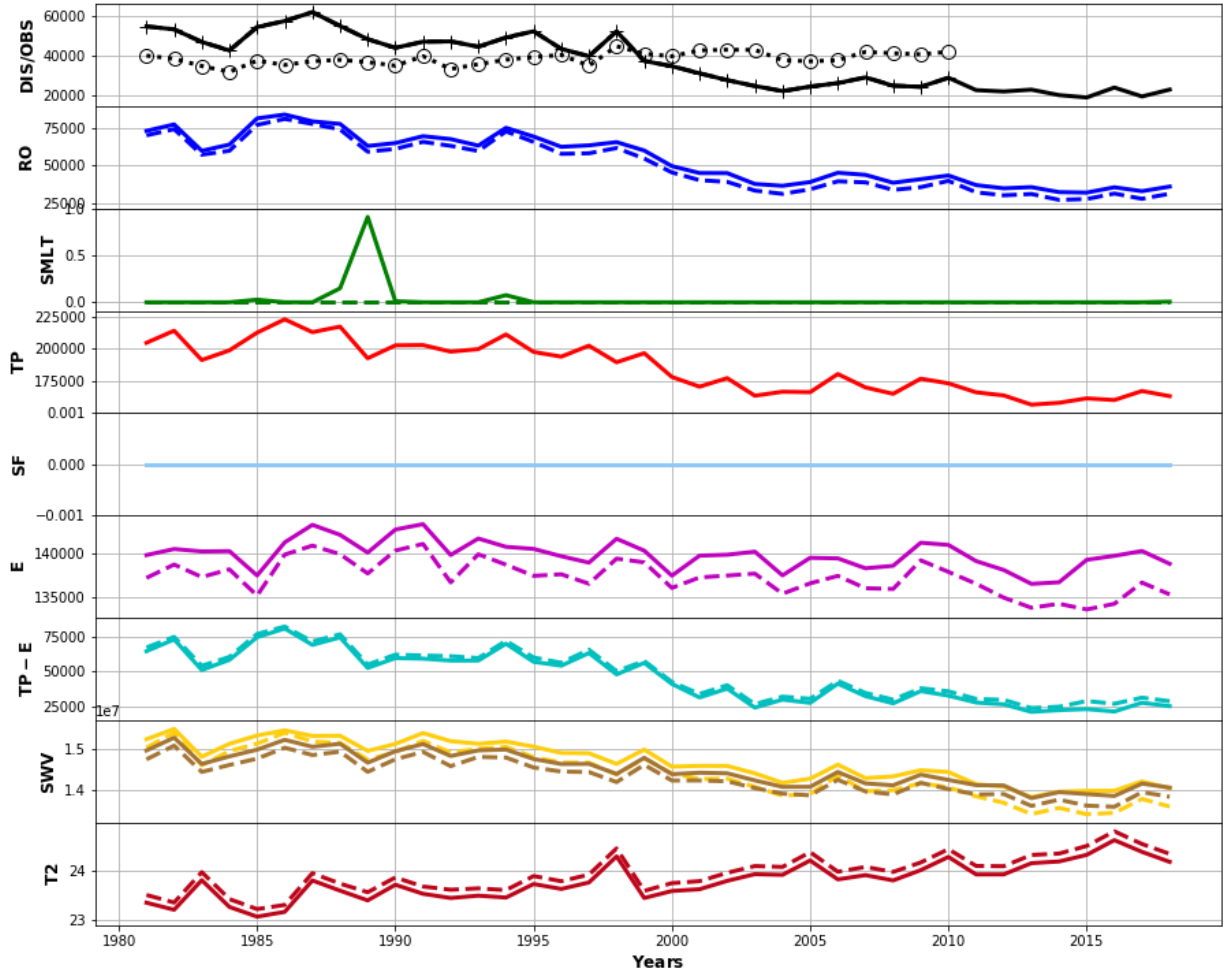
- Discharge T=0.14 M=73 S=37
- DisMatchObs T=-0.12 M=76 S=38
- DisOBS T=-0.08 M=267 S=107
- Precip T=-0.03 M=2.0k S=266
- Snowfall T=nan M=0 S=0
- Runoff T=0.12 M=98 S=43
- Runoff Land T=0.07 M=106 S=45
- -1*Evap T=-0.04 M=-2.2k S=144
- -1*Evap Land T=0.04 M=-1.9k S=177
- Snowmelt T=nan M=0 S=0
- Snowmelt Land T=nan M=0 S=0
- Prec - Eva T=-0.67 M=-227 S=291
- Prec - Eva Land T=0.25 M=77 S=152
- SoilMoist7cm T=-0.01 M=215.6k S=8.1k
- SoilMoist7cm Land T=-0.02 M=212.6k S=10.4k
- SoilMoist1m T=0.04 M=225.9k S=15.2k
- SoilMoist1m Land T=0.00 M=221.9k S=11.9k
- T2 T=0.17 M=28.01 S=0.34
- T2 Land T=0.21 M=28.25 S=0.38



Africa - No.5

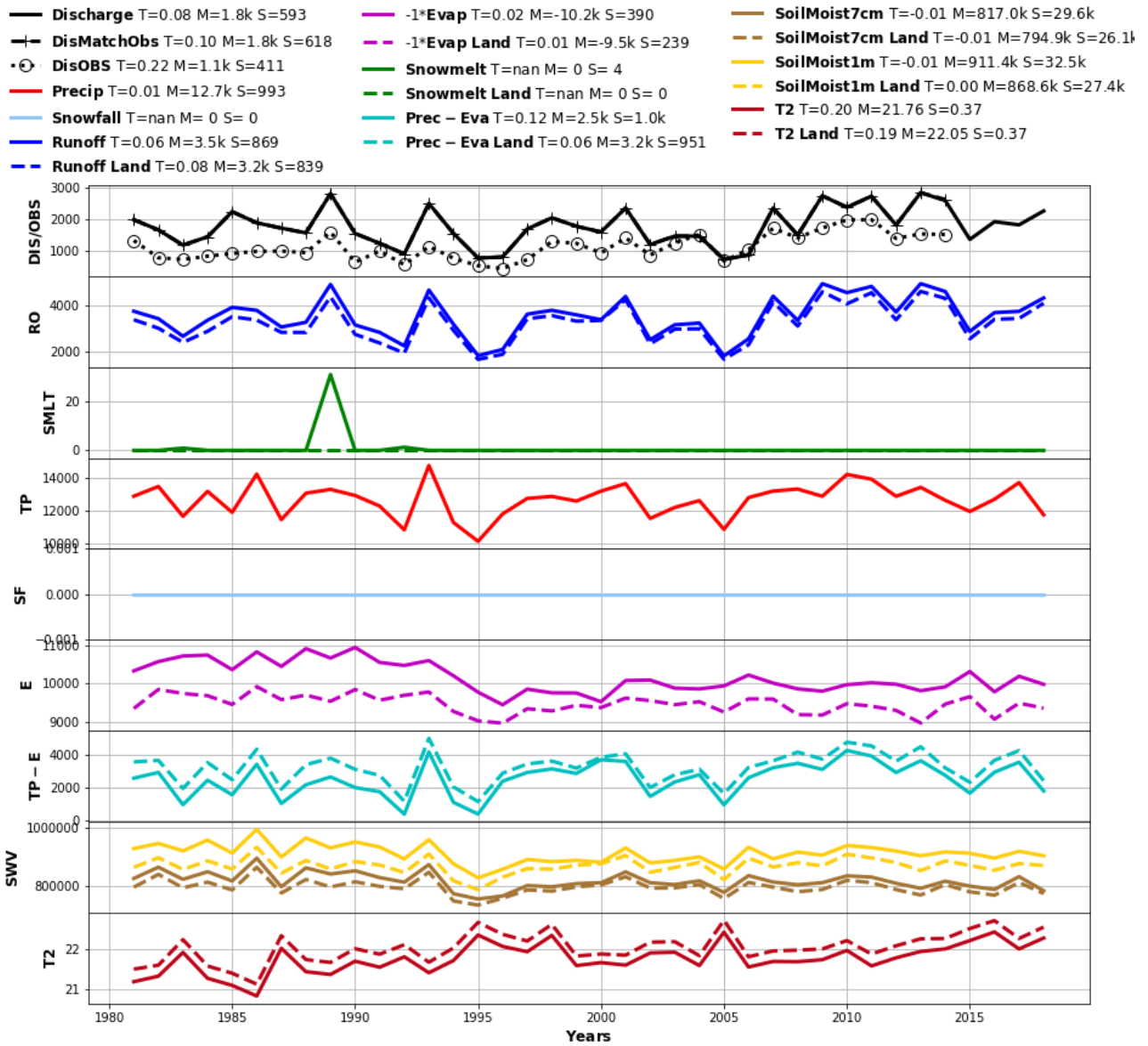
River: Congo, Outlet: [-4.05S; 15.65E], Area: 3618130 km²

- **Discharge** T=-0.30 M=36.8k S=13.4k
- **DisMatchObs** T=-0.29 M=41.0k S=12.0k
- **DisOBS** T=0.05 M=38.6k S=3.1k
- **Precip** T=-0.08 M=185.7k S=19.3k
- **Snowfall** T=nan M= 0 S= 0
- **Runoff** T=-0.25 M=54.1k S=16.4k
- **Runoff Land** T=-0.28 M=49.8k S=17.0k
- **-1*Evap** T=0.01 M=-140.0k S=1.7k
- **-1*Evap Land** T=0.01 M=-137.3k S=2.0k
- **Snowmelt** T=nan M= 0 S= 0
- **Snowmelt Land** T=nan M= 0 S= 0
- **Prec - Eva** T=-0.33 M=45.8k S=18.3k
- **Prec - Eva Land** T=-0.30 M=48.4k S=17.9k
- **SoilMoist7cm** T=-0.02 M=14.5m S=411.1k
- **SoilMoist7cm Land** T=-0.02 M=14.3m S=418.2
- **SoilMoist1m** T=-0.03 M=14.7m S=481.2k
- **SoilMoist1m Land** T=-0.03 M=14.4m S=583.0k
- **T2** T=0.28 M=23.79 S=0.37
- **T2 Land** T=0.28 M=23.95 S=0.37



Africa - No.6

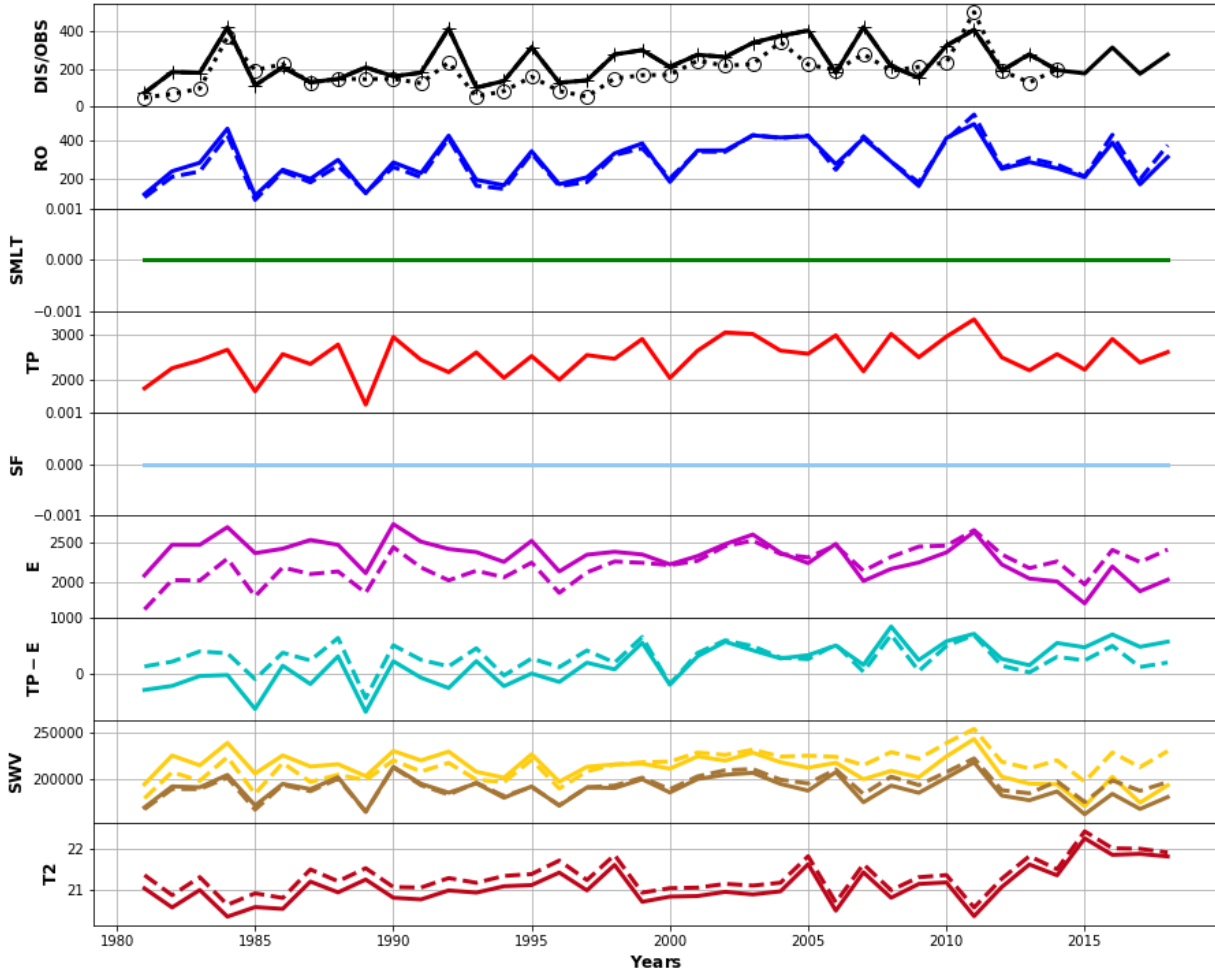
River: Zambesi-upstream, Outlet: [-17.45S; 24.35E], Area: 331113 km2



Africa - No.7

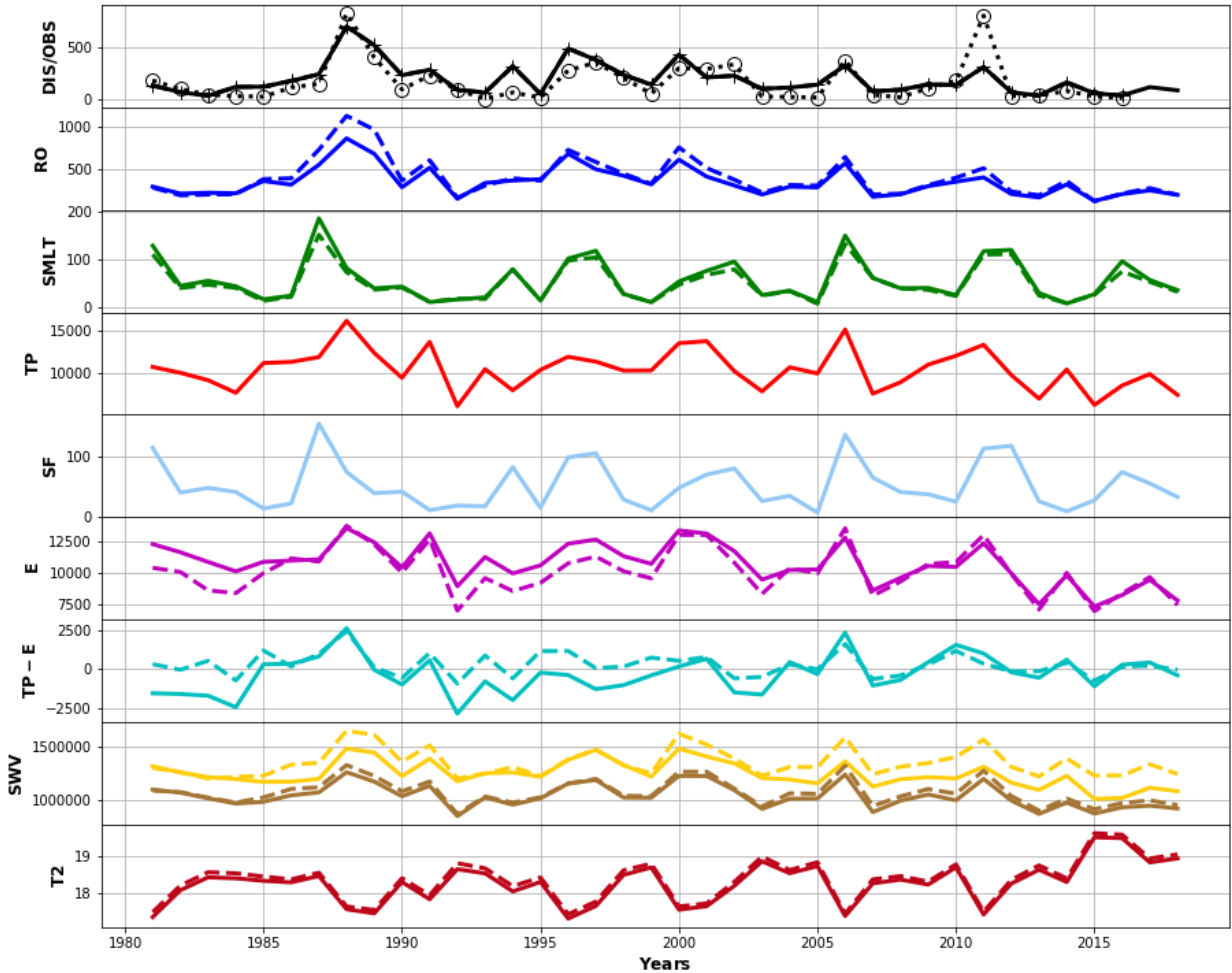
River: Cunene, Outlet: [-17.45S; 14.15E], Area: 85253 km2

- Discharge T=0.12 M=237 S=99
- DisMatchObs T=0.16 M=237 S=102
- DisOBS T=0.21 M=183 S=93
- Precip T=0.05 M=2.5k S=399
- Snowfall T=nan M= 0 S= 0
- Runoff T=0.09 M=284 S=104
- Runoff Land T=0.15 M=280 S=110
- -1*Evap T=0.05 M=-2.3k S=216
- -1*Evap Land T=-0.05 M=-2.2k S=205
- Snowmelt T=nan M= 0 S= 0
- Snowmelt Land T=nan M= 0 S= 0
- Prec - Eva T=1.25 M=190 S=357
- Prec - Eva Land T=0.09 M=288 S=248
- SoilMoist7cm T=-0.01 M=189.8k S=13.2k
- SoilMoist7cm Land T=0.02 M=193.5k S=12.8k
- SoilMoist1m T=-0.03 M=212.1k S=15.4k
- SoilMoist1m Land T=0.04 M=215.3k S=15.1k
- T2 T=0.22 M=21.09 S=0.44
- T2 Land T=0.18 M=21.32 S=0.42



River: Orange, Outlet: [-28.75S; 17.65E], Area: 734698 km2

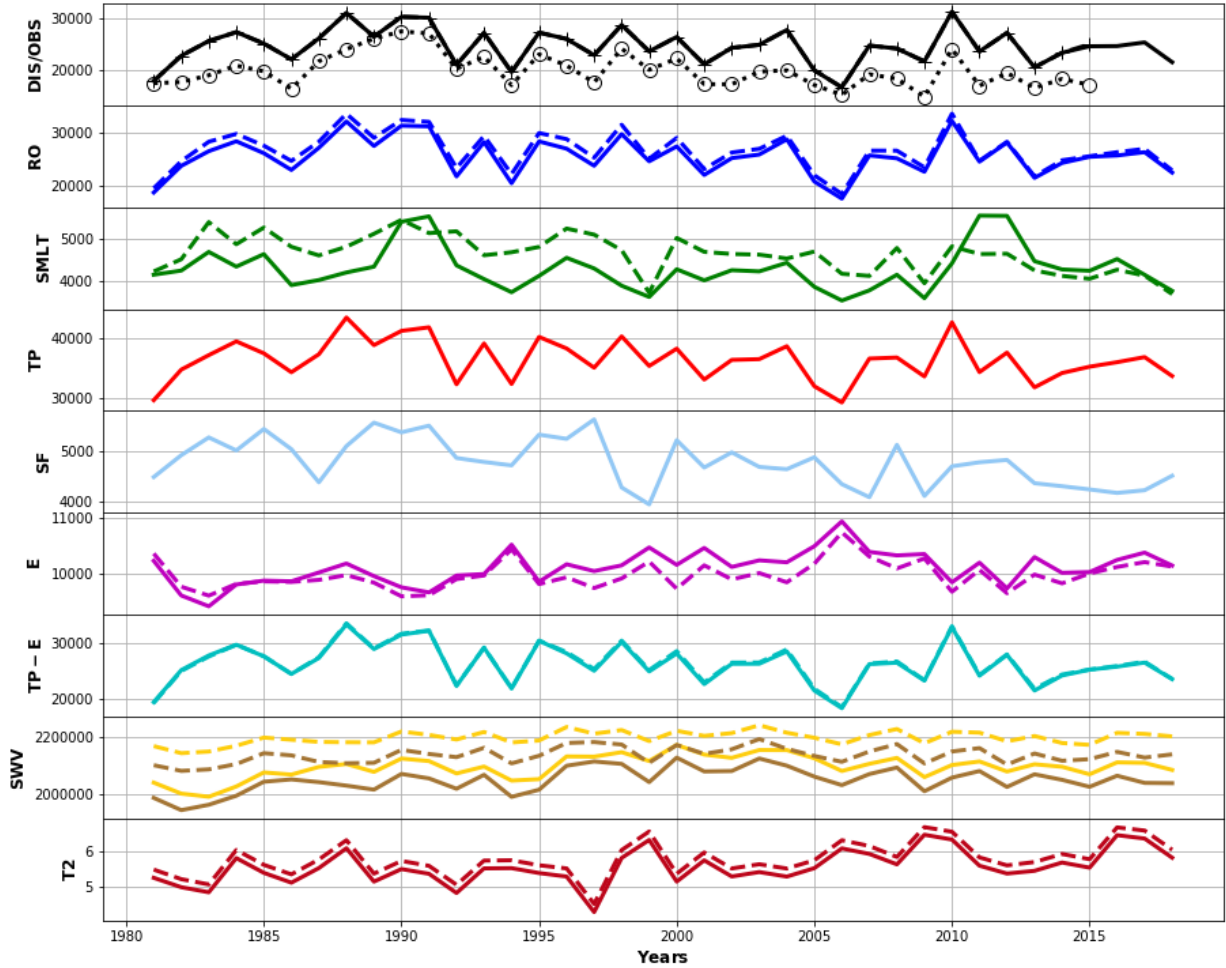
- Discharge T=-0.18 M=196 S=148
- DisMatchObs T=-0.16 M=200 S=151
- DisOBS T=-0.07 M=170 S=194
- Precip T=-0.04 M=10.4k S=2.3k
- Snowfall T=-0.02 M=53 S=38
- Runoff T=-0.14 M=351 S=167
- Runoff Land T=-0.15 M=401 S=226
- -1*Evap T=0.07 M=-10.7k S=1.6k
- -1*Evap Land T=0.03 M=-10.1k S=1.8k
- Snowmelt T=-0.03 M=56 S=43
- Snowmelt Land T=-0.02 M=51 S=37
- Prec - Eva T=0.94 M=-311 S=1.2k
- Prec - Eva Land T=-0.42 M=284 S=720
- SoilMoist7cm T=-0.03 M=1.0m S=107.9k
- SoilMoist7cm Land T=-0.02 M=1.1m S=114.4k
- SoilMoist1m T=-0.04 M=1.2m S=118.7k
- SoilMoist1m Land T=-0.00 M=1.3m S=127.7k
- T2 T=0.20 M=18.28 S=0.54
- T2 Land T=0.20 M=18.38 S=0.54



South Asia - No.1

River: Brahmaputra, Outlet: [25.15N; 89.65E], Area: 518898 km²

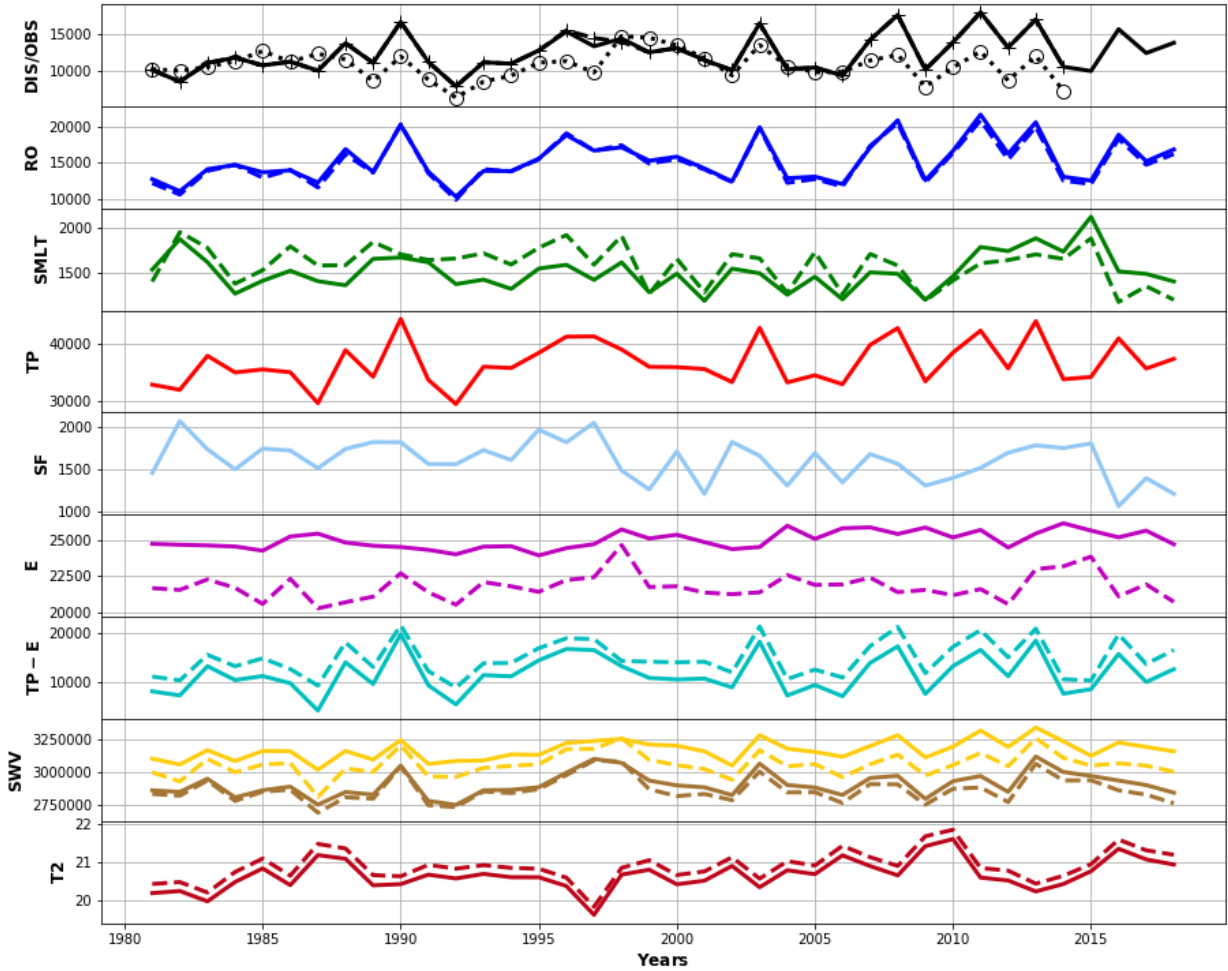
- Discharge T=-0.02 M=24.5k S=3.4k
- DisMatchObs T=-0.02 M=24.6k S=3.5k
- DisOBS T=-0.05 M=19.9k S=3.2k
- Precip T=-0.02 M=36.4k S=3.4k
- Snowfall T=-0.05 M=4.8 S=453
- Runoff T=-0.02 M=25.6k S=3.4k
- Runoff Land T=-0.03 M=26.6k S=3.6k
- -1*Evap T=-0.01 M=-10.1k S=292
- -1*Evap Land T=-0.01 M=-10.0k S=247
- Snowmelt T=-0.01 M=4.3k S=501
- Snowmelt Land T=-0.05 M=4.6k S=440
- Prec - Eva T=-0.03 M=26.3k S=3.6k
- Prec - Eva Land T=-0.03 M=26.4k S=3.6k
- SoilMoist7cm T=0.01 M=2.0m S=42.1k
- SoilMoist7cm Land T=0.00 M=2.1m S=27.6k
- SoilMoist1m T=0.01 M=2.1m S=40.3k
- SoilMoist1m Land T=0.00 M=2.2m S=22.4k
- T2 T=0.21 M=5.56 S=0.47
- T2 Land T=0.21 M=5.78 S=0.47



South Asia - No.2

River: Ganges, Outlet: [24.05N; 89.05E], Area: 951786 km2

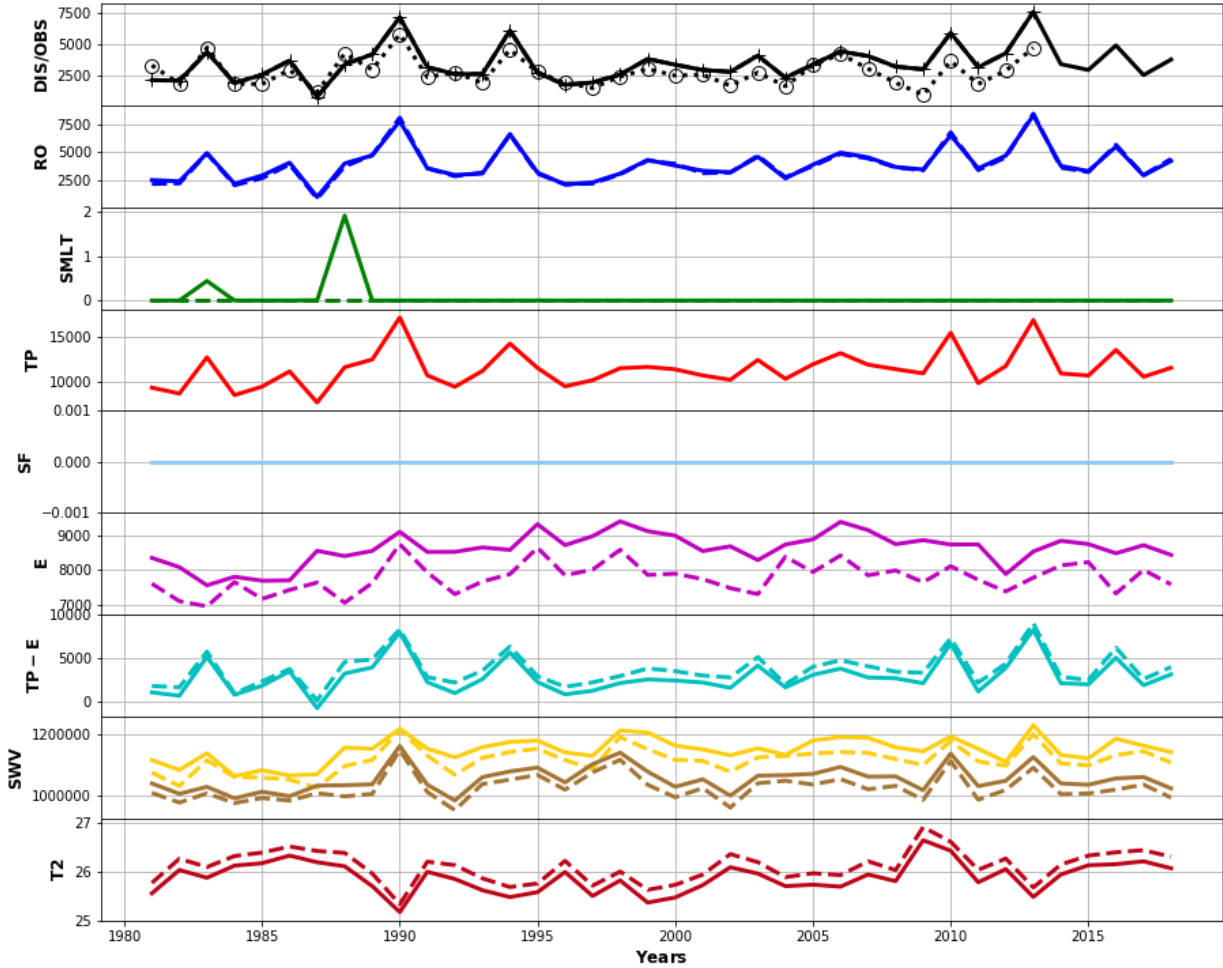
- Discharge T=0.07 M=12.5k S=2.6k
- DisMatchObs T=0.08 M=12.4k S=2.6k
- DisOBS T=-0.01 M=10.8k S=1.9k
- Precip T=0.03 M=36.6k S=3.8k
- Snowfall T=-0.05 M=1.6 S=232
- Runoff T=0.06 M=15.3k S=2.8k
- Runoff Land T=0.05 M=15.0k S=2.9k
- -1*Evap T=-0.01 M=-25.0k S=578
- -1*Evap Land T=-0.01 M=-21.8k S=886
- Snowmelt T=0.02 M=1.5k S=201
- Snowmelt Land T=-0.04 M=1.6k S=218
- Prec - Eva T=0.06 M=11.6k S=3.8k
- Prec - Eva Land T=0.05 M=14.8k S=3.6k
- SoilMoist7cm T=0.01 M=2.9m S=93.7k
- SoilMoist7cm Land T=0.00 M=2.9m S=98.3k
- SoilMoist1m T=0.01 M=3.2m S=76.1k
- SoilMoist1m Land T=0.01 M=3.1m S=91.0k
- T2 T=0.14 M=20.66 S=0.39
- T2 Land T=0.14 M=20.90 S=0.40



South Asia - No.3

River: Godavari, Outlet: [17.15N; 81.65E], Area: 311631 km2

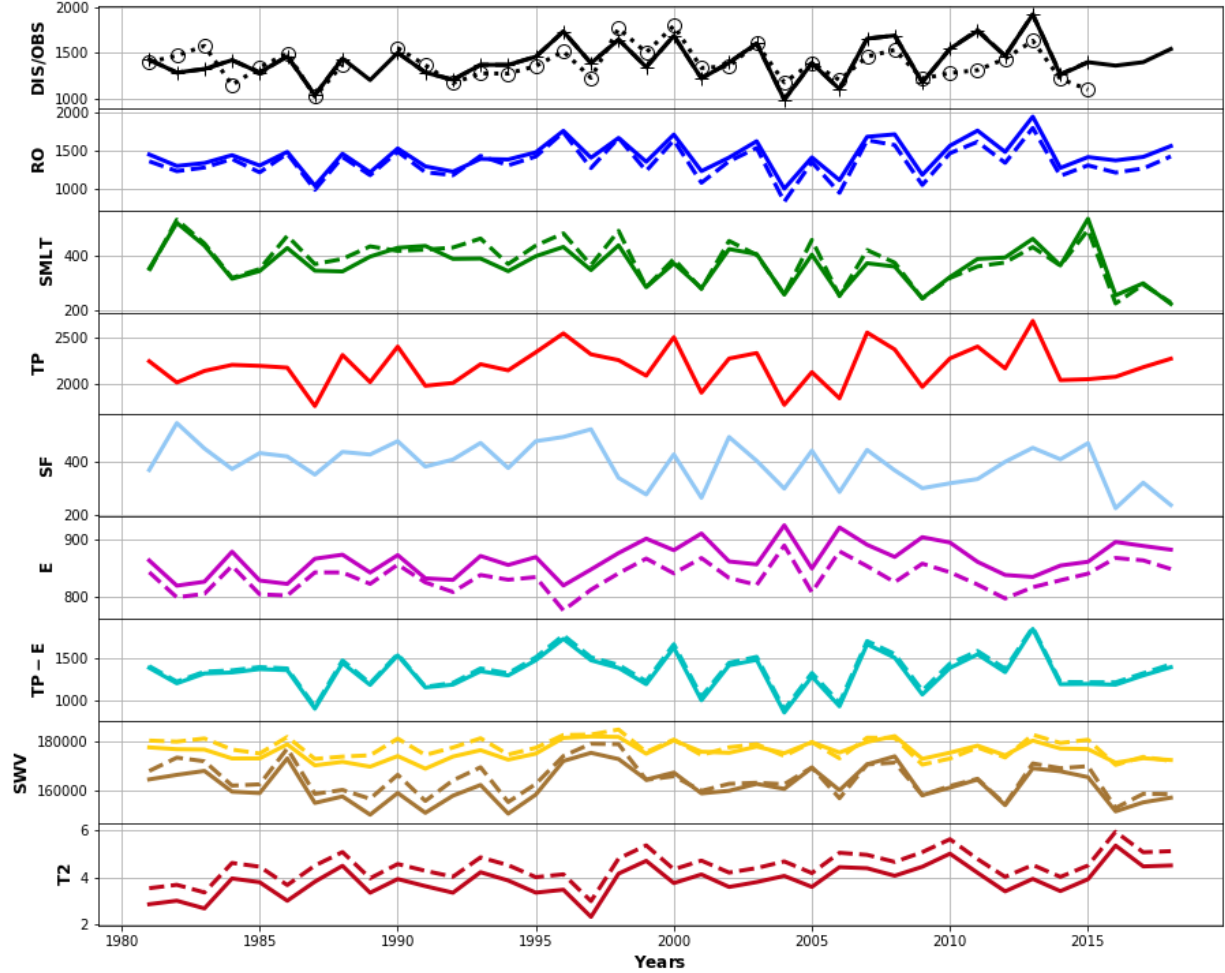
- Discharge T=0.10 M=3.5k S=1.4k
- DisMatchObs T=0.16 M=3.4k S=1.5k
- DisOBS T=-0.02 M=2.8k S=1.1k
- Precip T=0.05 M=11.5k S=2.0k
- Snowfall T=nan M= 0 S= 0
- Runoff T=0.10 M=3.9k S=1.5k
- Runoff Land T=0.11 M=3.9k S=1.6k
- -1*Evap T=-0.02 M=-8.6k S=444
- -1*Evap Land T=-0.01 M=-7.8k S=425
- Snowmelt T=nan M= 0 S= 0
- Snowmelt Land T=nan M= 0 S= 0
- Prec - Eva T=0.13 M=2.9k S=1.9k
- Prec - Eva Land T=0.12 M=3.7k S=1.9k
- SoilMoist7cm T=0.01 M=1.1m S=40.9k
- SoilMoist7cm Land T=0.01 M=1.0m S=42.2k
- SoilMoist1m T=0.01 M=1.1m S=40.7k
- SoilMoist1m Land T=0.01 M=1.1m S=41.8k
- T2 T=0.05 M=25.88 S=0.31
- T2 Land T=0.05 M=26.11 S=0.32



South Asia - No.4

River: Karnali, Outlet: [28.75N; 81.25E], Area: 46325 km2

- Discharge T=0.03 M=1.4k S=200
- DisMatchObs T=0.04 M=1.4k S=207
- DisOBS T=-0.01 M=1.4k S=179
- Precip T=0.01 M=2.2k S=204
- Snowfall T=-0.08 M=390 S=78
- Runoff T=0.03 M=1.4k S=204
- Runoff Land T=0.01 M=1.3k S=215
- -1*Evap T=-0.01 M=-865 S=27
- -1*Evap Land T=-0.01 M=-834 S=24
- Snowmelt T=-0.05 M=366 S=70
- Snowmelt Land T=-0.07 M=378 S=78
- Prec - Eva T=0.01 M=1.3k S=212
- Prec - Eva Land T=0.01 M=1.4k S=213
- SoilMoist7cm T=0.00 M=162.3k S=6.7k
- SoilMoist7cm Land T=-0.01 M=164.9k S=6.7k
- SoilMoist1m T=0.00 M=175.7k S=3.4k
- SoilMoist1m Land T=-0.00 M=177.3k S=3.8k
- T2 T=0.30 M=3.86 S=0.62
- T2 Land T=0.28 M=4.49 S=0.60



Australia - No.1

River: Murray, Outlet: [-34.35S; 139.65E], Area: 713793 km²

- Discharge T=-0.11 M=375 S=225
- DisMatchObs T=-0.18 M=375 S=218
- DisOBS T=-0.28 M=159 S=138
- Precip T=-0.07 M=12.3k S=2.8k
- Snowfall T=-0.13 M=49 S=22
- Runoff T=-0.10 M=823 S=375
- Runoff Land T=-0.14 M=783 S=381
- -1*Evap T=0.03 M=-15.1k S=1.7k
- -1*Evap Land T=0.06 M=-11.7k S=2.1k
- Snowmelt T=-0.19 M=71 S=40
- Snowmelt Land T=-0.13 M=52 S=24
- Prec - Eva T=-0.11 M=-2835 S=1.5k
- Prec - Eva Land T=-0.32 M=592 S=1.0k
- SoilMoist7cm T=-0.02 M=1.9m S=172.2k
- SoilMoist7cm Land T=-0.03 M=1.8m S=175.6k
- SoilMoist1m T=-0.03 M=2.1m S=179.9k
- SoilMoist1m Land T=-0.03 M=1.9m S=158.9k
- T2 T=0.30 M=17.53 S=0.60
- T2 Land T=0.31 M=17.74 S=0.62

